GFZ
Helmholtz Centre
POTSDAM

HELMHOLTZ CENTRE POTSDAM
GFZ GERMAN RESEARCH CENTRE
FOR GEOSCIENCES

Prof. Dr. Bernhard Grasemann
Handling Topical Editor Solid Earth

Bernhard Schuck
Section 4.2: Geomechanics and Scientific Drilling
Telegrafenberg
14473 Potsdam
bernhard.schuck@gfz-potsdam.de

Potsdam, 8 November 2019

Re-submission se-2019-109 "Fault zone architecture of a large plate-bounding strike-slip fault: a case study from the Alpine Fault, New Zealand"

Dear Prof. Grasemann,

We are grateful for the time spent by you and the reviewers on our manuscript. As already indicated in our comments in the interactive discussion, we modified and re-structured the manuscript by implementing the reviewer comments, making the message clear and compelling.

As a consequence, the outline of our discussion has a new structure and now includes specific sections on the "influence of shallow-depth conditions on fault gouge structure" (section 5.2), "implications of fault-core along-strike variations for fault zone architecture" (part of section 5.3.2), "further evidence for a more complex Alpine Fault Zone architecture" (part of section (5.3.2) and a final section dedicated to "the Alpine Fault's more complex geometry: a shallow-depth phenomenon?" (part of section (5.3.2).

Additionally, we outlined more explicitly that the Alpine Fault Zone is commonly perceived to accommodate displacement along a single principal slip zone – a geometry which is conceptualized by Caine et al. (1996) (lines 54 – 55; see also figures 1a and 2c). Our results contrast this view and support a conceptualized fault zone architecture following Faulkner et al. (2003) (lines 572 – 603, see also figures 1b and 11).

Furthermore, for completeness we included section 4.3.3 (mineralogy of the footwall), which was accidently not included in the initially submitted manuscript.

In the following we address individual aspects raised by the reviewers:

Reviewer Comment 1, aspect 1

To better constrain our results based on field observations, we more extendedly discussed our results in context of seismic investigations (see lines 604 – 615).

To account for the reviewer's criticism on lines 271 – 273 of the initially submitted manuscript, we stated in lines 282 – 284 that decreasing amount and size of clasts towards the PSZ observed by us in the field and in thin sections has also been found previously by other studies.

Furthermore, results of other studies on fault gouge thickness variations have been discussed in lines 554 – 556 and lines 563 – 571.

Reviewer Comment 1, aspect 2

We corrected typos in our equations 1 and 2.

To obtain more robust results of geochemical analyses we better constrained the protolith composition by including more data (see table S1). Furthermore, we briefly reviewed the possibilities to derive isocons and justified the approach we used (lines 219 – 226). Additionally, we state in lines 419 – 421 that results of isocon analyses are in general agreement with previous studies.

Reviewer Comment 1, aspect 3

We pointed out that data sparsity resulting from difficult outcrop conditions is an obstacle to understand the Alpine Fault Zone and that additional investigations are required to constrain our results (lines 476 – 480 and 627 – 629).

The discussion part "Implications of fault-core along-strike variations for fault zone architecture" (part of section 5.3.2) elaborates more detailed on potential factors controlling fault gouge thickness.

Reviewer Comment 1 – line by line

In response to the reviewer's comment on line 483 we referred to previous studies suggesting that investigated fault gouges have been exhumed actively, i.e. accommodate slip in the very near-surface (lines 83 – 84 and 122 – 124).

We stated that the models of Hull (1988) and Scholz (1987) on displacement-thickness-relationships are based on empirical observations (line 552).

To account for the reviewer's comments on lines 526 – 528 we elaborated in more detail on our assumption that the entire central segment of the Alpine Fault fails during an earthquake, hence four of the five locations investigated will be affected simultaneously (lines 557 – 562).

Stimulated by the reviewer's comment on line 534, the part "further evidence for a more complex Alpine Fault architecture" of section 5.3.2 (lines 574 – 602) discusses more extensively the implications of the Deep Fault Drilling Project on the Alpine Fault's geometry.

Figures 6 and 7 have been modified as suggested by the reviewer.

Reviewer Comment 3, aspect 3

We decided to not draw a conclusive sketch showing the main microstructures regarding to the different locations, because variations between different outcrops are minor and main microstructures have been presented in a conclusive sketch by Schuck et al. (2018) (see their figure 9). However, with figure 11 we decided to provide a conclusive sketch of the Alpine Fault Zone, which relates our observations to the model presented by Faulkner et al. (2003) (see our figure 1b) and the common perception of the Alpine Fault Zone (see figure 2c).

Reviewer Comment 3 – line by line

As suggested, we included the coordinates of the investigated outcrops in the caption of figure 2 and modified the symbol of DFDP-2 in figure 2b.

We are confident that all points raised have been addressed properly and that they helped to substantially improve the manuscript.

Yours sincerely,

Bernhard Schuck and co-authors

Fault zone architecture of a large plate-bounding strike-slip fault: a case study from the Alpine Fault, New Zealand

Bernhard Schuck[1,a], Anja M. Schleicher[2], Christoph Janssen[1], Virginia G. Toy[3,a], and Georg Dresen[1,4]

[1]Helmholtz Centre Potsdam, GFZ German Research Centre for Geosciences, Section 4.2: Geomechanics and Scientific Drilling, Potsdam, Germany
[2]Helmholtz Centre Potsdam, GFZ German Research Centre for Geosciences, Section 3.1: Inorganic and Isotope Geochemistry, Potsdam, Germany
[3]Department of Geology, University of Otago, Dunedin, New Zealand
[4]University of Potsdam, Institute of Geosciences, Potsdam, Germany
[a]now at: Johannes Gutenberg-Universität Mainz, Tectonics and Structural Geology, Mainz, Germany

Correspondence: Bernhard Schuck (bernhard.schuck@gfz-potsdam.de)

Abstract. New Zealand's Alpine Fault is a large, plate-bounding strike-slip fault, that ruptures in large ($M_W > 8$) earthquakes. ~~Its hazard potential is linked to its geometrical properties.~~ We conducted field and laboratory analyses of fault rocks to ~~elucidate their influence on~~ assess its fault zone architecture. Results reveal that the Alpine Fault zone has a complex geometry, comprising an anastomosing network of multiple slip planes that have accommodated different amounts of displacement. ~~Within it, slip zone width is demonstrably not related to lithological differences of quartzofeldspathic lithologies, which vary slightly along-strike. The~~ This contrasts with the previous perception of the Alpine Fault zone, which assumes a single principal slip zone accommodated all displacement. This interpretation is supported by results of drilling projects and geophysical investigations. Furthermore, observations presented here show that the young, largely unconsolidated sediments that constitute the footwall ~~in some outcrops have a much more~~ at shallow depths have a significant influence on fault gouge rheological properties and structure. ~~Additionally, seismic investigations indicate that the exposed complex fault zone architecture extends into the basement. This study reveals the Alpine Fault contains multiple slip zones surrounded by a broader damage zone; properties elsewhere associated with carbonate or phyllosilicate-rich faults.~~

1 Introduction

A fault, a planar discontinuity in rock where one side has moved relative to the other parallel to the discontinuity plane, constitutes a rheological and mechanical manifestation of localized deformation (Twiss and Moores, 2007; Ben-Zion, 2008; Fossen, 2016; Fossen and Cavalcante, 2017). ~~Many large~~ Large faults zones are typically composed of networks of smaller, individual, but related and interacting faults of self-similar geometry (Ben-Zion and Sammis, 2003; Twiss and Moores, 2007; Peacock et al., 2016). The structure, composition, hydrological properties and seismo-mechanical behavior of faults are typically intimately related. These interactions also govern strain distribution and depend on various factors, such as lithology (Faulkner et al., 2003; Schleicher et al., 2010; Holdsworth et al., 2011; Rybacki et al., 2011), fluid pressure (Hickman et al., 1995; Janssen

et al., 1998; Fagereng et al., 2010) and stress field and stress magnitudes (Sibson, 1985; Faulkner et al., 2006; Lindsey et al., 2014).

Faults control the strength of the Earth's lithosphere (Townend and Zoback, 2000; Bürgman and Dresen, 2008) and govern substantially fluid flow (Caine et al., 1996; Wibberley et al., 2008). Hydrocarbon production from fault-compartmentalized reservoirs (Van Eijs et al., 2006), exploitation of fault-hosted mineral deposits (Cox et al., 1986) and long-term integrity of potential nuclear waste repositories (Laurich et al., 2018) are practical examples demonstrating how important it is to understand fault zone properties and their spatial and temporal evolution. Furthermore, large, plate-bounding strike-slip faults such as the Alpine Fault (New Zealand), the North Anatolian Fault Zone (Turkey) or the San Andreas Fault (USA) rupture in large ($M_W > 7$) earthquakes (Toppozada et al., 2002; Sutherland et al., 2007; Bohnhoff et al., 2016). Many of these faults are located in densely populated areas so they pose a significant geohazard (Eguchi et al., 1998; Sahin and Tari, 2000; Martínez-Garzón et al., 2015). Thus, from a georesource, seismic hazard and risk perspective, it is important to characterize the seismo-mechanical properties of faults (Aksu et al., 2000; Zoback et al., 2007; Hollingsworth et al., 2017).

Caine et al. (1996) presented a conceptual model of the structure of fault zones that has three primary components (Fig. 1a). The protolith (I) hosts a damage zone (II) that is characterized by a fracture density significantly higher than the background values of the surrounding host rock (Chester et al., 1993; Biegel and Sammis, 2004; Faulkner et al., 2010). The damage zone contains the fault core (III) where most of the displacement has been accommodated (Caine et al., 1996). This conceptual framework has been found to be applicable to faults across the full range of natural and experimental spatial scales (Anders and Wiltschko, 1994). Biegel and Sammis (2004) suggested a fault core should be defined as the zone within a fault where strain leads to granulation of rocks, distinct from a damage zone within which fracture density is high but fracturing has "not [been] sufficient to produce distinct particles". A fault core can be structurally and lithologically heterogeneous, and most of the displacement it accommodated may be localized along one or more principal slip zones (PSZ) defined by ultracataclasites or fault gouges (Sibson, 2003; Janssen et al., 2014; Toy et al., 2015). Although most commonly less than 10 cm thick, PSZs may be up to 1 m thick (Sibson, 2003) and thicknesses tend to increase with increasing displacement (Evans, 1990; Faulkner et al., 2010; Ben-Zion and Sammis, 2003, and references therein). In general, fault zone thicknesses may range from millimeters (e.g. Antonellini and Aydin, 1994) to a few hundreds of meters (e.g. Bruhn et al., 1994).

The Punchbowl Fault, an inactive, exhumed part of the San Andreas Fault system, typifies this conceptual model of fault zone architecture. It has a single PSZ embedded in a fault core and surrounding damage zone. A single, continuous gouge layer with 30 cm thickness on average, hosts the ~1 mm thick PSZ. The core of the Punchbowl Fault is surrounded by an approximately 15 m thick damage zone (Chester and Logan, 1986; Chester et al., 2005).

However, other faults show a more complex structure with changing properties along strike or down dip (e.g. Wibberley et al., 2008; Faulkner et al., 2010). For example, detailed studies of the Carboneras Fault, Spain, yielded a conceptual model that is suitable for broader, typically phyllosilicate-rich fault zones, which tend to contain multiple high-strain zones (Fig. 1b; Faulkner et al. 2003). The Carboneras Fault is a predominantly strike-slip structure, that comprises an ~1 km thick tabular zone of continuous and anastomosing strands of phyllosilicate-rich fault gouge containing lenses of fractured protolith surrounded

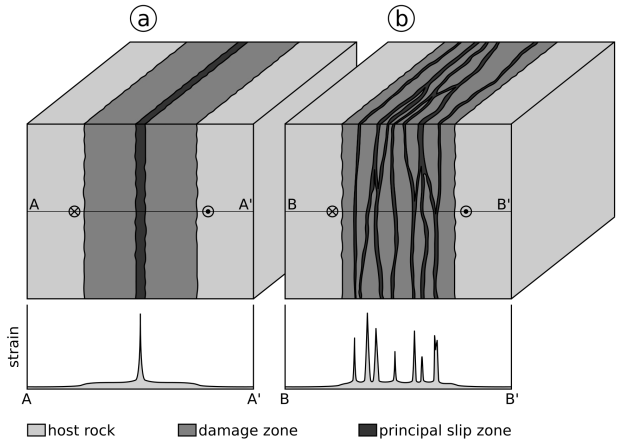

Figure 1. Conceptual end-member models of fault zone architecture. **(a)** According to the model of Caine et al. (1996) a fault is a relatively simple structure, where most of the strain is accommodated at a single, quite narrow fault core hosting a principal slip zone. **(b)** Faults being described by the model of Faulkner et al. (2003) are more complex and consist of a damage zone hosting multiple, anastomosing principal slip zones forming a complex network.

by an approximately 100 m wide damage zone. Scaly clays, which typically contain anastomosing shear planes, are examples of this distributed fault zone model on the hand-specimen scale (Vannucchi et al., 2003; Laurich et al., 2017).

The fault zone architecture of New Zealand's Alpine Fault, a large, transpressional plate-bounding fault and a significant geohazard, has attracted increasing attention in the last ten years~~(e.g. Barth et al., 2012; Sutherland et al., 2012; Barth et al., 2013; Toy et al., 20~~ ~~.~~. Considered to be appropriately described by the conceptual model of Caine et al. (1996), a single PSZ is commonly supposed to accommodate displacement along the Alpine Fault (e.g. Barth et al., 2012; Sutherland et al., 2012; Barth et al., 2013; Norris and Toy, 20 . Here, by combining results of these previous studies on the Alpine Fault's structure with new field observations, microstructural, mineralogical and geochemical analyses we show that the Alpine Fault has a complex fault geometry ~~at and above seismogenic depths. Atypical for fault zones hosted in quartzofeldspathic protoliths, this~~ manifested by PSZ thicknesses differing substantially between investigated outcrops. This complexity is not ~~a function of lithologyand~~ controlled by lithology, which is unexpected given that the Alpine Fault is hosted in a quartzofeldspathic protolith, which commonly fosters localization compared to phyllosilicate host rocks (Faulkner et al., 2003). This implies that the Alpine Fault does not fit ~~the classical~~ our paradigmatic models of fault zone architecture.

2 Geological Setting

2.1 The Alpine Fault and associated hazard

The Alpine Fault localizes most of the deformation associated with the relative displacement between the Australian Plate and the Pacific Plate. The fault is dominantly dextral transpressive and runs through the South Island of New Zealand. The straight,

800 km long surface trace extends from Milford Sound in the SW to Hokitika in the NE, where it transfers displacement onto the four main fault strands of the Marlborough Fault System (the Wairau, Awatare, Clarence and Hope Faults; Fig. 2a). The Alpine Fault maintains a constant NE-SW strike for its entire length, but the fault dip changes from 80-90° SE SW of the Dun Mountain Ophiolite Belt (DMOB) to 30-50° SE in the central segment (Barth et al., 2013). The shallowest 1-2 km of the fault NE of Haast display 'serial partitioning', i.e. northerly-striking oblique thrust sections ~~and~~ alternate with easterly-striking dextral strike slip sections of 1-10 km length (Norris and Cooper, 1995; Barth et al., 2012).

A 470 km right-lateral offset of the DOMB defines the minimum cumulative displacement along the fault (Sutherland et al., 2007) . Displacement-normal shortening is on the order of 90 ± 20 km (Little et al., 2005). Strike-slip displacement rates are between 21 mm yr^{-1} and 29 ± 6 mm yr^{-1} (Norris and Cooper, 2000) corresponding to 60-80 % of the total relative velocity between the bounding plates (DeMets et al., 2010). Seismic investigations indicate a maximum exhumation of ~35 km from a deep crustal, subhorizontal, NE-dipping detachment (Stern et al., 2001; Little et al., 2005). Long-term exhumation rates of 6-9 mm yr^{-1} are inferred from $^{40}Ar/^{39}Ar$ ages encountered between Franz Josef Glacier and Fox Glacier (Little et al., 2005). A combination of these high exhumation rates and meteoric fluid circulation driven by steep topographic gradients results in a very high geothermal gradient of up to 125 °C km^{-1} encountered in valleys (Menzies et al., 2016; Sutherland et al., 2017).

Currently, the Alpine Fault does not exhibit creep and is thought to be seismically locked to a depth of 12-18 km (Beavan et al., 2007). It is known to rupture in large earthquakes ($M_W > 8$), while generating up to 8-9 m of lateral and up to 1 m of normal displacement (Sutherland et al., 2007; Nicol et al., 2016). Offset and deformed Quaternary features demonstrate that Alpine Fault earthquakes rupture the ground surface (e.g. Cooper and Norris, 1990; Berryman et al., 2012; Schuck et al., 2018). While events like the most recent one in 1717 AD might rupture the entire fault, differing recurrence intervals of 263 ± 68 years for the central segment and 291 ± 23 years for the southern segment demonstrate that individual sections of the fault might fail independently (Fig. 2a; Sutherland et al. 2007; Howarth et al. 2018 and references therein). Considering the potential to produce large magnitude earthquakes and the time passed since the last event, the Alpine Fault is late in its seismic cycle and thus constitutes one of the South Island's major geohazards.

2.2 Lithology

The Australian Plate footwall assemblage encompasses Paleozoic to Cretaceous plutonic rocks intruded into metasediments (Fig. 2b). As these units are mostly overlain by Quaternary fluvioglacial sediments, footwall rocks are poorly exposed (e.g. Toy et al., 2015). In the Pacific Plate hanging-wall, a narrow, 12-25 km wide, elongate belt of metamorphosed sediments, the Alpine Schist, is exposed from SW of Jackson Bay to the fault's north-eastern termination (e.g. Sibson et al., 1979; Grapes and Watanabe, 1992; Scott et al., 2015). The Alpine Schist originates mostly from the Torlesse Terrane. This terrane is a polygenetic metamorphic suite with the Alpine Schist being its high-grade, and most recently-formed ~~part (Roser and Cooper, 1990).~~ (Late Cretaceous) part (Roser and Cooper, 1990; Scott et al., 2015).

The amphibolite-greenschist facies rocks of the Alpine Schist have dominantly metapelitic to metapsamitic compositions, with rare metabasite and metachert. Metamorphic grade decreases from K-feldspar and oligoclase amphibolite facies through garnet, biotite and chlorite greenschist facies to pumpellyite-actinolite and prehnite-pumpellyite facies with increasing SE-

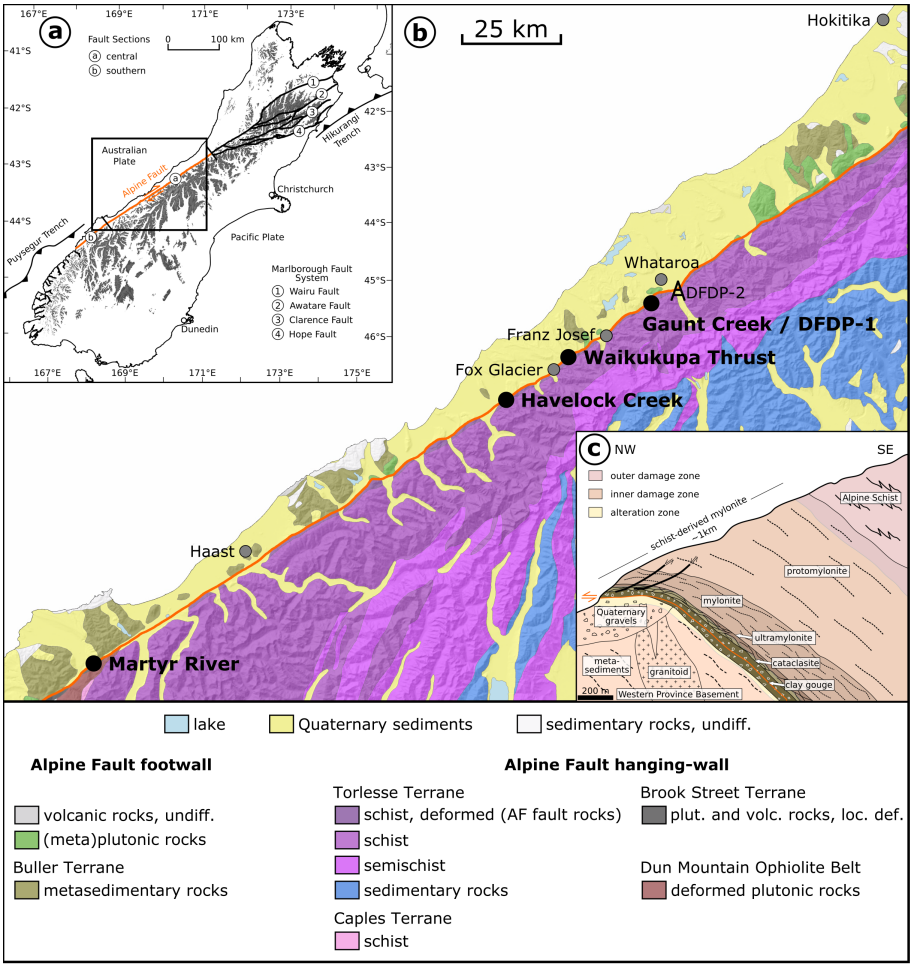

Figure 2. **(a)** Plate tectonic setting of New Zealand's South Island with the Alpine Fault's onshore segment being highlighted in orange. Position of (b) is indicated by black box. **(b)** Simplified geological map of the study area. Alpine Fault trace shown in orange. Locations of investigated outcrops: Martyr River: S43° 7' 47" E168° 33' 40"; Havelock Creek: S43° 32' 15" E169° 52' 15"; Waikukupa Thrust: S43° 26' 22" E170° 4' 8"; Gaunt Creek: S43° 18' 58" E170° 19' 20". Map is based on the geological map of New Zealand's South Island (Edbrooke et al., 2015) and the digital elevation model of Columbus et al. (2011). **(c)** Typical shallow-depth sequence of Alpine Fault rocks. Figure was modified from Norris and Cooper (2007). Extents of alteration zone were derived from Sutherland et al. (2012) and extents of inner and outer damage zone from Townend et al. (2017).

distance from the fault plane (e.g. Grapes and Watanabe, 1992; Scott et al., 2015). However, a combination of significant right-lateral displacement and high-exhumation rates resulted in 200-300 m wide inverted metamorphic sequences cropping out structurally above brittle fault rocks in the central segment (Cooper and Norris, 2011). Irrespective of local variations, typical mineral phases encountered in Alpine Schist-derived fault rocks are quartz, feldspar, garnet, muscovite, biotite, other minor phases and, in case of metabasites, hornblende and epidote (Norris and Cooper, 2007). At the Waikukupa Thrust there

are remnants of highly disrupted, intensely strained and sheared granite pegmatites indicating simple shear strains of more than 150 and coeval pure shear stretches of ~3.5 (Norris and Cooper, 2003; Toy et al., 2013).

~~**(a)** Plate tectonic setting of New Zealand's South Island with the Alpine Fault's onshore segment being highlighted in orange. Position of (b) is indicated by black box. **(b)** Simplified geological map of the study area. Alpine Fault trace shown in orange. Locations of investigated outcrops are highlighted with bold font. Map is based on the geological map of New Zealand's South Island (Edbrooke et al., 2015) and the digital elevation model of Columbus et al. (2011). **(c)** Typical shallow-depth sequence of Alpine Fault rocks. Figure was modified from Norris and Cooper (2007). Extents of alteration zone were derived from Sutherland et al. (2012) and extents of inner and outer damage zone from Townend et al. (2017).~~

Whereas the Alpine Schist constitutes the protolith of fault rocks in the central portion of the Alpine Fault, a comparatively small (~550 m thick) sliver of the Brook Street Terrane (BST) is the protolith of samples from the southern segment (Fig. 2b). The sliver is surrounded by the DMOB and bound to the NE by the Alpine Fault. The BST is the remnant of a Permian island-arc system, mainly composed of basaltic to andesitic volcaniclastic and sedimentary rocks of prehnite to pumpellyite and locally greenschist metamorphic grade (Spandler et al., 2005).

2.3 Fault rocks of the Alpine Fault

Exhumation from deep-crustal levels resulted in the formation of an approximately one kilometer wide characteristic sequence of hanging-wall fault rocks (e.g. Reed, 1964; Sibson et al., 1979; Cooper and Norris, 2011; Toy et al., 2015, Fig. 2c). Progressive north-westward-increasing ~~shear~~ strain of the Alpine Schist yielded proto- to ultramylonites that are overprinted by a cataclastic fault zone displaying increasing damage towards the PSZ (Williams et al., 2016). Cataclastic shears in the ultramylonites are filled with phyllosilicates and exhibit strike-slip, normal and reverse kinematics. Cataclasites are composed of comminuted mylonite fragments within a matrix of pulverized host rock, authigenic chlorite, muscovite and illite (Sibson et al., 1979; Norris and Cooper, 2007; Boulton et al., 2012). Intense chloritization imparted a typical pale-green color to these 10-30 m wide cataclasites (Warr and Cox, 2001), which are cemented by authigenic phases, dominantly phyllosilicates and carbonates (Sutherland et al., 2012; Toy et al., 2015; Williams et al., 2016). The fault's PSZ ~~is~~ cross-cuts all other structures, which indicates that it is the last active part of the fault system and accommodates the coseismic displacements that manifest as offset Quaternary features (e.g. Cooper and Norris, 1990; Berryman et al., 2012; Schuck et al., 2018). It is an incohesive and fine-grained gouge up to ~50 cm in thickness (Norris and Cooper, 2007; Boulton et al., 2012). Authigenic phyllosilicates cement the PSZ converting it into an impermeable hydraulic barrier preventing cross-fault fluid flow (Sutherland et al., 2012; Menzies et al., 2016). There is no location providing a continuous section from hard-rock hanging- to hard-rock footwall (Townend et al., 2009).

2.4 The Deep Fault Drilling Project

Studying the physical character of tectonic deformation at depth within a continental fault late in its interseismic period provided the motivation for the Deep Fault Drilling Project (DFDP, Fig. 3a, Townend et al., 2009). Phase 1 drilled two ~100 m (DFDP-1A) and ~150 m (DFDP-1B) deep pilot holes in January 2011 (Sutherland et al., 2012; Toy et al., 2015). These DFDP-1

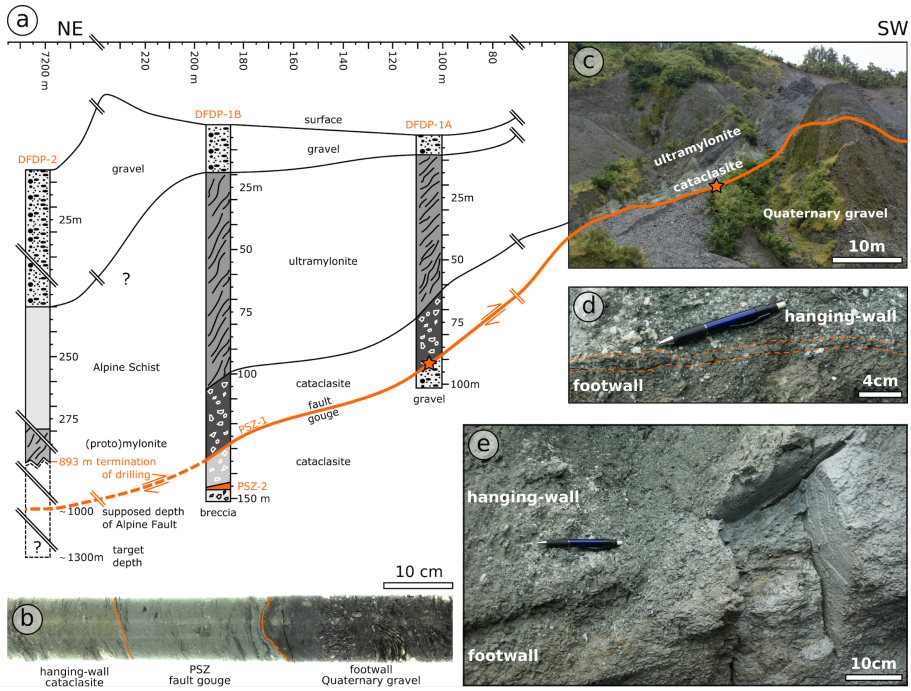

Figure 3. **(a)** Schematic overview of Deep Fault Drilling Project (DFDP) boreholes drilled in phase 1 at Gaunt Creek and phase 2 within the Whataroa River Valley. Star at DFDP-1A indicates location of b. **(b)** Segment of 180° scan of PSZ encountered at DFDP-1A drill core (run 66, section1). **(c)** Individual fault rock units of the Alpine Fault zone are well-recognizable at the outcrop Gaunt Creek, in close proximity to the DFDP boreholes. Star indicates location of d and e. **(d)** An approximately 1 cm thick, brown layer indicated by stippled orange lines, was interpreted to represent the PSZ at Gaunt Creek. **(e)** Sample location (specimen shown in figure 5b) some 10s of centimeter SW of location shown in d. Figure modified according to Sutherland et al. (2012) and Boulton et al. (2014).

boreholes provide a continuous section of fault rocks from hanging-wall ultramylonites to footwall gravels enabling lithological (Toy et al., 2015), mineralogical (Schleicher et al., 2015), geomechanical (Boulton et al., 2014; Carpenter et al., 2014) and geophysical analysis (Sutherland et al., 2012; Townend et al., 2013). In total, three ~20 cm thick PSZs were encountered. In DFDP-1A the PSZ is located between 90.67 and 90.87 m depth (Figs. 3a & b), and in DFDP-1B two PSZs were encountered at 128.30-128.50 m and 143.96-144.16 m depth, respectively (Fig. 3a, Toy et al., 2015).

Another two boreholes were drilled in DFDP phase 2 (DFDP-2A: 212.6 m MD - measured depth, DFDP-2B: 893.1 m MD) about 7.5 km ENE of the location of DFDP-1 (Fig. 2b, Toy et al., 2017). Phase 2 yielded cuttings for petrographic investigations (Toy et al., 2017) and provided various insights into fault zone architecture by wireline logs (e.g. Janku-Capova et al., 2018; Massiot et al., 2018) but was not able to penetrate and sample the fault core due to scientific and technical difficulties (Toy et al., 2017). DFDP boreholes from both phases provide the opportunities for long-term monitoring of the Alpine Fault (e.g. Sutherland et al., 2015).

2.5 Study locations

For this study, all known outcrops with accessible PSZ between Martyr River in the SW and Kokatahi River, SSE of Hokitika in the NE were investigated in the austral summer 2015/16 (Fig. 2b). Furthermore, cataclasite and fault gouge samples were available from the DFDP-1A core. Four of the five investigated locations, Havelock Creek, Waikukupa Thrust, Gaunt Creek and the core of DFDP-1A, are in the central segment of the Alpine Fault with the Alpine Schist as hanging-wall host rock. Rocks of the BST constitute the host of fault rocks encountered at Martyr River, the fifth and southwestern-most location. All outcrops are located along river banks providing good outcrop conditions.

Waikukupa Thrust is the only studied site that is considered to be inactive. Incision of the Waikukupa River resulted in a geomechanically unfavorable geometry leading to the abandonment of this thrust segment and re-localization of deformation approximately 700 m to the NE at Hare Mare Creek (Norris and Cooper, 1997).

3 Methods

3.1 Sampling

Fault rocks at Martyr River and Havelock Creek were sampled using hammer and chisel. At Waikukupa Thrust and Gaunt Creek samples were recovered using a hand-held chainsaw equipped with a silicon-carbide chain. After recovery, all outcrop samples were immediately wrapped in aluminum and plastic foil to slow down drying. This procedure allowed continuous transects across the PSZ, which juxtapose hanging-wall cataclasites and footwall gravels, to be sampled from Martyr River and Waikukupa Thrust. However, the samples broke apart along the PSZ during shipping. An intact contact of PSZ on footwalls material was only preserved from Gaunt Creek.

In summary, hanging-wall fault rocks are available from Martyr River, Waikukupa Thrust and DFDP-1A. PSZ samples originate from all five locations and footwall rocks were taken at Martyr River, Waikukupa Thrust and Gaunt Creek.

3.2 Microstructural analysis

Samples from Martyr River, Waikukupa Thrust and Gaunt Creek were cut dry with a low-speed saw perpendicular and parallel to the fault trace. From all locations, subsamples were selected for microstructural analyses and subsequently embedded in resin prior to the preparation of 29 dry-polished thin sections using otherwise standard techniques.

Microstructural investigations were conducted using optical microscopy, scanning electron microscopy (SEM), transmission electron microscopy (TEM) and cathodoluminescence analyses (CL). Thin sections were studied with a Leica DM RX optical microscope and a FEI Quanta 3D SEM with focused ion beam (FIB; dual-beam machine). The SEM, equipped with a field emission gun, operated at 20 kV in backscatter electron mode (BSE) and allowed semi-quantitative geochemical analyses with its EDAX energy dispersive X-ray analyzer (EDX). For TEM analyses, a platinum strip was deposited on the sites selected with the FIB of the SEM to enable subsequent preparation of 14 thin foils ($10 \times 8 \times 0.15$ µm) with a FEI FIB 200 following the procedure outlined by (Wirth, 2004, 2009). A FEI Tecnai G2 F20 X-Twin TEM with Gatan Tidiem energy filter, Fishione

high-angle annular dark field detector (HAADF) and EDX operated at 200 kV and allowed nanoscale investigations. Cathodoluminescence analyses on calcite veins and cement were performed on thin sections using an Olympus polarizing microscope. The Lumic HC1-LM hot cathode CL microscope operated at 14 kV, 0.0001 mbar and ~0.6 mA electron beam and 2.5 A filament current, respectively.

Microstructural analyses are mostly based on qualitative observations, but some quantitative information was obtained by image analysis using the open source software FIJI / ImageJ (Schindelin et al., 2012; Schneider et al., 2012).

3.3 Mineralogical and geochemical investigations

18 bulk rock powder samples for mineralogical and geochemical analyses were prepared with a jaw crusher ~~, subsequent sieving~~ and subsequently sieved to grain sizes < 62 µm~~and a~~. A McCrone micronization mill ~~providing~~ provided the < 10 µm grain size fraction for the quantitative mineralogical analysis.

3.3.1 X-ray diffraction analysis

The mineralogical compositions of the samples were determined by X-ray diffraction (XRD) analysis on random powder samples loaded from the back-side of the sample holders (∅ 16 mm). XRD analyses were performed with a PANalytical Empyrean X-ray diffractometer operating with Bragg-Brentano geometry at 40 mA and 40 kV with CuKα radiation and a PIXel 3d detector at a step size of 0.013 °2Θ from 4.6 to 85 °2Θ and 60 s per step.

Mineralogy was determined qualitatively with the EVA software (version 11.0.0.3) by Bruker. Rietveld refinement for quantitative mineralogy was performed using the program BGMN and the graphical user interface Profex (version 3.10.2, Döbelin and Kleeberg, 2015) calibrated for the used diffractometer. The error of quantitative analyses is expected to be in the range of 3 wt%. Goodness of fit was assessed by visually inspecting the differences between measured and modelled diffractograms and by aiming to obtain R_{wp}-values lower than 3, a value arbitrarily chosen (Toby, 2006).

Bulk powder subsamples (45 mg), dispersed in 1.5 ml of de-ionized water and disaggregated in an ultrasonic bath, were placed on round (∅ 3.1 cm) glass slides and air-dried for subsequent smectite and chlorite analyses. Identification of smectite was performed after ethylene glycolation at 45 °C for at least 12 h (2.4 – 25 °2Θ), and heating to 500 °C for one hour allowed to differentiate between chlorite and kaolinite (2.4 – 25 °2Θ, Moore and Reynolds, 1997).

Illite polytype analyses to differentiate between authigenic and detrital (i.e. comminuted muscovite) species were conducted on selected samples with high illte and / or muscovite concentrations (Moore and Reynolds, 1997; Haines and van der Pluijm, 2008). Diffractograms for polytype analyses were acquired between 16 and 44 °2Θ at a step size of 0.013 °2Θ with 200 s per step. All diffractograms and R_{wp}-values are provided in the supplementary material.

3.3.2 X-ray fluorescence spectrometry

X-ray fluorescence spectrometry (XRF) with a PANalytical AXIOS Advanced spectrometer enabled ~~to study~~ study of geochemical variations of major elements. For this purpose, after drying of ~1.1 g of bulk rock powder overnight at 105 °C, 1

g of sample material, 6 g of $LiBO_2$ and 0.5-0.7 g of ammonium nitrate, acting as oxidizing agent, were fusion digested at increasing temperatures from 400 °C to 1150 °C with a dilution of 1:6. The loss on ignition (LOI) providing volatile contents was determined on 20-30 mg of powder samples with an Euro EA Elemental Analyzer.

To evaluate fluid-related element mobilization, XRF data were analyzed based on the equation of Gresens (1967) for composition-volume relationships resulting from metasomatic alterations, employing the isocon method (Grant, 1986, 2005). In this, the chemical composition of each investigated fault rock sample (i.e. altered rock) is plotted against the chemical composition of the host rock (i.e. unaltered rock). An isocon, a straight line through the origin, separates species enriched relative to the host rock plotting above from those depleted plotting below. It follows the equation

$$C_{A}^{A} = m \times C_{H}^{H} \tag{1}$$

with C_{A}^{A} and C_{H}^{H} being element concentrations of the altered and the host rock, respectively, and m referring to the isocon's slope. ~~A linear best-fit through all data points is used to determine the slope (Grant, 1986, 2005).~~ Enrichment or depletion (ΔC_i) of an element i relative to its host rock equivalent is calculated as follows:

$$\frac{\Delta C_i}{C_i^H} = m^{-1} \times \frac{C_i^A}{C_i^H} - 1 \tag{2}$$

The inverse of the isocon's slope (m^{-1}) indicates overall mass gain ($m^{-1} > 1$) or loss ($m^{-1} < 1$), respectively. Mass gains [%] are calculated as ($m^{-1} - 1$) × 100 %. A negative mass gain corresponds to a mass loss [%].

To derive isocon slopes, Grant (2005) suggested five approaches: (I) clustering of C_i^A / C_i^H, (II) a best-fit of data forming a linear array through the origin on an isocon diagram as graphical equivalent to (I), (III) assuming that certain elements are immobile, or assuming (IV) mass or (V) volume to be constant during alteration. However, it has previously been shown that Al and Ti - elements commonly assumed to be not affected by fluid-related alteration, e.g. Grant (2005), Dolejš and Manning (2010) - are mobilized by fluid-related alteration at the Alpine Fault. Furthermore, authigenic mineral formation is thought to affect both fault rock mass, and rock volume (Schuck et al., 2018). As identification of clusters (I) or linear arrays (II) selects only a subset of all data points, and these selections may be biased, we used a linear best-fit through all data points to determine isocon slopes.

Identification of the host rock is just as important as correctly determining the ~~slope of the isocon~~ slopes of the isocons (Grant, 1986). We defined a reference protolith composition for fault rocks from Havelock Creek, Waikukupa Thrust, Gaunt Creek and DFDP-1A ~~as~~ (Table S1) based on the average of geochemical compositions of Alpine Schist ~~samples derived from DFDP-2B cuttings (Table S1, Table 4 in Toy et al., 2017)~~data reported by Grapes et al. (1982), Roser and Cooper (1990) and Toy et al. (2017). These analyses are derived form the entire central segment of the Alpine Fault and individual data points display little variation.

~~To assess fluid-related alteration at~~ At Martyr River, the ~~geochemistry presented in Table 1 by Spandler et al. (2005) has been averagedto be~~ geochemical compositions by Spandler et al. (2005, see their table 1) have been averaged, and used as host rock

composition (Table S1). ~~However, data~~ Their analyses from Bluff Complex and Takitimu Mountains ~~have been~~ were excluded, because the origin and some geochemical features, respectively, are different from the bulk BST (Spandler et al., 2005). We also ~~note there are limitations to the ability of the~~ noteh the isocon-method ~~to understand~~ has limitations for understanding of fluid-assisted alteration related to fault activity at Martyr River. This is because the width of the Alpine Fault deformation zone at this location is larger than the thickness of the BST (Fig. 2b), so faulting-related fluid-rock-interaction likely occurred with the DMOB ~~likely occurred~~ and the geochemical composition of the reference protolith was already affected by fluid-related alteration. Furthermore, the BST is compositionally very heterogeneous due to magmatic differentiation so it is difficult to choose a single representative ~~geochemical composition of the host rock~~ host rock geochemical composition. Fortunately, these variations only substantially affect the absolute quantification. The method nevertheless allows relative geochemical changes within the fault zone at this location to be accounted for.

The limitations regarding absolute quantification of concentration changes as result of hydrothermal alteration also apply to the Alpine Schist~~, too~~.

4 Results

4.1 Field observations

Individual ~~fault rock units~~ units of the Alpine Fault rock sequence - (ultra)mylonites, cataclasites and footwall gravels - can be identified clearly at all sites investigated. However, weathering and landslides ~~obscure~~ complicate the unambiguous identification of the PSZ ~~, hence the fault core,~~ at Gaunt Creek and Havelock Creek. This is exemplified by an approximately 1 cm thick, fine-grained, brown, fractured and discontinuous layer interpreted to represent the PSZ at Gaunt Creek (Figs. 3c-e) that was identified through sampling to be a footwall-feature approximately 8 cm below the PSZ (see section 4.2.3). ~~Due to these difficult outcrop conditions~~Furthermore, measurements of fault orientation are only robust in the well-exposed outcrops at Waikukupa Thrust (50° / 44° SE) and Martyr River (59° / 51° SE) and ~~have to treated with caution at~~ those from Gaunt Creek (61° / 32° SE) and Havelock Creek (102° / 55° SE) should be treated with caution.

Thicknesses of fault gouges constituting the PSZ ~~varies~~ vary between individual locations, including the DFDP-1A core (Figs. 3-5), and ~~decreases~~ decrease in the following order: Havelock Creek (~50 cm; Figs. 4a & 5a), Gaunt Creek (~30-40 cm; Figs. 3c-e & 5b), DFDP-1A (20 cm; Fig. 3b), Waikukupa Thrust (~4 cm; Figs. 4b & 5c) and Martyr River (~1-2 cm; Figs. 4c, d & 5d). ~~These thickness variations appear to be not systematically controlled by protolith lithology~~ Except for Martyr River, these locations have the same protolith (Fig. 2b; see section 4.3)~~and highlight that the fault has a very variable character at different locations.~~ . Furthermore, there is no systematic variation of PSZ thickness in distance along strike in these outcrops.

4.2 Microstructures

The fault rocks of Alpine Fault hanging-wall, PSZ and footwall contain clasts embedded in a fine-grained matrix. We define matrix as ~~very~~ fine particles - detrital and authigenic - belonging to the clay-size fraction, i.e. < 2 µm (Fig. 6a). In fact, the

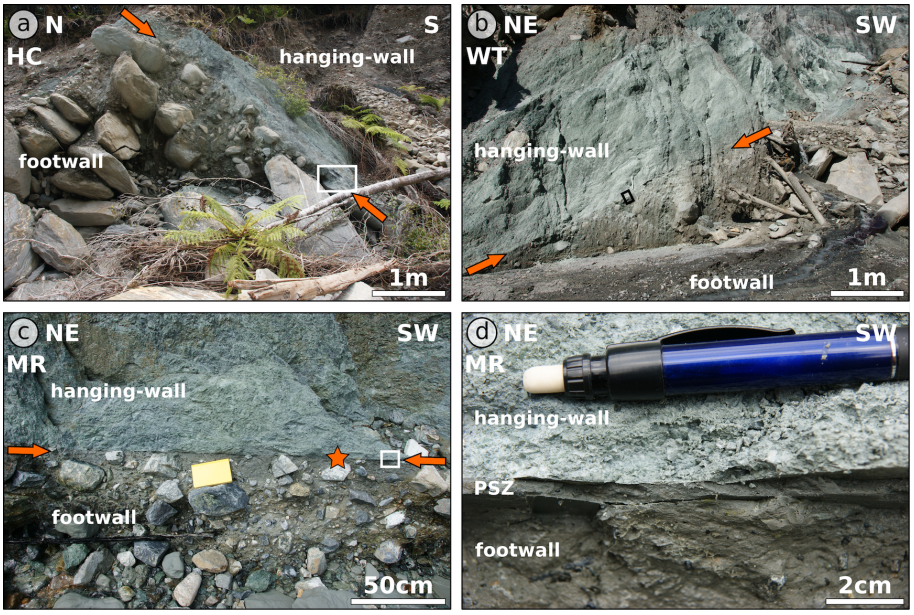

Figure 4. Outcrops of Alpine Fault zone rocks. **(a)** Whereas pale-green hanging-wall cataclasites and larger Quaternary footwall gravels are clearly identified at Havelock Creek, the contacts and hence thickness of the PSZ (indicated by arrows) to over- and underlying units, respectively, are only poorly constrained. White box indicates position of figure 5a. **(b)** The PSZ at Waikukupa Thrust as indicated by arrows is well-defined and straight. Black box gives location of sample presented in figure 5c. **(c)** At Martyr River, hanging- and footwall rocks are sharply separated by a well-defined PSZ (indicated by arrows). White box indicates position of (d). Star gives sample location for specimen shown in figure 5d. **(d)** The PSZ at Martyr River is between 1 and 2 cm thick. HC: Havelock Creek; WT: Waikukupa Thrust; MR: Martyr River.

typical matrix grain size is $\ll 1$ µm. The matrix is composed of abundant ~~, predominantly authigenic phyllosilicates - mostly chlorite - and~~ phyllosilicates of detrital (see section 4.3) and authigenic (e.g. Fig. 6a) origin and detrital particles, ~~mainly~~ mostly quartz and feldspar. The ~~detrital particles are of~~ latter are subangular to rounded in shape with elongate to moderate sphericity and commonly with edges that have been affected by dissolution and mineral alteration processes (Fig. 6a).

~~In contrast, the clasts that are~~ Clasts embedded in the fault rock matrix are predominantly comminuted quartz, feldspar and mica grains, as well as fragments of Alpine Schist and mylonite. In addition, there are two more groups of clasts. The first one comprises compact, almost pore-free, fine particles with distinct boundaries but similar composition compared to the surrounding matrix (Fig. 6b). This group of clasts is termed *matrix clasts* in the following. The second group comprises small areas, which are microstructurally similar to *matrix clasts*. These features are characterized by brighter grey-values in BSE-mode, and typically high porosities ~~allowing to distinguish them~~ so they are easy to differentiate from the surrounding material (Fig. 6c). EDX analyses demonstrate that they are compositionally identical to the surrounding matrix. ~~As a~~ Because comparison of optical and scanning electron microscopy images reveals that these structures ~~appear to be similar to~~ look like

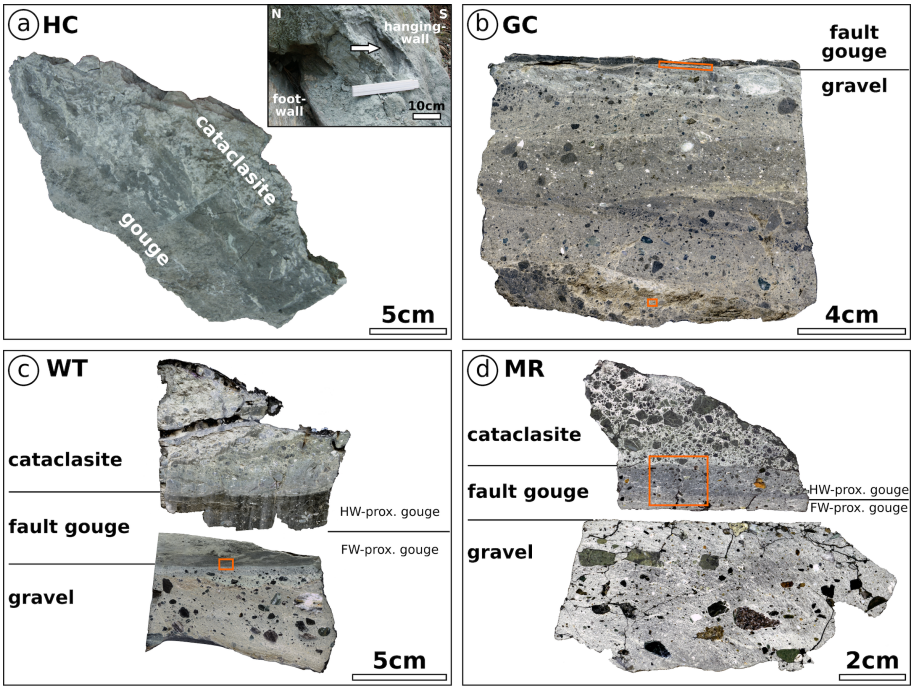

Figure 5. Investigated outcrop samples. **(a)** The contact between hanging-wall cataclasites and thick fault gouge at Havelock Creek is poorly developed and appears to be transitional over ~8 cm. Inset provides zoom to sample location (indicated by arrow). **(b)** Identifying the fault gouge in field at location Gaunt Creek turned out to be difficult. Consequently, only the lowermost part of the PSZ has been sampled. Contact between PSZ and footwall is sharp. Orange box at the contact indicates location of figures 7k-m; orange box at the bottom indicates location of figure 6d. **(c)** The thin fault gouge at Waikukupa Thrust consists of a hanging-wall-proximal and footwall-proximal layer. Orange box gives location of figure 7j. **(d)** The contacts of the thin PSZ with hanging- and footwall rocks, respectively, are sharp at Martyr River. Fault gouge consists of a hanging-wall-proximal and a footwall-proximal layer. Orange box gives location of figures 7a & b. HC: Havelock Creek; GC: Gaunt Creek; WT: Waikukupa Thrust; MR: Martyr River.

matrix clasts under plain polarized light (Figs. 6d & e), ~~they will be termed~~ we refer to them as *bright matrix clasts* in the following.

The distinct lithological and (micro-to-macro) structural characteristics of all units are described in detail in the following sections and summarized in Tables 1 (hanging-wall), 2 (PSZ) and 3 (footwall).

295 #### 4.2.1 Hanging-wall cataclasites

Clasts embedded in the fine-grained cataclasite matrix at DFDP-1A and Waikukupa Thrust are mostly quartz and feldspars~~with often~~, with commonly fractured, dissolved and altered edges (Fig. 6a). Furthermore, matrix clasts are encountered ~~within close distance~~ close to the contact with the PSZ (< 1.35 m at DFDP-1A and < 10 cm at Waikukupa Thrust, respectively). In contrast, quartz and feldspars only constitute ~5 % of clasts at Martyr River. There, most clasts ~~, green on outcrop- and~~

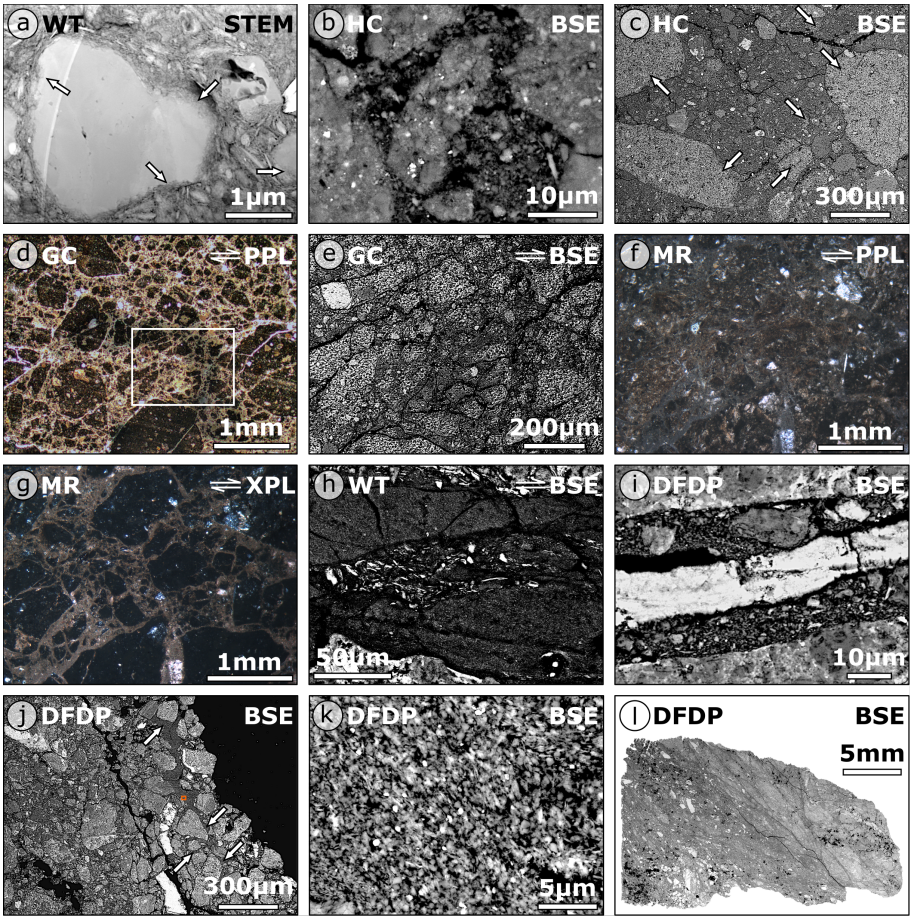

Figure 6. **(a)** Particles forming the fault rock matrix are defined to be smaller than 2 µm. Abundant authigenic phyllosilicates cement the matrix. Arrows indicate albite dissolution and alteration to phyllosilicates. **(b)** Matrix clasts, low-porosity, compact and clast-like areas of similar composition as the matrix, are embedded within the fault rock matrix at all outcrops. **(c)** Bright matrix clasts (arrows) surrounded by fine-grained matrix and some clasts. **(d)** Lens of matrix clasts within footwall gravels at Gaunt Creek (see figure 5b). White box indicates location of (e). **(e)** SEM analysis shows that clasts within a lens ~8-8.5 cm below the PSZ at Gaunt Creek are bright matrix clasts. **(f & g)** Corresponding PPL (f) and XPL (g) photomicrographs of hanging-wall clasts at Martyr River. Identification of constituting mineral phases – mostly quartz, feldspar, chlorite – is only possible by EDX analysis. **(h)** Mature microfault filled by fine-grained authigenic phyllosilicates with typical grain sizes < 2 µm and a core of coarser-grained material. **(i)** Microfault displaying a calcite vein within its core surrounded by fine-grained matrix and some larger clasts. **(j)** Locally, pores and cracks are cemented by fine-grained, authigenic phyllosilicates (arrows). Orange box indicates location of (k). **(k)** Matrix-cementing authigenic phyllosilicates are mostly flake- to needle-shaped chlorite crystallites.**(l)** Foliated cataclasite (top left to bottom right) sampled 25 cm above the PSZ. WT: Waikukupa Thrust; HC: Havelock Creek; GC: Gaunt Creek; MR: Martyr River; DFDP: Deep Fault Drilling Project core 1A; STEM: scanning transmission electron microscopy; BSE: backscatter electron microscopy; PPL: plane polarized light; XPL: cross-polarized light.

~~hand specimen-scale (Fig. 5d) but dark-brown to black on the optical microscale (Figs. 6f & g), are identified to be~~ are polymineralic aggregates consisting of quartz, feldspar, chlorite, rarely biotite and fragments of calcite veins ~~by EDX analyses. At all locations, there~~ (Figs. 6f & g). There are subordinately fragments of Alpine Schist (all locations) and mylonites (~~only~~ Waikukupa Thrust). At DFDP-1A and Waikukupa Thrust ~~they~~ these fragments display ~150 µm wide, gouge-filled microfaults (Table 1). At Waikukupa Thrust, there are also clay-clast aggregates (CCA; Boutareaud et al., 2008). ~~Amount and~~ At both thin section and outcrop scale, amount and size of clasts generally decrease towards the PSZ and both vary systematically with PSZ thickness ~~(Table 1)~~(Table 1; see also Boulton et al., 2012; Toy et al., 2015): locations with thinner PSZ contain more clasts in the hanging-wall, which tend to be larger, compared to locations with thicker PSZ.

Open cracks, typically several millimeters long and up to hundreds of micrometer wide, increase in abundance towards the PSZ at DFDP-1A and Waikukupa Thrust. Furthermore, microfaults (~5-130 µm ~~wide~~thick) cross-cut cataclasites at these locations. They contain comminuted particles and authigenic phyllosilicates and range in maturity: ~~whereas~~ mature microfaults display a well-developed fine-grained fault gouge with particles up to tens of micrometer in size but mostly smaller than 2 µm (Fig. 6h). In contrast, juvenile microfaults contain poorly sorted particles up to a few hundreds of micrometer in size with the majority being larger than 10 µm. In addition, some microfaults have cores made of coarser-grained matrix and clasts (Fig. 6h) or calcite veins (Fig. 6i) surrounded by fine-grained gouge.

Locally, there are patches almost completely devoid of clastic particles but with abundant authigenic flake- to needle-shaped chlorite crystals cementing pores and fractures at Waikukupa Thrust and DFDP-1A (Figs. 6j & k). The amount of these chlorite-dominated areas as well as authigenic phyllosilicates in general increases with decreasing distance to the PSZ and progressively cements the fault rocks. Furthermore, the matrix is cemented by calcite (Table 1). Whereas finely-dispersed calcite is abundant at Martyr River, calcite at Waikukupa Thrust is mostly present only in direct vicinity (< 3 cm) to the PSZ. There, mutually cross-cutting calcite veins (~15 µm thick) display small (< 20 µm) dextral offsets (see figure 3f in Schuck et al., 2018). Furthermore, there are < 100 µm large calcite-cemented breccias composed of angular fragments of clastic particles and *matrix clasts* (see figure 3c in Schuck et al., 2018). At DFDP-1A, calcite is encountered in lenses and veins, which frequently cross-cut clasts but rarely the matrix and generally increase in abundance towards the PSZ.

Locally, cataclasites are foliated. At DFDP-1A, clasts together with microfaults define a weak foliation (Fig. 6l) varying non-systematically across the investigated interval, locally displaying SC-geometry. At Waikukupa Thrust and close to the PSZ, cataclastic lenses exhibit a very weak foliation parallel to ~~displacement~~the shear plane.

4.2.2 Principal Slip Zone fault gouges

The type of contact between hanging-wall cataclasites and fault gouge ~~correlates~~ appears to correlate with PSZ thickness: where the PSZ is thicker, contacts are transitional manifested by decreasing grain sizes (Table 2)~~and correlate with increasing amounts of phyllosilicates~~, as exemplified at Havelock Creek with its transitional, poorly-developed contact over 8 cm (Fig. 5a). In contrast, Waikukupa Thrust has a sharp contact on the outcrop and hand-specimen scale (Figs. 4b & 5c), but displays a transition over 4 mm from a porous, clast-rich cataclasite-matrix to a very dense PSZ-matrix as revealed by microscopic

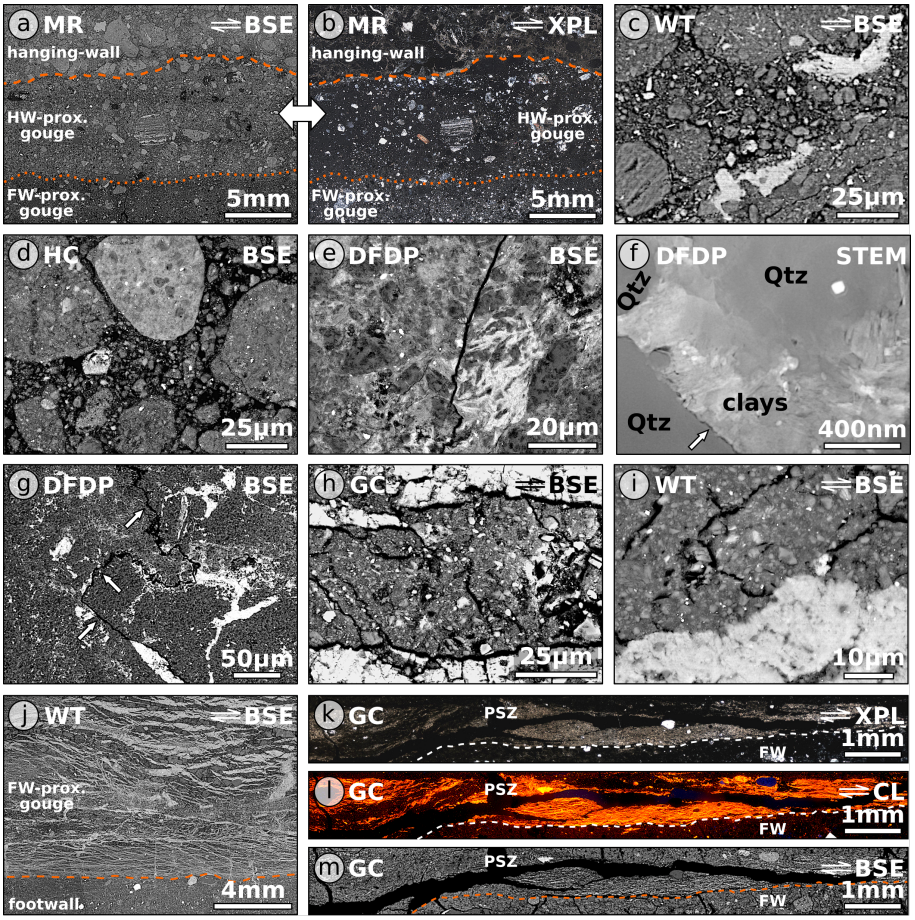

Figure 7. ~~**(a & b)** Corresponding~~ **(a)** BSE ~~(a)~~ and **(b)** XPL ~~(b)~~ photomicrographs of the fault core at Martyr River. Identification of the contact between hanging-wall and PSZ (stippled line) as well as hanging-wall and footwall-proximal gouge (dotted line), respectively, is difficult. **(c & d)** The hanging-wall proximal gouge at Waikukupa Thrust (c) with its large amount of matrix clasts is microstructurally similar to the PSZ at Havelock Creek (d). **(e)** Photomicrograph of typical microstructures of cemented PSZ at DFDP-1A core. **(f)** Cemented PSZ matrix of the DFDP-1A core. Pores between comminuted and dissolved (arrow) quartz grains are cemented by authigenic phyllosilicates, ~~mainly~~ mostly chlorite. **(g)** Slickolite (white arrows) indicative of pressure solution. **(h & i)** Fault gouge at Gaunt Creek (h) is microstructurally similar to footwall-proximal gouge at Waikukupa Thrust (i). **(j)** Network of anastomosing calcite veins within footwall-proximal gouge layer at Waikukupa Thrust. The contact between fault gouge and footwall (orange line) is sharp. **(k-m)** The basal part of the PSZ at Gaunt Creek hosts a network of calcite veins terminating at the sharp contact (white / orange stippled line) with the footwall (FW). MR: Martyr River; WT: Waikukupa Thrust; HC: Havelock Creek; DFDP: Deep Fault Drilling Project conA; GC: Gaunt Creek; BSE: backscatter electron microscopy; XPL: cross-polarized light; STEM: scanning transmission electron microscopy; CL: cathodoluminescence.

inspection (see figure 3a in Schuck et al., 2018). Identification of the sharp but undulating contact at Martyr River is simple ~~on~~ in outcrop- and hand-specimen (Figs. 4c, d & 5d), but difficult on microscale (Figs. 7a & b).

Matrix clasts are the prevailing type of clast at Waikukupa Thrust and Havelock Creek (Figs. 7c & d), but constitute less than 5 % of clasts at Martyr River. Furthermore, ~~unlike Martyr River~~ the phyllosilicate-cemented fault gouge at Martyr River hosts individual mineral phases, which is distinctly different from its hanging-wall, where large, fine-grained chloritized particles dominate ~~in the hanging-wall, the calcite-poor, phyllosilicate-cemented fault gouge at this location hosts individual mineral phases~~ (Fig. 7b). *Bright matrix clasts* are present at all locations, but are abundant only at Havelock Creek and Gaunt Creek, where they, in addition to clast-like shapes, occupy several hundreds of micrometer large areas. In general, amount and size of clasts weakly ~~correlates~~ correlate with PSZ thickness (Table 2). Where the PSZ is thinner, clasts tend to be more abundant and sizes tend to be larger. Clast sizes increase in the following order: Gaunt Creek (~75 µm), Havelock Creek (~75 µm), Waikukupa Thrust (~100 µm) and Martyr River (tens of micrometer to ~200 µm).

It is not possible to determine the amount and size of clasts within the DFDP-1A core, because more than 90 % of this unit is cemented by authigenic phyllosilicates, mostly chlorite (Figs. 7e & f). Authigenic phyllosilicates tend to nucleate along crack and grain boundaries of fractured grains. Additionally, newly formed phyllosilicates replace dissolved larger particles and mimic their original shape. Non-cemented areas are restricted to fractures. Many of these fractures contain up to 350 µm wide calcite cores, locally surrounded by gouge, microstructurally similar to microfaults observed within the DFDP-1A cataclasites (see Fig. 6i). ~~It is at these~~ These non-cemented, fracture-related locations ~~that there are~~ host patches of fine-grained, randomly oriented and needle-shaped, authigenic chlorite crystallites. The presence of these patches within the PSZ is restricted to DFDP-1A.

We only saw evidence of pressure solution at one location, DFDP-1A~~is the only location investigated, where there are indications of deformation by pressure-solution as evidenced by~~ , where there is a slickolite (Fig. 7g), a stylolite with teeth oblique to the stylolite surface (cf. Passchier and Trouw, 2005). However, enrichment of insoluble material or secondary phases along teeth-crowns is not observed.

PSZs at Waikukupa Thrust and Martyr River are layered and display a hanging-wall-proximal and a footwall-proximal layer, respectively (Figs. 5c & d). At Martyr River, the contact is best recognized on the hand-specimen scale (Figs. 4d, 5d, 7a & b), where the fault gouge is blueish-grey proximal to the hanging-wall and green-grey proximal to the footwall. Minor differences between both gouge layers are manifested by slightly more and larger clasts in the ~0.8-1 cm thick hanging-wall-proximal layer than the ~0.3-0.5 cm thick footwall-proximal layer (20-25 % vs. 25-30 %; Table 2).

At Waikukupa Thrust, a sharp but undulating contact separates a brown-dark grey hanging-wall-proximal layer with 5-10 % clasts from a medium-light grey footwall-proximal layer, which is clast-poor (< 1 % clasts; usually < 5 µm large).

The dense, clast-poor (< 1 % clasts) fault gouge at Gaunt Creek is microstructurally identical to the footwall-proximal layer at Waikukupa Thrust (Figs. 7h & i). Furthermore, both gouges exhibit calcite vein networks close to the contact with the footwall (Figs. 7j-m). At Waikukupa Thrust, veins display mutual cross-cutting relationships with dextral offsets. For a detailed description of these calcite veins, the reader is referred to the preceding work of Schuck et al. (2018). At Gaunt Creek, the 350-800 µm wide vein network (Figs. 7k-m) ~~is subject to~~ has been subsequently affected by intensive fracturing and calcite dissolution, which hampers the identification of cross-cutting relationships. Furthermore, the contact between calcite veins and

surrounding gouge is poorly-developed. Veins are typically 5-10 µm wide and tend to be thicker, less dissolved and deformed close to the footwall. CL colors are yellow-orange but slightly brighter and more yellow towards the footwall (Fig. 7l).

Apart from these vein networks, calcite veins cross-cut *matrix clasts* at Martyr River and the hanging-wall-proximal gouge layer of Waikukupa Thrust, but are very rare at Havelock Creek. Additional hanging-wall-proximal microstructures are clasts forming a weak foliation parallel to displacement at Martyr River and CCAs at Waikukupa Thrust. Furthermore, hanging-wall proximal microstructures at Waikukupa Thrust are similar to those of Havelock Creek (Figs. 7c & d), except that clasts are not ~~homogenously~~ homogeneously distributed but cluster randomly at Havelock Creek. Apart from the hanging-wall-proximal fault gouge layer of Waikukupa Thrust, where typical clast size decreases while the size of *matrix clasts* increases towards the footwall, trends regarding microstructures are not observed. Most remarkably, ~~there are no~~ discrete slip planes are not observed within the fault gouges.

4.2.3 Footwall gravels

~~The~~ Where sufficiently exposed, the contact between clast-poor PSZ and clast-bearing footwall is sharp (Figs. 4b-d; 5b & c; 7j–m). Footwall gravels are compositionally similar to overlying hanging-wall cataclasites and fault gouges (Table 3). Furthermore, the same correlations regarding amount and size of clasts ~~as~~ observed in hanging-wall cataclasites and fault gouges are ~~valid~~ seen within footwall gravels ~~, too~~ (Table 3): locations with thin PSZ tend to contain more and larger clasts than locations with thicker PSZ. In addition, grain size increases with increasing distance from the PSZ. Whereas there are some bright *matrix clasts* at Martyr River and Gaunt Creek, *matrix clasts* are only encountered at Gaunt Creek. At Martyr River, footwall clasts are slightly imbricated and have a weak foliation parallel to displacement.

Calcite is absent at Martyr River and restricted to a ~3 mm thick layer immediately adjacent to the PSZ at Waikukupa Thrust. There, calcite constitutes finely dispersed cement, veinlets and < 5 µm thick rims at grain edges parallel to displacement. In contrast, at Gaunt Creek, calcite is predominantly found in veins and lenses cross-cutting matrix and detrital clasts.

The ~1 cm thick, fine-grained, brown layer erroneously interpreted as PSZ at Gaunt Creek (Figs. 3d & e), is mainly composed of fractured, subangular to subrounded *matrix clasts* (Fig. 6d). The amount of quartzofeldspathic clasts within this lens is < 5 %. Fractures between the individual clasts are filled with a fine-grained matrix. SEM analysis reveals that these clasts are actually *bright matrix clasts* (Fig. 6e).

4.3 Mineralogy

There are only minor variations in qualitative fault rock composition (Table 4). Quartz, feldspar, calcite and phyllosilicates, (chlorite, kaolinite, muscovite, illite, and biotite) and traces of apatite, pyrite and rutile are always present. Additionally, Waikukupa Thrust and Havelock Creek contain amphiboles, mainly hornblende, and there is epidote at Waikukupa Thrust and Martyr River. Serpentine minerals are only encountered within the fault gouge at Martyr River. Analyzed fault rocks do not contain smectite, and kaolinite is present only in traces. Furthermore, polytype analysis demonstrates that illite identified by Rietveld refinement predominantly constitutes detrital but comminuted muscovite (see supplement).

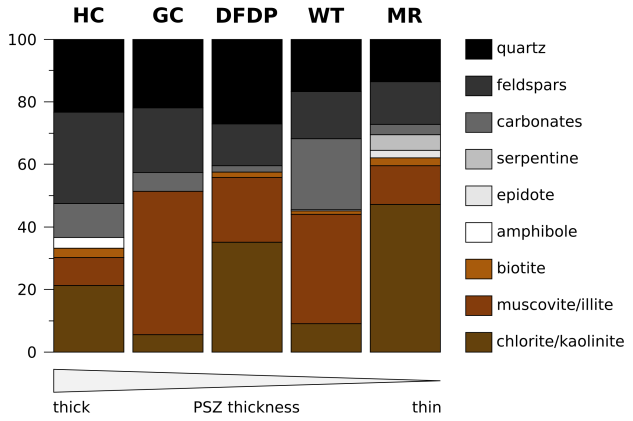

Figure 8. Simplified mineralogical composition of investigated PSZs based on results presented in Table 4. HC: Havelock Creek; GC: Gaunt Creek; DFDP: Deep Fault Drilling Project core 1A.; WT: Waikukupa Thrust; MR: Martyr River.

4.3.1 Hanging-wall cataclasites

Quartz and feldspars are the dominant mineral phases in hanging-wall cataclasites. They do not exhibit any clear trend towards the PSZ (Table 4). Phyllosilicates appear to decrease in content towards the PSZ. This probably is an artefact of Rietveld refinement based on the < 10 µm instead of the clay-size fraction. In the DFDP-1A drill core material, the concentrations of detrital muscovite/illite decrease towards the PSZ compared to authigenic chlorite/kaolinite~~showing~~, which show an opposite trend. Furthermore, calcite also increases towards the PSZ at DFDP-1A.

4.3.2 Principal Slip Zone fault gouges

Quartz and feldspar contents vary by more than 50 % between individual locations (21 wt% at Waikukupa Thrust vs. 52 wt% at Havelock Creek; Fig. 8; Table 4). In general, these clastic phases tend to be less abundant in thinner than in thicker PSZs (Fig. 8). Phyllosilicate concentrations exhibit the opposite pattern: thinner PSZs tend to be more phyllosilicate-rich than ticker PSZs. Furthermore, chlorite/kaolinite and muscovite/illte show inverse correlations but do not vary systematically with respect to PSZ thickness. Calcite concentrations of Waikukupa Thrust (29 %) and Gaunt Creek (6 %) reflect mineralization manifested in vein networks. As calcite veins are rare at Havelock Creek, the relatively high (11 %) concentrations potentially reflect calcite cementation. In contrast, calcite concentrations within PSZs of DFDP-1A and Martyr River are lower compared to the hanging-wall.

4.3.3 Footwall gravels

At Gaunt Creek, quartz and feldspar concentrations increase with increasing distance from the PSZ, whiile those of phyllosilicates decrease, and calcite concentrations remain constant (Table 4). Conversely, at Waikukupa Thrust, footwall concentrations of

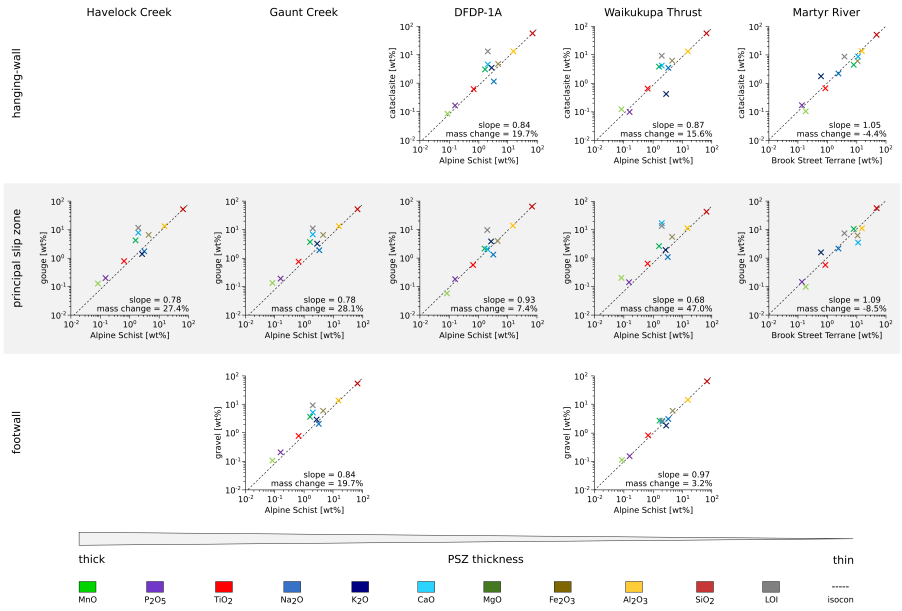

Figure 9. Isocon analysis of locations investigated. In case of multiple measurements per structural unit (hanging-wall, PSZ, footwall), data were averaged to derive single values. Values are given in Table S1.

clastic phases and calcite are comparable to those of the hanging-wall close to the contact with the PSZ, and phyllosilicates are slightly more abundant in the footwall compared to the hanging-wall adjacent to the PSZ. Compared to the PSZ, clastic phases are significantly more abundant and amounts of phyllosilicate are lower.

4.4 Geochemistry

Element concentrations commonly scatter and, if at all, increase or decrease only slightly towards the PSZs (Table 5). The isocon analysis reveals a slight but recognizable correlation between the amount of fluid-related alteration and PSZ thickness: using the slope of the isocon as a proxy to assess the overall degree of fluid-related alteration, with a larger deviation from one indicating a higher amount of alteration, the hanging- and footwalls of ~~sample locations with~~ locations characterized by thinner PSZ are generally less affected by metasomatism (Fig. 9; ~~Table 6; Tables S1 & S2~~Tables 6 & S1). The PSZs display the same trend, but less pronounced. This is especially valid for the PSZ at Waikukupa Thrust, which is affected by a fluid-related mass change of up to ~~79 %~~ 68 % (Table 6). However, microstructural observations (see section 4.2.2 and Schuck et al., 2018) ~~indicate~~ suggest this is most likely related to the extraordinarily large amount of calcite veins.

Enrichment of individual elements confirms this correlation: enrichment of Al_2O_3, CaO~~and LOI~~, LOI, MnO, P_2O_5 and TiO_2 in hanging- and footwall rocks is more pronounced at locations with thicker PSZ compared to those with thinner PSZ (Table 6; Table S2). Element enrichment of PSZ fault gouges exhibits a similar but less pronounced trend~~with CaO~~. Comparable to the

general pattern of isocon slopes described above, the PSZ at Waikukupa Thrust ~~being remarkably more enriched than expected due to formation~~ represents an outlier, because the large volume of calcite veins results in extraordinarily enriched CaO.

Looking at cross-fault transects, ~~the degree of metasomatism at~~ PSZs are more affected by metasomatism than hanging- and footwalls. Furthermore, footwalls are generally less affected by metasomatism than hanging-walls. However, DFDP-1A constitutes an exception, because the PSZ is less affected by metasomatism than the hanging-wall cataclasites: the degree of fluid-related alteration increases towards the PSZ and displays highest hanging-wall amounts immediately adjacent to ~~the PSZ~~ it (Table 6). ~~Furthermore, whereas the PSZ at DFDP-1A has been less affected by fluid-related alteration compared to the hanging-wall, samples of Waikukupa Thrust~~This contrasts with Waikukupa Thrust, where samples display a continuing trend to higher amounts of fluid-related alteration from the hanging-wall to the base of the PSZ close to the footwall.

~~Footwalls are generally less affected by metasomatism than hanging-walls and PSZs. Despite limited sample numbers, the degree of metasomatism at Gaunt Creek appears to decrease with increasing distance to the PSZ.~~

5 Discussion

5.1 Fluid-related alteration and fluid transport within Alpine Fault rocks

Isocon analyses clearly demonstrate that all investigated fault rocks have been substantially altered by fluids (Fig. 9; Table 6), which is also shown by the presence of authigenic phyllosilicates (Figs. 6a & k) and calcite vein networks ~~and authigenic phyllosilicates.~~ (Figs. 7j - m). In general, metasomatic alteration of the fault rocks resulted in element enrichment and mass gain, which is in agreement with previous work (Schuck et al., 2018). Analyses of Martyr River fault rocks seem to show an opposite pattern but this may be an artefact related to inappropriate choice of the protolith's geochemical composition (see section 3.3.1).

~~While the degree~~ It is recognized that the Alpine Fault's PSZ constitutes an impermeable barrier restricting fluid circulation to its hanging-wall (Sutherland et al., 2012; Menzies et al., 2016). Consequently, fluid-related element mobilization can be expected in the hanging-wall. This is confirmed by isocon analyses: DFDP-1A samples show increasing amounts of fluid-related alteration ~~correlates slightly with fault gouge thickness~~ towards the PSZ with peak-values immediately above it. However, at all other locations the fault gouges are more affected by fluid-related alteration than either hanging- or footwall rocks (Fig. 9~~; Table 6), it is correlated negatively with phyllosilicate content (Figs. 8 & 9). Furthermore, except~~). This suggest, in combination with networks of anastomosing calcite veins (Figs. 7j-m; Schuck et al., 2018), that there is repeated transient fluid-flow within the PSZ, most-likely along-fault, because the veins are parallel to the shear plane.

Overall, results of isocon analyses confirm outcomes of previous studies, which demonstrated that fluid-related alteration significantly changed the petrophysical, mineralogical, geochemical and geomechanical properties of the Alpine Fault zone (e.g. Boulton et al., 2012; Townend et al., 2013; Carpenter et al., 2014). This supports the proposal of Sutherland et al. (2012) that an 'alteration zone' within ~50 m of the PSZ should be included as a fundamental and additional part of the Alpine Fault zone architectural model (Fig. 2c).

Except for the slickolite observed in the DFDP-1A fault core (Fig. 7g), there is no unambiguous microstructural evidence for pressure-solution such as dissolution seams or indented and embayed clasts . Considering the large amounts of annual was not found. Annual rainfall along the NW edge of the Southern Alps , it is likely is very high (e.g. Norris and Cooper, 1997, and references therei , and we suggest the observed dissolution of grain edges is related to weathering rather than fault deformation processes.

In summary, both microstructures and the predominant enrichment of elements show that fluids are not responsible for stress-driven dissolution processes or for substantial mass transfer out of the fault zone. Except for Ca-enrichment due to formation of calcite networks at Gaunt Creek and Waikukupa ThrustHowever, given that amount of phyllosilicates and degree of fluid-related alteration are negatively correlated (Figs. 8 & 9), the results of this study do not identify alteration mechanisms that completely explain the observed element mobilization within the fault rocks. , except at Waikukupa Thrust and Gaunt Creek, where Ca-enrichment is associated with the formation of calcite networks (Figs. 7j - m).

It is recognized that the Alpine Fault's PSZ constitutes an impermeable barrier restricting fluid circulation to its hanging-wall (Sutherland et al., 2012; Menzies et al., 2016). Consequently, fluid-related element mobilization can be expected in the hanging-wall. This is confirmed by isocon analyses: DFDP-1A samples show increasing degrees of fluid-related alteration towards the PSZwith peak-values immediately above it

5.2 Influence of shallow-depth conditions on fault gouge structure

In the following, we consider to what extent the fault gouges formed at shallow-depths, thus do not provide information about deeper fault zone architecture.

Fault gouges at Waikukupa Thrust and Martyr River are layered. Continuous transects across the fault core would sample contacts of fault gouge with both hanging- and footwall rocks. Furthermore, they would allow microstructures to be described across the entire PSZ. However, all other locations display fault gouges more affected by fluid-related alteration than these continuous transects are only available from Waikukupa Thrust and Martyr River. Consequently, the absence of layered fault gouges at other locations seems to be more appropriately explained by a sampling bias than by fault gouge layers being site-specific features.

Cowan et al. (2003) analyzed low-angle detachment faults in the Death Valley. There, layered fault gouges, consisting of a hanging- and footwall rocks, respectively. In combination with networks of anastomosing calcite veins (Figs. 7j-m; Schuck et al., 2018) , this suggests that there is repeated transient fluid-flow within the PSZ, most-likely along-fault as indicated by veins oriented parallel to displacement.

Results of isocon analyses also confirm outcomes of previous studies, which demonstrated that a footwall-proximal layer, separate footwall cataclasites from weakly consolidated hanging-wall sediments. They compare the footwall-proximal gouge layer to the hanging-wall-proximal layer (i.e. the layer juxtaposed to the weakly consolidated sediments), finding the former is fine-grained, clast-poor and supposed to have accommodated most of the strain. Cowan et al. (2003) interpret the formation of these layered fault gouges to reflect changing p-T-conditions during exhumation, which in combination with fluid-related alteration significantly changed the petrophysical, mineralogical, geochemical and geomechanical properties of alteration, formed authigenic phyllosilicates within the PSZs before fault rocks were brought in contact with weakly consolidated hanging-wall

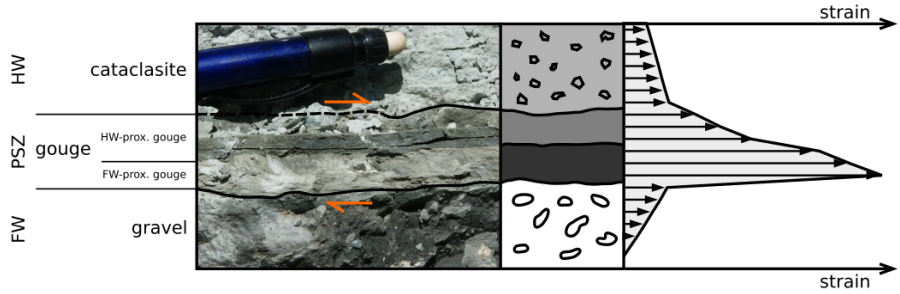

Figure 10. Conceptual model providing a potential explanation how layered principal slip zones observed at Martyr River and Waikukupa Thrust could have been formed. Resulting from the juxtaposition of weakly consolidated sediments in the footwall and relatively competent fault rocks, strain localized non-homogenously in the PSZ. The photographed example is from Waikukupa Thrust. Stippled line indicates where the contact between cataclasite and gouge is obscured by debris. Figure was modified from Cowan et al. (2003).

sediments. This juxtaposition resulted in mechanical layering enabling the hanging-wall-proximal layer to accommodate most of the strain.

By considering the different fault kinematics of the Alpine Fault compared to these faults in the Death Valley (thrust vs. low-angle detachment fault), the Alpine Fault with its layered gouges described in this and previous work (e.g. Boulton et al., 2012; Schuck is structurally identical to the faults analyzed in the Death Valley (Fig. 10; for details see Biegel and Sammis, 2004). Furthermore, studied fault gouges bound footwall-gravels, which are poorly consolidated and thus assumed to be mechanically weak. In addition, fault gouge layers juxtaposed on these weakly consolidated rocks (footwall-proximal layer at the Alpine Fault; hanging-wall-proximal layer in the Death Valley) are microstructurally comparable, as they contain fewer and preferentially smaller clasts than the other layers of the fault gouges (see also Table 2). Furthermore, microstructures of the calcite network in the footwall-proximal layer at Waikukupa Thrust suggest localized and cyclic faulting (Schuck et al., 2018) supporting the interpretation that this gouge unit accommodated most of the strain. Consequently, layered fault gouges and associated microstructures demonstrate that strain localization and associated structural complexities within the Alpine Fault core are, at least partially, affected by shallow, hence late, processes, considered that exhumation of investigated rocks to subaerial level is accommodated entirely by the Alpine Fault~~zone (e.g. Boulton et al., 2012; Townend et al., 2013; Carpenter et al., 2014). This supports the proposal of Sutherland et al. (2012) that an 'alteration zone' within ~50 m of~~'s PSZ (e.g. Little et al., 2005; Toy et al., 2015) .

This interpretation has major consequences for structural investigations of the Alpine Fault's PSZ, because it implies that formation of microstructures observed in outcrops was influenced by boundary conditions not representative of those along most of the fault rocks' exhumation path. This highlights the importance of continuing to attempt to obtain samples for microstructural investigations of Alpine Fault rocks from locations and / or depths where hanging-wall and PSZ fault rocks are not juxtaposed on weakly consolidated footwall sediments. Acknowledging that there is no outcrop where hard-rock hanging-wall is in contact with hard-rock footwall (Townend et al., 2009), drilling projects aiming to penetrate the ~~PSZ should~~

~~be included as a fundamental and additional part of the~~ Alpine Fault ~~zone architectural model (Fig. 2c).~~ at depths where Quaternary gravels do not constitute the footwall appear to be the only promising approach to achieve this end. This would also overcome the problem of data sparsity due to the limited amount of outcrops. This would improve the robustness of results.

5.3 Architecture of Alpine Fault zone

5.3.1 Alpine Fault damage zone

Norris and Cooper (2007) suggested an average brittle damage zone width of ~100 m, which is based on a compilation of outcrop studies in the fault's central segment~~of ~100 m~~. More recent investigations indicate wider damage zones: Alpine Fault outcrops in the segment south of Haast have damage zone widths between 90 and 240 m (Barth et al., 2013). Analyses of downhole geophysical data and recovered cores from the DFDP-2 borehole indicate that the Alpine Fault's hydrologically active damage zone ~~, where fluids circulate in fractures that are more common than in the surrounding rock mass,~~ contains an 'inner zone' affected by earthquake rupture processes that is 0.5 km wide at up to 8 km depth and about 1 km wide at the surface (Fig. 2c). This inner damage zone is surrounded by an up to a few kilometers wide 'outer zone', which might be a near-surface, topographically-controlled feature only (Townend et al., 2017; Massiot et al., 2018; Williams et al., 2018).

Outcrop and drillcore investigations demonstrate quite constant fracture densities within at least 500 m of the PSZ in the hanging-wall and 30 m in the footwall (Williams et al., 2016, 2018), which is different to decreasing fracture densities towards the fault cores observed elsewhere (e.g. Chester et al., 2005; Faulkner et al., 2006; Mitchel and Faulkner, 2009). In fact, DFDP investigations show that apparent fracture density decreases with depth, i.e. towards the PSZ (Townend et al., 2013; Williams et al., 2016). However, this is considered as an artefact resulting from rapid exhumation and associated unloading (Williams et al., 2016). Furthermore, despite its presence across the entire damage zone, gouge-filled fractures within < 160 m of the PSZ tend to be thinner (< 1 cm) and more abundant (Williams et al., 2018).

5.3.2 Alpine Fault core

Extent of fault core

As a result of the pervasive alteration zone surrounding the PSZ, the fault core of the Alpine Fault is rather diffuse (Sutherland et al., 2012; Townend et al., 2013; Williams et al., 2018). Commonly, the fault gouge forming the PSZ and part of the surrounding cataclasites are considered to constitute the fault core (e.g. Williams et al., 2017). However, there is some ambiguity when it comes to actually defining the width of the fault core: Toy et al. (2015) consider a 20-30 m wide zone around the PSZ as fault core, Sutherland et al. (2012) and Townend et al. (2017) narrow it down to 2 m surrounding the PSZ with an additional degree of localization manifested in the < 0.5 m wide PSZ (Sutherland et al., 2012; Williams et al., 2016). However, by defining the damage zone as having elevated fracture densities compared to the host rock (Chester et al., 1993; Faulkner et al., 2010) and noting that there is no observable variation in fracture density within 30 m of the PSZ (Williams et al., 2016), it seems

reasonable to exclusively consider the fault gouge forming the PSZ as core of the Alpine Fault's central segment. This view is supported by fault gouge microstructures: microfaults (Figs. 6h & i), predominantly encountered in hanging-wall cataclasites but also present in fault gouges (Table 3), show that strain is localized to discrete structures within the PSZ. Furthermore, ~~these structures~~ the fault breccias encountered in these microfaults exhibit a broad range in degree of sorting (poorly – very well) and grain size (< 2-100s of micrometer), which demonstrates that they accommodated different amounts of strain. However, microfaults appear to be a local phenomenon and there are no continuous, discrete slip planes within the PSZ, despite the large finite displacement accommodated.

This interpretation is further backed by distinct geophysical (e.g. Townend et al., 2013), petrophysical (e.g. Carpenter et al., 2014), mineralogical (e.g. Schleicher et al., 2015), microstructural (e.g. Toy et al., 2015) and geochemical (Schuck et al., 2018) properties of the PSZ. To the SW of the study area, the fault core might be more complex, because of its different lithological composition and fault orientation (Barth et al., 2013).

~~Fault-core~~ Implications of fault-core along-strike variations for fault zone architecture

~~Despite mostly comparable~~ Investigated fault rocks are mostly comparable in terms of microstructures and mineralogy ~~of investigated fault rocks~~ (Tables 1-4)~~, there are complex along-strike variations of fault gouge properties. In the following, we relate the results of our microstructural and geochemical investigation to the geometry of the Alpine Fault zone and its spatial variations. Furthermore, we examine whether the fault core structures result from shallow-depth phenomena, thus do not provide information about deeper fault zone architecture.~~

~~Fault gouges at Waikukupa Thrust and Martyr River are layered. However, continuous transects across the fault core, which sample contacts of fault gouge with hanging- as well as footwall rocks respectively, and which allow microstructures to be described across the entire PSZ, are only available from these two outcrops. Consequently, the absence of layered fault gouges at other locations seems to be more appropriately explained by a sampling bias than by fault gouge layers being site-specific features.~~

~~Cowan et al. (2003) analyzed low-angle detachment faults in the Death Valley, where layered fault gouges separate footwall cataclasites from weakly consolidated hanging-wall sediments. Compared to the footwall-proximal gouge layer, the hanging-wall-proximal layer is fine-grained~~. However, ~~clast-poor and supposed to have accommodated most of the strain. Changing boundary conditions during exhumation, namely decreasing temperature and pressure, as well as fluid-related alteration leading to the formation of authigenic phyllosilicates and juxtaposition of fault rocks with hanging-wall sediments resulted in mechanical layering enabling the hanging-wall-proximal layer to accommodate most of the strain.~~ individual outcrops display distinct differences, which will be discussed in context of the Alpine Fault Zone's architecture in the following.

~~By considering the different fault kinematics (low-angle detachment vs. thrust fault), the Alpine Fault with its layered gouges described in this and previous work (e.g. Boulton et al., 2012; Schuck et al., 2018) is structurally identical to the faults analyzed in the Death Valley (Fig. 10; for details see Biegel and Sammis, 2004). The footwall-proximal layer of Alpine Fault gouge contains fewer and preferentially smaller clasts than the overlying hanging-wall-proximal layer (Table 2) and bounds mechanically weak gravels. Furthermore, microstructures of the calcite network in the footwall-proximal layer at Waikukupa~~

~~Thrust attest to localized and cyclic faulting (Schuck et al., 2018) supporting the interpretation that this gouge unit accommodated most of the strain. Consequently, layered fault gouges and associated microstructural evidence demonstrate that strain localization and associated structural complexities within the Alpine Fault core are, at least partially, affected by shallow, hence late, processes.~~

~~Conceptual model providing a potential explanation how layered principal slip zones observed at Martyr River and Waikukupa Thrust could have been formed. Resulting from the juxtaposition of weakly consolidated sediments in the footwall and relatively competent fault rocks, strain localized non-homogenously in the PSZ. Example is from Waikukupa Thrust. Stippled line indicates where contact between cataclasite and gouge is obscured by debris. Figure was modified according to Cowan et al. (2003)~~ ~~.~~

~~This interpretation has major consequences for structural investigations of the Alpine Fault's PSZ, because it implies that formation of microstructures observed in outcrops was influenced by boundary conditions not representative of those along most of the fault rocks' exhumation path. This highlights the importance of continuing to attempt to obtain samples for microstructural investigations of Alpine Fault rocks from locations and / or depths, where hanging-wall and PSZ fault rocks are not juxtaposed on weakly consolidated footwall sediments.~~

The most remarkable difference between individual locations is the variation in PSZ thickness by a factor of of 25 (2 cm at Martyr River vs. 50 cm at Havelock Creek; Figs. 3-5). ~~Furthermore, locations with thicker PSZ tend to have poorly defined contacts with hanging- and footwall respectively, than locations with thinner PSZ (Table 2)~~Similar along-strike variations of PSZ thickness have been reported previously from other faults (e.g. Sagy and Brodsky, 2009; Kirkpatrick et al., 2018). It has been suggested that such variations may ~~result from different~~ be a result of the active mechanisms of deformation ~~(Hobbs et al., 1990; Schrank et al., 2008)~~(Hobbs et al., 1990; Schrank et al., 2008; Sagy and Brodsky, 2009), or initial presence of heterogeneities subsequently amplified during continuous deformation (Segall and Pollard, 1983; Schrank et al., 2008; Norris and Toy, 2014; Fossen and Cavalcante, 2017). Common examples are variations in mechanical strength reflecting differing viscosities as result of compositional heterogeneities (Chester et al., 1993; Faulkner et al., 2003; Schrank et al., 2008; Rybacki et al., 2014; Nardini et al., 2018), varying geometric properties (Cowan et al., 2003; Schrank et al., 2008) or a combination of ~~all or some of~~ these factors (Schrank et al., 2008; Boese et al., 2012; Czaplinska et al., 2015).

~~These~~ As will be elaborated in the following, these explanations do not appear to be responsible for observed variations~~as there is no correlation between PSZ thickness and sample location~~. PSZ thickness does not vary systematically along-strike in the sampled locations (Fig. 2b). Furthermore, all locations, except Martyr River, are in the central segment of the Alpine Fault where Torlesse Terrane Alpine Schist is the protolith. This demonstrates that variations of protolith mineralogy have no significant influence on observed differences in PSZ thickness. However, fault gouge thickness correlates with mineralogy: thicker gouges at Havelock Creek, Gaunt Creek and the DFDP-1A core are richer in clastic phases and poorer in phyllosilicates than the thin gouges of Martyr River and Waikukupa Thrust (Fig. 8). This is astonishing, because elsewhere phyllosilicate-rich fault gouges generally tend to be wider ~~(Faulkner et al., 2003; ?) owing~~ (Faulkner et al., 2003) owing to the frictionally weak nature of these phases (Moore et al., 1997; Moore and Lockner, 2007; Lockner et al., 2011; Carpenter et al., 2015). ~~Furthermore, the very narrow fault gouge at Martyr River contains frictionally extraordinary weak serpentine phases which elsewhere have~~

~~typically dominated in fairly thick fault zones (Moore et al., 1997; ?; ?). Conversely,~~ Conversely, other fault zones with ~~similar quartzofeldspathic composition to~~ quartzofeldspathic compositions like the Alpine Fault ~~are typically narrower~~ have been found to be fairly narrow (Chester et al., 1993; Faulkner et al., 2003). Consequently, unlike ~~other fault zonesworldwide~~these fault zones, the Alpine Fault displays a negative correlation between phyllosilicate content and fault core thickness. This suggests that strain localization within the fault core might be governed by processes insensitive ~~of~~ to rheological variations caused by differing fault rock composition~~.~~

, although observed slight microstructural differences such as grains size (see also Table 1-3) could influence localization. However, data are too scarce to derive robust conclusions. In addition, orientation of the fault (Figs. 2a & b), magnitude of stress and the stress field itself (Boese et al., 2012; Warren-Smith et al., 2017) are fairly constant along the central segment of the Alpine Fault, thus it is ~~unlikely~~ less likely that these parameters are responsible for observed variations of fault gouge thickness. However, it is still possible that the extreme variations in topography typical of the Alpine Fault hanging-wall generated quite different stress fields at our investigated sites (c.f. Upton et al., 2017). Biegel and Sammis (2004) suggested to ~~explain~~ along-strike variations of gouge thickness ~~as record of~~ record rupture arrest. However, our observations (and the nature of Alpine Fault outcrops in general) do not easily lend themselves to a systematic analysis of this kind in the Alpine Fault zone.

Another approach to explain observed thickness variations is to examine the relation between fault core width and displacement. Wear models based on empirical observations describe a positive correlation between gouge thickness and displacement (e.g. Hull, 1988; Scholz, 1987). However, quantitative models of fault core evolution have so far failed to reproduce datasets compiled on natural faults (e.g. Blenkinsop, 1989; Evans, 1990; Sibson, 2003). Nevertheless, faults that accommodated larger displacements do appear to generally have thicker fault cores ~~(Evans, 1990; Faulkner et al., 2010; Ben-Zion and Sammis, 2003, and referen~~ (Evans, 1990; Ben-Zion and Sammis, 2003; Sagy and Brodsky, 2009; Faulkner et al., 2010, and references therein). In other words: the more earthquakes a fault has seen, the thicker its PSZ may be (Ma et al., 2006; Li et al., 2013). ~~However, by keeping in mind that four~~ Four of the five fault gouges investigated are located in the Alpine Fault's central segment, which is considered to rupture entirely during an earthquake (Sutherland et al., 2007; Howarth et al., 2018) ~~, and in absence of other processes considered likely, PSZ thickness variations suggest that~~ and to have done so for at least the last ~8000 years (Berryman et al., 2012). If we employ the simple relationship that shear strain in a fault zone is equal to zone width multiplied by boundary displacement, and assume constant strain distribution within the PSZ gouges, the PSZ thickness variations we describe suggest the studied fault gouges accommodated different amounts of ~~displacement. This implies the~~ coseismic displacement.

Other examples where PSZ thickness varies by one order of magnitude within tens of meters along strike are not comparable to the Alpine Fault, because these faults accommodated substantially less displacement than the Alpine Fault: Shervais and Kirkpatrick (201 and Kirkpatrick et al. (2018) investigate a fault which accommodated displacement of the order of 10 - 30 km. The fault core contains at least 13 individual slip layers, suggesting that slip accommodated by these individual slip layers is most likely substantially smaller than the overall fault displacement. Consequently, observed PSZ thickness variations potentially reflect fault roughness, which is supposed to smooth as displacement increases (Sagy and Brodsky, 2009; Brodsky et al., 2011). In contrast, the Alpine Fault not only accommodated at least 470 km displacement (Sutherland et al., 2007), its fault gouge also

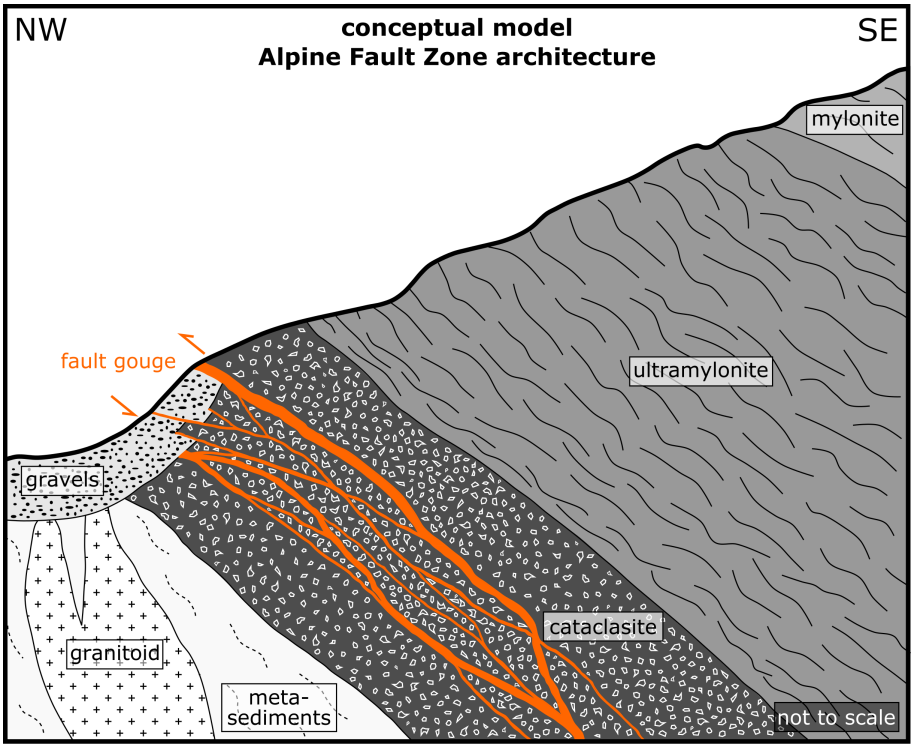

Figure 11. Proposed conceptual model of the Alpine Fault Zone architecture. Multiple fault strands, with gouge thicknesses varying between a few centimeters and several tens of centimeters, accommodate displacement. Different fault gouge thicknesses represent different amounts of displacement accommodated by individual fault strands. This demonstrates the difficulty to identify the fault strand active during the last event.

does not display discrete slip planes (see section 4.2.2). Furthermore, contacts between between fault gouge and hanging- and footwall, respectively, are - where sufficiently exposed - smooth (Figs. 4b-d & 5b-d).

Consequently, Alpine Fault PSZ thickness variations reflecting different amounts of displacement imply that the studied PSZs are not part of the same shear plane, and that the Alpine Fault zone hosts multiple fault strands, which may not be active simultaneously ~~during the same events (Fig~~(Figs. 1b ~~).~~ & 11). Figure 11 demonstrates how difficult it will be to identify the fault strand active during the most recent event.

Further evidence for a more complex Alpine Fault Zone architecture

This assumption of a more complex Alpine Fault zone geometry is further supported by microstructural, mineralogical and geophysical observations to be discussed in the following. Most obviously, ~~the two PSZs encountered in the DFDP-1B core (Fig. 3a; Toy et al., 2015)~~ DFDP results promote a more complex view of the fault zone architecture ~~.~~ of the Alpine Fault: DFDP-1B is the only location in the fault's central segment where there are two PSZs, both bound by brittle fault rocks

(Fig. 3a; Sutherland et al., 2012; Toy et al., 2015) . This is substantially different from other locations at the Alpine Fault, where multiple fault strands have been identified in poorly-consolidated, several tens to a few hundred meters thick Quaternary sediments covering hanging- and footwall (Kaiser et al., 2009; Carpentier et al., 2012). The presence of these two PSZs in DFDP-1B could reflect that displacement was accommodated by more than one PSZ, which is dissimilar to the paradigm of uplift along a single fault plane (e.g. Little et al., 2005; Toy et al., 2015), and / or that one PSZ was abandoned and displacement transferred to another PSZ. Fault gouge dating could help answer this question, but is beyond the scope of this paper.

Furthermore, although the shallower DFDP-1B PSZ and the PSZ of DFDP-1A have so far been ~~considered~~ assumed to belong to the same fault plane (Fig. 3a), they exhibit different mineralogical and hence geomechanical properties (Boulton et al., 2014; Schleicher et al., 2015). This is unexpected given the ~~small separation between~~ close proximity of the boreholes and thus sample spacing of less than 100 m (Sutherland et al., 2012)~~.~~, because the distinct mineral compositions of these two PSZs represent high (DFDP-1A) and low (DFDP-1B) temperature alteration, respectively. Considering the proximity of the two drillsites, the distinct mineralogies reflecting different temperatures - hence depths - of formation appear to go beyond what one would expect as common along-strike variation observed in the field. Similarly, although mineralogically comparable (Fig. 8), fault gouge microstructures of DFDP-1A and Gaunt Creek, also within only ~100 m distance (Fig. 3a), differ remarkably, as exemplified by the almost completely cemented DFDP-1A PSZ compared to the PSZ at Gaunt Creek (Table 2; Figs. 7e, f, k-m).

In light of this interpretation, the ~1 cm thick, *matrix clast*-bearing layer sampled ~8 cm below the PSZ at Gaunt Creek (Figs. 3d, e, 5b & 6d), which is microstructurally similar to the investigated fault gouges at Havelock Creek and Waikukupa Thrust (hanging-wall-proximal layer), could be considered to constitute another PSZ of the Alpine Fault, currently starting to accommodate larger amounts of slip, or an inactive one as observed in the fault's southern segment (Barth et al., 2013).

~~Consequently, this multidisciplinary approach~~ Geometric and spatial relationships, mineralogical composition and geomechanical properties of the various (potential) PSZs at Gaunt Creek / DFDP-1 (Fig. 3a) support our hypothesis that displacement along the Alpine Fault is accommodated by more than one PSZ.

The Alpine Fault's more complex geometry: a shallow-depth phenomenon?

The multidisciplinary approach presented here reveals that the Alpine Fault zone has a complex geometry (see Fig. 1b), which is ~~atypical for~~ different from other quartzofeldspathic faults but typical for carbonate or phyllosilicate-hosted ones ~~.~~ ~~Nonetheless~~(Faulkner et al., 2003).However, it cannot be excluded that the observations we present in favor of a more complex fault zone geometry simply reflect shallow-depth phenomena like layered fault gouges do. ~~However, seismic investigations that extend into the basement~~ Active seismic source investigations at the DFDP-2 site and around Haast also support a more complex fault zone model. These studies imaged a series of subparallel reflectors, interpreted as multiple fault strands (Lay et al., 2016; Lukács et al., 2018)~~.~~, which are comparable to those hosted by the Quaternary sediments covering hanging- and footwall (Kaiser et al., 2009; Carpentier et al., 2012). There are also indications that these fault strands at the DFDP-2 site and around Haast extend into the basement. So far, it is debated if these separate fault strands are isolated or anastomosing and if they are/were active contemporaneously or consecutively (Lukács et al., 2018). Note that this structural complexity differs

from the situation encountered at Waikukupa Thrust, as the second fault strand encountered at Hare Mare Creek, 700 m to the NE of this location, resulted from incision of the Waikukupa River and subsequent stress reorientation (Norris and Cooper, 1997).

6 Conclusions

~~Rheological~~ Layered fault gouges reflect a structural complexity of the Alpine Fault's PSZ, which originates from shallow-depth processes. At depths where Quaternary gravels comprise the footwall, rheological contrasts resulting from the juxtaposition of these poorly consolidated and mechanically weak footwall sediments with more competent hanging-wall cataclasites control ~~strain localization~~ the distribution of strain within the fault gouge and result in ~~a~~ the layered structure at shallow depths. ~~The possibility that topography also influences gouge thickness at shallow depth should be considered based on further work combining field, laboratory and geomorphologic investigations~~Consequently, rheological interpretations based on these rocks are biased as their microstructures mostly record modifications in just the latest part of the exhumation trajectory. These results also show that careful analyses are necessary in order to study actively ~~exhumed fault zones as microstructures may rather record shallow-depth artefacts than deformation history~~exhuming fault zones and that samples should be taken at greater depths to fully investigate these kinds of faults.

~~Field and borehole observations supported by microstructural, mineralogical and geochemical analyses provide evidence that~~ Variations of PSZ fault gouge thickness between individual study sites suggest that fault rocks at these locations accommodated different amounts of displacement. Assuming that the Alpine Fault~~zone is more complex than suggested by previous field investigations, which were hampered by the dense vegetation of the study area. These results highlight that the fault has a very variable character at different locations, and that this character is demonstrably not systematically controlled by the protolith lithology. Interestingly, PSZ width is not only unaffected by mineralogical composition but also correlates negatively with phyllosilicate content, which is different from other fault zones around the world where phyllosilicate-rich faults tend to be less localized.~~'s central segment, where most of the sites are located, is activated entirely during an earthquake, these thickness variations suggest that investigated PSZs are not located on the same fault plane. This implies that multiple fault strands accommodate Alpine Fault displacement. These findings, which are based on field and microstructural analyses, are further supported by the results of the Deep Fault Drilling Project and geophyiscal investigations.

Consequently, ~~these combined microstructural, mineralogical and geochemical analyses, considered in context of other studies,~~ these results show the Alpine Fault zone architecture is more appropriately described by the broad and complex conceptual model of Faulkner et al. (2003) rather than the simple, single PSZ model of Caine et al. (1996). ~~This suggests that investigated fault gouges are not part of the same fault plane but represent distinct slip planes within a complex network of anastomosing shear planes forming the core of the Alpine Fault, surrounded by a broader damage zone. As other commonly invoked approaches, such as compositional heterogeneities, do not explain observed differences, varying fault gouges thicknesses demonstrate that individual slip planes accommodated different amounts of displacement, hence strain. Dating encountered fault gouges would allow assessment of whether multiple slip zones are active contemporaneously.~~

Data availability. Underlying diffractograms and supporting data of isocon analysis for this paper can be found in the Supplement.

Author contributions. BS, CJ and VT conducted field work and obtained the samples. Microstructures were analysed by BS. BS and AS performed XRD and XRF analyses. All authors contributed to manuscript preparation but BS had primary responsibility.

Competing interests. The authors declare that they have no conflict of interest.

Acknowledgements. We thank Stefan Gehrmann for the preparation of thin sections as well as Hartmut Liep and Marina Ospald for preparing powder samples. We would also like to thank Lina Harfenmeister and Andrea Gotsche for help with XRF and Marie Bonitz for assistance with XRD analyses. Anja Schreiber and Richard Wirth are acknowledged for TEM-foil preparation and TEM analysis, respectively. Uwe Wollenberg (EMR Group, Geological Institute, RWTH Aachen University) enabled access to and provided help with CL analyses. We are grateful to Christoph Schrank and an anonymous reviewer who stimulated fruitful discussions that helped to substantially improve the manuscript. This project was funded by ~~DFD~~ grant JA 573/8-2 of the German Research Foundation (DFG). Furthermore, we acknowledge support by the Royal Society of New Zealand Rutherford Discovery Fellowship (RDF) 16-UOO-1602.

References

Aksu, A., Calon, T., and Hiscott, R.: Anatomy of the North Anatolian Fault Zone in the Marmara Sea, Western Turkey: Extensional basins above a continental transform, GSA Today, 6, 3 – 7, 2000.

Anders, M. and Wiltschko, D.: Microfracturing, paleostress and the growth of faults, Journal of Structural Geology, 16, 795 – 815, 1994.

Antonellini, M. and Aydin, A.: Effect of faulting on fluid flow in porous sandstones: Petrophysical properties, AAPG Bulletin, 78, 355 – 377, 1994.

Barth, N., Toy, V., Langridge, R., and Norris, R.: Scale dependence of oblique plate-boundary partitioning: New insights from LiDAR, central Alpine Fault, New Zealand, Lithosphere, 4, 435 – 448, https://doi.org/10.1130/L201.1, 2012.

Barth, N., Boulton, C., Carpenter, B., Batt, G., and Toy, V.: Slip localization on the southern Alpine Fault, New Zealand, Tectonics, 32, 620 – 640, https://doi.org/10.1002/tect.20041, 2013.

Beavan, J., Ellis, S., Wallace, L., and Denys, P.: Kinematic constraints from GPS on oblique convergence of the Pacific and Australian plates, central South Island, New Zealand, In: Okaya, D., Stern, T.A. and Davey, F. (eds.): A continental plate boundary: Tectonics at South Island, New Zealand. AGU Geophysical Monograph, 175, 75 – 94, 2007.

Ben-Zion, Y.: Collective behavior of earthquakes and faults: Continuum-discrete transitions, progressive evolutionary changes, and different dynamic regimes, Reviews of Geophysics, 46, https://doi.org/10.1029/2008RG000260, 2008.

Ben-Zion, Y. and Sammis, C.: Characterization of fault zones, Pure and Applied Geophysics, 160, 677 – 715, 2003.

Berryman, K., Cochran, U., Clark, K., Biasi, G., Langridge, R., and Villamor, P.: Major Earthquakes Occur Regularly on an Isolated Plate Boundary Fault, Science, 336, 1690 – 1693, 2012.

Biegel, R. and Sammis, C.: Relating fault mechanics to fault zone structures, Advances in Geophysics, 47, 65 – 111, 2004.

Blenkinsop, T.: Thickness-displacement relationships for deformation zones: Discussion, Journal of Structural Geology, 11, 1051 – 1054, 1989.

Boese, C., Townend, J., Smith, E., and Stern, T.: Microseismicity and stress in the vicinity of the Alpine Fault, central southern Alps, New Zealand, Journal of Geophysical Research, 117, https://doi.org/10.1029/2011JB008460, 2012.

Bohnhoff, M., Martínez-Garzón, P., Bulut, F., Stierle, E., and Ben-Zion, Y.: Maximum earthquake magnitudes along different sections of the North Anatolian Fault Zone, Tectonophysics, 674, 147 – 165, https://doi.org/10.1016/j.tecto.2016.02.028, 2016.

Boulton, C., Carpenter, B., Toy, V., and Marone, C.: Physical properties of surface outcrop cataclastic fault rocks, Alpine Fault, New Zealand, Geochemistry, Geophysics, Geosystems, 13, 238 – 265, https://doi.org/10.1029/2011GC003872, 2012.

Boulton, C., Moore, D., Lockner, D., Toy, V., Townend, J., and Sutherland, R.: Frictional properties of exhumed fault gouges in DFDP-1 cores, Alpine Fault, Geophysical Research Letters, 41, 356 – 362, https://doi.org/10.1002/2013GL058236, 2014.

Boutareaud, S., Calugaru, D.-G., Han, R., Fabbri, O., Mizoguchi, K., Tsutsumi, A., and Shimamoto, T.: Clay-clast aggregates: a new textural evidence for seismic fault sliding?, Geophysical Research Letters, 35, https://doi.org/10.1029/2007GL032554, 2008.

Brodsky, E., Gilchrist, J., Sagy, A., and Collettini, C.: Fault smooth gradually as a function of fault slip, Earth and Planetary Science Letters, 302, 185 – 193, 2011.

Bruhn, R., Parry, W., Yonkee, W., and Thompson, T.: Fracturing and hydrothermal alteration in normal fault zones, Pure and Applied Geophysics, 142, 609 – 644, 1994.

Bürgman, R. and Dresen, G.: Rheology of the lower crust and upper mantle: Evidence from rock mechanics, geodesy and field observations, Annual Reviews of Earth and Planetary Sciences, 36, 531 – 567, https://doi.org/10.1146/annurev.earth.36.031207.124326, 2008.

Caine, J., Evans, J., and Forster, C.: Fault zone architecture and permeability structure, Geology, 24, 1025 – 1028, 1996.

Carpenter, B., Kitajima, H., Sutherland, R., Townend, J., Toy, V., and Saffer, D.: Hydraulic and acoustic properties of the active Alpine Fault, New Zealand: Laboratory measurements on DFDP-1 drill core, Earth and Planetary Science Letters, 390, 45 – 51, https://doi.org/10.1016/j.epsl.2013.12.023, 2014.

Carpenter, B., Saffer, D., and Marone, C.: Composition, alteration, and texture of fault-related rocks from SAFOD core and surface outcrop analogs: evidence for deformation processes and fluid-rock interaction, Pure and Applied Geophysics, 172, 5273 – 5289, https://doi.org/10.1002/ 2015JB011963, 2015.

Carpentier, S., Green, A., Langridge, R., Boschetti, S., Doetsch, J., Abächerli, A., Horstmeyer, H., and Finnemore: Flower structures and Riedel shears at a step over zone along the Alpine Fault (New Zealand) inferred from 2D and 3D GPR images, Journal of Geophysical Research, 117, https://doi.org/10.1029/2011JB008749, 2012.

Chester, F. and Logan, J.: Implications for mechanical properties of brittle faults from observations of the Punchbowl Fault Zone, California, Pure and Applied Geophysics, 124, 79 – 106, 1986.

Chester, F., Evans, J., and Biegel, R.: Internal structure and weakening mechanisms of the San Andreas Fault, Journal of Geophysical Research, 98, 771 – 786, 1993.

Chester, J., Chester, F., and Kronenberg, A.: Fracture surface energy of the Punchbowl Fault, San Andreas System, Nature Letters, 437, 133 – 136, https://doi.org/10.1038/nature03942, 2005.

Columbus, J., Sirguey, P., and Tenzer, R.: A free fully assessed 15 meter digital elevation model for New Zealand, Survey Quarterly, 66, 16 – 19, 2011.

Cooper, A. and Norris, R.: Estimates for the timing of the last coseismic displacement on the Alpine Fault, northern Fiordland, New Zealand, New Zealand Journal of Geology and Geophysics, 33, 303 – 307, 1990.

Cooper, A. and Norris, R.: Inverted metamorphic sequences in Alpine Fault mylonites produced by oblique shear within a plate boundary fault zone, New Zealand, Geology, 39, 1023 – 1026, 2011.

Cowan, D., Cladouhos, T., and Morgan, J.: Structural geology and kinematic history of rocks formed along low-angle normal faults, Death Valley, California, GSA Bulletin, 115, 1230 – 1248, 2003.

Cox, S., Etheridge, M., and Wall, V.: The role of fluids in syntectonic mass transport and the localization of metamorphic vein-type ore deposits, Ore Geology Reviews, 2, 65 – 86, 1986.

Czaplinska, D., Piazolo, S., and Zibra, I.: The influence of phase and grain size distribution on the dynamics of strain localization in polymineralic rocks, Journal of Structural Geology, 72, 15 – 32, https://doi.org/10.1016/j.jsg.2015.01.001, 2015.

DeMets, C., Gordon, R., and Argus, D.: Geologically current plate motion, Geophysical Journal International, 181, 1 – 80, https://doi.org/10.1111/j.1365-246X.2009.04491.x, 2010.

Döbelin, N. and Kleeberg, R.: Profex: A graphical user interface for the Rietveld refinement program BGMN, Journal of Applied Crystallography, 48, 1573 – 1580, https://doi.org/10.1107/S16000576715014685, 2015.

Dolejš, D. and Manning, C.: Thermodynamic model for mineral solubility in aqueous fluids: theory, calibration and application to model fluid-flow systems, Geofluids, 10, 20 – 40, https://doi.org/10.1111/j.1468-8123.2010.00282.x, 2010.

Edbrooke, S., Hern, D., Forsyth, P., and Jongens, R.: Geological Map of New Zealand 1:1,000,000, GNS Science Geological Map 2. Lower Hut, New Zealand. GNS Science, 2015.

Eguchi, R., Goltz, J., Taylor, C., Chang, S., Flores, P., Johnson, L., Seligson, H., and Blais, N.: Direct economic losses in the Northridge Earthquake: A three-year post-event perspective, Earthquake Spectra, 14, 245 – 264, 1998.

Evans, J.: Thickness-displacement relationships for fault zones, Journal of Structural Geology, 12, 1061 – 1065, 1990.

Fagereng, A., Remitti, F., and Sibson, R.: Shear veins observed within anisotropic fabric at high angles to the maximum compressive stress, Nature Geoscience, 3, 482 – 485, https://doi.org/10.1038/NGE898, 2010.

Faulkner, D., Lewis, A., and Rutter, E.: On the internal structure and mechanics of large strike-slip fault zones: field observations of the Carboneras Fault in southeastern Spain, Tectonophysics, 367, 235 – 251, https://doi.org/10.1016/S0040-1951(03)00134-3, 2003.

Faulkner, D., Mitchell, T., Healy, D., and Heap, M.: Slip on 'weak' faults by the rotation of regional stress in the fracture damage zone, Nature Letters, 444, 922 – 925, https://doi.org/10.1038/nature05353, 2006.

Faulkner, D., C.A.L., J., Lunn, R., Schlische, R., Shipton, Z., Wibberley, C., and Withjack, M.: A review of recent developments concerning the structure, mechanics and fluid flow properties of fault zones, Journal of Structural Geology, 32, 1557 – 1575, https://doi.org/10.1016/j.jsg.2010.06.009, 2010.

Fossen, H.: Structural Geology, Cambridge University Press, 2nd edn., 2016.

Fossen, H. and Cavalcante, G.: Shear zones - A review, Earth-Science Reviews, 171, 434 – 455, https://doi.org/10.1016/j.earscirev.2017.05.002, 2017.

Grant, J.: The Isocon Diagram – a simple solution to Gresens' equation for metasomatic alteration, Economic Geology, 81, 1976 – 1982, 1986.

Grant, J.: Isocon analysis: a brief review of the method and applications, Physics and Chemistry of the Earth, 30, 997 – 1004, https://doi.org/10.1016/j.pce.2004.11.003, 2005.

Grapes, R. and Watanabe, T.: Metamorphism and uplift of Alpine Schist in the Franz Josef - Fox Glacier area of the Southern Alp, New Zealand, Journal of Metamorphic Geology, 10, 171 – 180, 1992.

Grapes, R., Watanabe, T., and Palmer, K.: XRF analyses of quartzofeldspathic schists and metacherts, Franz Josef - Fox Glacier area, Southern Alps of New Zealand, Victoria University of Wellington Geology Department publication, 25, 11, 1982.

Gresens, R.: Composition-volume relationships of metasomatism, Chemical Geology, 2, 47 – 65, 1967.

Haines, S. and van der Pluijm, B.: Clay quantification and Ar–Ar dating of synthetic and natural gouge: Application to the Miocene Sierra Mazatán Detachment Fault, Sonora, Mexico, Journal of Structural Geology, 30, 525 – 538, https://doi.org/10.1016/j.jsg.2007.11.012, 2008.

Hickman, S., Sibson, R., and Bruhn, R.: Introduction to special section: mechanical involvement of fluids in faulting, Journal of Geophysical Research, 100, 12 831 – 12 840, 1995.

Hobbs, B., Mühlhaus, H.-B., and Ord, A.: Instability, softening and localization of deformation, In: Knipe, R.J. and Rutter, E.H. (eds.): Deformation Mechanisms, Rheology and Tectonics, Geological Society Special Publication, 54, 143 – 165, 1990.

Holdsworth, R., van Diggelen, E., Spiers, C., de Bresser, J., Walker, R., and Bowen, L.: Fault rocks from the SAFOD core samples: implications for weakening at shallow depths along the San Andreas Fault, California, Journal of Structural Geology, 33, 132 – 144, https://doi.org/10.1016/j.jsg.2010.11.010, 2011.

Hollingsworth, J., L., Y., and Avouac, J.-P.: Dynamically triggered slip on a splay fault in the M_W 7.8, 2016 Kaikoura (New Zealand) earthquake, Geophysical Research Letters, 44, 3517 – 3525, https://doi.org/10.1002/2016GL072228, 2017.

Howarth, J., Cochran, U., Langridge, R., Clark, K., Fitzsimons, S., Berryman, K., Villamor, P., and Strong, D.: Past large earthquakes on the Alpine Fault: paleoseismological progress and future directions, New Zealand Journal of Geology and Geophysics, 61, 309 – 328, https://doi.org/10.1080/00288306.2018.1464658, 2018.

Hull, J.: Thickness-displacement relationships for deformation zones, Journal of Structural Geology, 10, 431 – 435, 1988.

Janku-Capova, L., Sutherland, R., Townend, J., Doan, M.-L., Massiot, C., Coussens, J., and Célérier, B.: Fluid flux in fractured rock of the Alpine Fault hanging-wall determined from temperature logs in the DFDP-2B borehole, New Zealand, Geochemistry, Geophysics, Geosystems, 9, https://doi.org/10.1029/2017GV007317, 2018.

Janssen, C., Laube, N., Bau, M., and Gray, D.: Fluid regime in faulting deformation of the Waratah Fault Zone, Australia, as inferred from major and minor element analyses and stable isotopic signatures, Tectonophysics, 204, 109 – 130, 1998.

Janssen, C., Wirth, R., Wenk, H.-R., Morales, L., Naumann, R., Kienast, M., Song, S.-R., and Dresen, G.: Faulting processes in active faults - evidences from TCDP and SAFOD drill core samples, Journal of Structural Geology, 65, 100 – 116, https://doi.org/10.1016/j.jsg.2014.04.004, 2014.

Kaiser, A., Green, A., Campbell, F., Horstmeyer, H., Manukyan, E., Langridge, R., McClymont, A., Mancktelow, N., Finnemore, M., and Nobes, D.: Ultrahigh-resolution seismic reflection imaging of the Alpine Fault, New Zealand, Journal of Geophysical Research, 114, https://doi.org/10.1029/2009JB006338, 2009.

Kirkpatrick, J., Shervais, K., and Ronayne, M.: Spatial Variation in the Slip Zone Thickness of a Seismogenic Fault, Geophysical Research Letters, 45, 7,542 – 7,550, 2018.

Laurich, B., Urai, J., and Nussbaum, J.: Microstructures and deformation mechanisms in Opalinus Clay: insights from scaly clay from the Main Fault in the Mont Terri Rock Laboratory (CH), Solid Earth, 8, 27 – 44, https://doi.org/19.5194/se-8-27-2017, 2017.

Laurich, B., Urai, J., Vollmer, C., and Nussbaum, C.: Deformation mechanisms and evolution of the microstructure of gouge in the Main Fault in Opalinus Clay in the Mont Terri Rock Laboratory (CH), Solid Earth, 9, 1 – 24, https://doi.org/10.5194/se-9-1-2018, 2018.

Lay, V., Buske, S., Lukács, A., Gorman, A., Bannister, S., and Schmitt, D.: Advanced seismic imaging techniques characterize the Alpine Fault at Whataroa (New Zealand), Journal of Geophysical Research: Solid Earth, 121, https://doi.org/10.1002/2016JB013534, 2016.

Li, H., Wang, H., Xu, Z., Si, J., Pei, J., Li, T., Huang, Y., Song, S.-R., Kuo, L.-W., Sun, Z., Chevalier, M.-L., and Liu, D.: Characteristics of the fault-related rocks, fault zones and the principal slip zone in the Wenchuan Earthquake Fault Scientific Drilling Project Hole-1 (WFSD-1), Tectonophysics, 584, 23 – 42, https://doi.org/10.1016/j.tecto.2012.08.021, 2013.

Lindsey, E., Fialko, Y., Bock, Y., Sandwell, D., and Bilham, R.: Localized and distributed creep along the southern San Andreas Fault, Journal of Geophysical Research: Solid Earth, 119, 7909 – 7922, https://doi.org/10.1002/2014JB011275, 2014.

Little, T., Cox, S., Vry, J., and Batt, G.: Variations in exhumation level and uplift rate along the oblique-slip Alpine Fault, central Southern Alps, New Zealand, GSA Bulletin, 117, 707 – 723, https://doi.org/10.1130/B25500.1, 2005.

Lockner, D., Morrow, C., Moore, D., and Hickman, S.: Low strength of deep San Andreas Fault gouge from SAFOD core, Nature, 472, 82 – 86, https://doi.org/10.1038/nature09927, 2011.

Lukács, A., Gorman, A., and Norris, R.: Quaternary structural and paleo-environmental evolution of the Alpine Fault near Haast, New Zealand, from 2D seismic reflection and gravity data, New Zealand Journal of Geology and Geophyics, 31, 181 – 213, https://doi.org/10.1080/00288306.2018.1544153, 2018.

Ma, K., Tanaka, H., Song, S.-R., Wang, C.-Y., Hung, J.-H., Tsai, Y.-B., Mori, J., Song, Y., Yeh, E., Soh, W., Sone, H., Kuo, L.-W., and Wu, H.-Y.: Slip zone and energetics of a large earthquake from the Taiwan Chelungpu-fault Drilling Project, Nature, 444, 473 – 475, https://doi.org/10.1038/nature05253, 2006.

Martínez-Garzón, P., Bohnhoff, M., Ben-Zion, Y., and Dresen, G.: Scaling of maximum observed magnitudes with geometrical and stress properties of strike-slip faults, Geophysical Research Letters, 42, https://doi.org/10.1093/gji/ggx169, 2015.

Massiot, C., Célérier, B., Doan, M.-L., Little, T., Townend, J., McNamara, D., Williams, J., Schmitt, D., Toy, V., Sutherland, R., Janku-Capova, L., Upton, P., and Pezard, P.: The Alpine Fault hanging-wall viewed from within: Structural analysis of ultrasonic image logs in the DFDP-2B borehole, New Zealand, Geochemistry, Geophysics, Geosystems, 19, https://doi.org/10.1029/2017GC007368, 2018.

Menzies, C., Teagle, D., Niedermann, S., Cox, S., Craw, D., Zimmer, M., Cooper, M., and Erzinger, J.: Frictional strength of wet and dry montmorillonite, Earth and Planetary Science Letters, 455, 125 – 135, https://doi.org/10.1016/j.epsl.2016.03.046, 2016.

Mitchel, T. and Faulkner, D.: The nature and origin of off-fault damage surrounding strike-slip fault zones with a wide range of displacements: A field study from the Atacama fault system, northern Chile, Journal of Structural Geology, 31, 802 – 816, 2009.

Moore, D. and Lockner, D.: Friction of smectite clay montmorillonite, in: The Seismogenic Zone of Subduction Thrust Faults, p. 317–345, Columbia University Press, 2007.

Moore, D. and Reynolds, Jr., R.: X-Ray Diffraction and the Identification of clay Minerals, Oxford University Press, Oxford, 1997.

Moore, D., Lockner, D., Shengli, M., Summers, R., and Byerlee, J.: Strength of serpentinite gouges at elevated temperatures, Journal of Geophysical Research, 102, 14 787 – 14 801, https://doi.org/10.1029/2010GL046129, 1997.

Nardini, L., Rybacki, E., Döhmann, M., Morales, L., Brune, S., and Dresen, G.: High-temperature shear zone formation in Carrara marble: The effect of loading conditions, Tectonophysics, 749, 120 – 139, https://doi.org/10.1016/j.tecto.2018.10.022, 2018.

Nicol, A., Robinson, R., Van Dissen, R., and Harvison, A.: Variability of recurrence interval and single-event slip for surface-rupturing earthquakes in New Zealand, New Zealand Journal of Geology and Geophysics, 59, 97 – 116, https://doi.org/10.1080/00288306.2015.1127822, 2016.

Norris, R. and Cooper, A.: Origin of small-scale segmentation and transpressional thrusting along the Alpine Fault, New Zealand, GSA Bulletin, 107, 231 – 240, 1995.

Norris, R. and Cooper, A.: Erosional control on the structural evolution of a transpressional thrust complex on the Alpine Fault, New Zealand, Journal of Structural Geology, 19, 1323 – 1342, 1997.

Norris, R. and Cooper, A.: Late Quaternary slip rates and slip partitioning on the Alpine Fault, New Zealand, Journal of Structural Geology, 23, 507 – 520, https://doi.org/10.1002/2016JB013658, 2000.

Norris, R. and Cooper, A.: Very high strains recorded in mylonites along the Alpine Fault, New Zealand: Implications for the deep structure of plate boundary faults, Journal of Structural Geology, 25, 2141 – 2157, 2003.

Norris, R. and Cooper, A.: The Alpine Fault, New Zealand: Surface geology and field relationships, In: Okaya, D., Stern, T.A. and Davey, F. (eds.): A continental plate boundary: Tectonics at South Island, New Zealand. AGU Geophysical Monograph, 175, 157 – 175, 2007.

Norris, R. and Toy, V.: Continental transforms: A view from the Alpine Fault, Journal of Structural Geology, 64, 3 – 31, https://doi.org/10.1016/j.jsg.2014.03.003, 2014.

Passchier, C. and Trouw, R.: Microtectonics, Springer, 2nd edn., 2005.

Peacock, D., Nixon, C., Rotevatn, A., Sanderson, D., and Zuluaga, L.: Glossary of fault and other fracture networks, Journal of Structural Geology, 92, 12 – 29, https://doi.org/10.1016/j.jsg.2016.09.008, 2016.

Reed, J.: Myonites, cataclasites, and associated rocks along the Alpine Fault, South Island, New Zealand, New Zealand Journal of Geology and Geophysics, 7, 645 – 684, https://doi.org/10.1080/00288306.1964.10428124, 1964.

Roser, B. and Cooper, A.: Geochemistry and terrane affiliation of Haast schist from the western southern Alps, New Zealand, New Zealand Journal of Geology and Geophysics, 33, 1 – 10, https://doi.org/10.1080/00288306.1990.10427567, 1990.

Rybacki, E., Janssen, C., Wirth, R., Chen, K., Wenk, H.-R., Stromeyer, D., and Dresen, G.: Low-temperature deformation in calcite veins of SAFOD core samples (San Andreas Fault) – microstructural analysis and implications for fault rheology, Tectonophysics, 509, 107 – 119, https://doi.org/10.1016/j.tecto.2011.05.014, 2011.

Rybacki, E., Morales, L., Naumann, M., and Dresen, G.: Strain localization during high temperature creep of marble: The effect of inclusions, Tectonophysics, 634, 182 – 197, https://doi.org/10.1016/j.tecto.2014.07.032, 2014.

Sagy, A. and Brodsky, E.: Geometric and rheological asperities in an exposed fault zone, Journal of Geophysical Research, 114, https://doi.org/10.1029/2008JB005701, 2009.

Sahin, M. and Tari, E.: The August 17 Kocaeli and the November 12 Düzce earthquakes in Turkey, Earth Planets Space, 52, 753 – 757, https://doi.org/10.1016/j.tecto.2011.05.014, 2000.

Schindelin, J., Arganda-Carreras, I., Frise, E., Kaynig, V., Longair, M., Pietzsch, T., Preibisch, S., Rueden, C., Saalfeld, S., Schmid, B., Tinevez, J.-Y., White, D., Hartenstein, V., Eliceiri, K., Tomancak, P., and Cardona, A.: Fiji: an open-source platform for biological-image analysis, Nature methods, 9, 676 – 682, 2012.

Schleicher, A., van der Pluijm, B., and Warr, L.N.: Nanocoatings of clay and creep of the San Andreas Fault at Parkfield, Geology, 38, 667 – 670, https://doi.org/10.1130/G31091.1, 2010.

Schleicher, A., Sutherland, R., Townend, J., Toy, V., and van der Pluijm, B.: Clay mineral formation and fabric development in the DFDP-1B borehole, central Alpine Fault, New Zealand, New Zealand Journal of Geology and Geophysics, 58, 13 – 21, https://doi.org/10.1080/00288306.2014.979841, 2015.

Schneider, C., Rasband, W., and Eliceiri, K.: NIH Image to ImageJ: 25 years of image analysis, Nature methods, 9, 671 – 675, 2012.

Scholz, C.: Wear and gouge formation in brittle faulting, Geology, 15, 493 – 495, 1987.

Schrank, C., Handy, M., and Fusseis, F.: Multiscaling of shear zones and the evolution of the brittle-to-viscous transition in continental crust, Journal of Geophysical Research, 113, https://doi.org/10.1029/2006JB004833, 2008.

Schuck, B., Janssen, C., Schleicher, A., Toy, V., and Dresen, G.: Microstructures imply cataclasis and authigenic mineral formation control geomechanical properties of New Zealand's Alpine Fault, Journal of Structural Geology, 110, 172 – 186, https://doi.org/10.1016/jsg.2018.03.001, 2018.

Scott, J., Auer, A., Muhling, J., Czertowicz, T., Cooper, A., Billia, M., and Kennedy, A.: New P-T and U-Pb constraints on Alpine Schist metamorphism in south Westland, New Zealand, New Zealand Journal of Geology and Geophysics, 58, 385 – 397, https://doi.org/10.1080/00288306.2015.1093005, 2015.

Segall, P. and Pollard, D.: Nucleation and growth of strike slip faults in granite, Journal of Geophysical Research, 88, 555 – 568, https://doi.org/10.1080/00288306.2015.1093005, 1983.

Shervais, K. and Kirkpatrick, J.: Smoothing and re-roughening processes: The geometric evolution of a single fault zone, Journal of Structural Geology, 98, 130 – 143, 2016.

Sibson, R.: A note on fault reactivation, Journal of Structural Geology, 7, 751 – 754, 1985.

Sibson, R.: Thickness of the Seismic Slip Zone, Bulletin of the Seismological Society of America, 93, 1169 – 1178, 2003.

Sibson, R., White, S., and Atkinson, B.: Fault rock distribution and structure within the Alpine Fault Zone: A preliminary account, In: Walcott, R.I. and Cresswell, M.M. (eds.): The origin of the Southern Alps. Bulletin of the Royal Society of New Zealand, 18, 55 – 65, 1979.

Spandler, C., Worden, K., Arculus, R., and Eggins, S.: Igneous rocks of the Brook Street Terrane, New Zealand: implications for Permian tectonics of eastern Gondwana and magma genesis in modern intra-oceanic volcanic arcs, New Zealand Journal of Geology and Geophysics, 48, 167 – 183, 2005.

Stern, T., Kleffmann, S., Okaya, D., Scherwath, M., and Bannister, S.: Low seismic-wave speeds and enhanced fluid pressure beneath the Southern Alps of New Zealand, Geology, 29, 679 – 682, 2001.

Sutherland, R., Eberhart-Phillips, D., Harris, R., Stern, T., Beavan, J., Ellis, S., Henrys, S., Cox, S., Norris, R., Berryman, K., Townend, J., Bannister, S., Pettinga, J., Leitner, B., Wallace, L., Little, T., Cooper, A., Yetton, M., and Stirling, M.: Do great earthquakes occur on the Alpine Fault in central South Island, New Zealand?, In: Okaya, D., Stern, T.A. and Davey, F. (eds.): A continental plate boundary: Tectonics at South Island, New Zealand. AGU Geophysical Monograph, 175, 235 – 251, 2007.

Sutherland, R., Toy, V., Townend, J., Cox, S., Eccles, J., Faulkner, D., Prior, D., Norris, R., Mariani, E., Boulton, C., Carpenter, B., Menzies, C., Little, T., Hasting, M., De Pascale, G., Langridge, R., Scott, H., Lindroos, Z., Fleming, B., and Kopf, A.: Drilling reveals fluid control on architecture and rupture of the Alpine Fault, New Zealand, Geology, 40, 1143 – 1146, https://doi.org/10.1130/G33614.1, 2012.

Sutherland, R., Townend, J., Toy, V., Allen, M., Baratin, L., Barth, N., Becroft, L., Benson, l., Boese, C., Boles, A., Boulton, C., Capova, l., Carpenter, B., Célérier, B., Chamberlain, C., Conze, R., Cooper, A., Coussens, J., Coutts, A., Cox, S., Craw, L., Doan, M., Eccles, J., Faulkner, D., Grieve, J., Grochowski, J., Gulley, A., Henry, G., Howarth, J., Jacobs, K., Jeppson, T., Kato, N., Keys, S., Kirilova, M., Kometani, Y., Kovacs, A., Langridge, R., Lin, W., Little, T., Mallyon, D., Mariani, B., Marx, R., Massiot, C., Mathewson, L., Melosh, B., Menzies, C., Moore, J., Morales, L., Morgan, C., Mori, H., Niemeijer, A., Nishikawa, O., Nitsch, O., Paris Cavailhès, J., Pooley, B., Prior, D., Pyne, A., Sauer, K., Savage, M., Schleicher, A., Schmitt, D., Shigematsu, N., Taylor-Offord, S., Tobin, H., Upton, P., Valdez, R., Weaver, K., Wiersberg, T., J., W., Yeo, S., and Zimmer, M.: Deep Fault Drilling Project (DFDP), Alpine Fault Boreholes DFDP-2A and DFDP-2B Technical Completion Report, GNS Science Report 2015/50, 2015.

Sutherland, R., Townend, J., Toy, V., Upton, P., Coussens, J., Allen, M., Baratin, L.-M., Barth, N., Becroft, L., Boese, C., Boles, A., Boulton, C., Broderick, N., Janku-Capova, L., Carpenter, B., Célérier, B., Chamberlain, C., Cooper, A., Coutts, A., Cox, S., Craw, L., Doan, M.-L., Eccles, J., Faulkner, D., Grieve, J., Grochowski, J., Gulley, A., Hartog, A., Howarth, J., Jacobs, K., Jeppson, T., Kato, N., Keys, S., Kirilova, M., Kometani, Y., Langridge, R., Lin, W., Little, T., Lukacs, A., Mallyon, D., Mariani, E., Massiot, C., Mathewson, L., Melosh, B., Menzies, C., Moore, J., Morales, L., Morgan, C., Mori, H., Niemeijer, A., Nishikawa, O., Prior, D., Sauer, K., Savage, M., Schleicher, A., Schmitt, D., Shigematsu, N., Taylor-Offord, S., Teagle, D., Tobin, H., Valdez, R., Weaver, K., Wiersberg, T., Williams, J., Woodman, N., and Zimmer, M.: Extreme hydrothermal conditions at an active plate-bounding fault, Nature, 545, https://doi.org/doi: 10.1038/nature22355, 2017.

Toby, B.: R factors in Rietveld analysis: How good is good enough?, Powder Diffraction, 21, 67 – 70, 2006.

Toppozada, T., D.M., B., Reichle, M., and Hallstrom, C. L.: San Andreas Fault Zone, California: M geq 5.5 earthquake history, Bulletin of the Seismological Society of America, 92, 2555 – 2601, 2002.

Townend, J. and Zoback, M.: How faulting keeps the crust strong, Geology, 28, 399 – 402, 2000.

Townend, J., Sutherland, R., and Toy, V.: Deep Fault Drilling Project - Alpine Fault, New Zealand, Scientific Drilling, 8, 75 – 82, 2009.

Townend, J., Sutherland, R., Toy, V., Eccles, J., Boulton, C., Cox, S., and McNamara, D.: Late-interseismic state of a continental plate-bounding fault: Petrophysical results from DFDP-1 wireline logging and core analysis, Alpine Fault, New Zealand, Geochemistry, Geophysics, Geosystems, 14, 3801 – 3820, https://doi.org/10.1002/ggge.20236, 2013.

Townend, J., Sutherland, R., Toy, V., Doan, M.-L., Célérier, B., Massiot, C., Coussens, J., Jeppson, T., Janku-Capova, L., Remaud, L., Upton, P., Schmitt, D., Williams, J., Allen, M., Baratin, L.-M., Barth, N., Becroft, L., Boese, C., Boulton, C., Broderick, N., Carpenter,

B., Chamberlain, C., Cooper, A., Coutts, A., Cox, S., Craw, L., Eccles, J., Faulkner, D., Grieve, J., Grochowski, J., Gulley, A., Hartog, A., Henry, G., Howarth, J., Jacobs, K., Kato, N., Keys, S., Kirilova, M., Kometani, Y., Langridge, R., Lin, W., Little, T., Lukacs, A., Mallyon, D., Mariani, E., Mathewson, L., Melosh, B., Menzies, C., Moore, J., Morales, L., Mori, H., Niemeijer, A., Nishikawa, O., Nitsch, O., Paris, J., Prior, D., Sauer, K., Savage, M., Schleicher, A., Shigematsu, N., Taylor-Offord, S., Teagle, D., Tobin, H., Valdez, R., Weaver, K., Wiersberg, T., and Zimmer, M.: Petrophysical, geochemical, and hydrological evidence for extensive fracture-mediated fluid and heat transport in the Alpine Fault's hanging-wall damage zone, Geochemistry, Geophysics, Geosystems, 18, 4709 – 4732, https://doi.org/10.1002/2017GC007202, 2017.

Toy, V., Norris, R., Prior, D., Walrond, M., and Cooper, A.: How do lineations reflect the strain history of transpressive shear zones? The example of the active Alpine Fault Zone, New Zealand, Journal of Structural Geology, 50, 187 – 198, https://doi.org/10.1016/j.jsg.2012.06.006, 2013.

Toy, V., Boulton, C., Sutherland, R., Townend, J., Norris, R., Little, T., Prior, D., Mariani, E., Faulkner, D., Menzies, C., Scott, H., and Carpenter, B.: Fault rock lithologies and architecture of the central Alpine Fault, New Zealand, revealed by DFDP-1 drilling, Lithosphere, 7, 155 – 173, https://doi.org/10.1130/L395.1, 2015.

Toy, V., Sutherland, R., Townend, J., Allen, M., Becroft, L., Boles, A., Boulton, C., Carpenter, B., Cooper, A., Cox, S., Daube, C., Faulkner, D., Halfpenny, A., Kato, N., Keys, S., Kirilova, M., Kometani, Y., Little, T., Mariani, E., Melosh, B., Menzies, C., Morales, L., Morgan, C., Mori, H., Niemeijer, A., Norris, R., Prior, D., Sauer, K., Schleicher, A., Shigematsu, N., Teagle, D., Tobin, H., Valdez, R., Williams, J., Yea, S., Baratin, L.-M., Barth, N., Benson, A., Boese, C., Célérier, B., Chamberlain, C., Conze, R., Coussens, J., Craw, L., Doan, M.-L., Eccles, J., Grieve, J., Grochowski, J., Gulley, A., Howarth, J., Jacobs, K., Janku-Capova, L., Jeppson, T., Langridge, R., Mallyon, D., Marx, R., Massiot, C., Mathewson, L., Moore, J., Nishikawa, O., Pooley, B., Pyne, A., Savage, M., Schmitt, D., Taylor-Offord, S., Upton, P., Weaver, K., Wiersberg, T., Zimmer, M., and DFDP-2 Science Team: Bedrock geology of DFDP-2B, central Alpine Fault, New Zealand, New Zealand Journal of Geology and Geophysics, https://doi.org/10.1080/00288306.2017.1375533, 2017.

Twiss, R. and Moores, E.: Structural Geology, W.H. Freeman and Company, 2nd edn., 2007.

Upton, P., Song, B., and Koons, P.: Topographic control on shallow fault structure and strain partitioning near Whataroa, New Zealand demonstrates weak Alpine Fault, New Zealand Journal of Geology and Geophysics, https://doi.org/10.1080/00288306.2017.1397706, 2017.

Van Eijs, R., Mulders, F., Nepveu, M., Kenter, C., and Scheffers, B.: Correlation between hydrocarbon reservoir properties and induced seismicity in the Netherlands, Engineering Geology, 84, 99 – 111, https://doi.org/19.1016/j.enggeo.2006.01.002, 2006.

Vannucchi, O., Maltman, A., Bettelli, G., and Clennell, B.: On the nature of scaly fabric and scaly clay, Journal of Structural Geology, 25, 673 – 688, 2003.

Warr, L. and Cox, S.: Clay mineral transformations and weakening mechanisms along the Alpine Fault, New Zealand, In: Holdsworth, R.E., Strachan, R.A., Magloughlin, J.F. and Knipe, R.J. (eds.): The nature and tectonic significance of fault zone weakening. Geological Society, London, Special Publications, 186, 85 – 101, 2001.

Warren-Smith, E., Lamb, S., and Stern, T.: Stress field and kinematics for diffuse microseismicity in a zone of continental transpression, South Island, New Zealand, Journal of Geophysical Research: Solid Earth, 122, https://doi.org/10.1002/2017JB013942, 2017.

Wibberley, C., Yielding, G., and Di Toro, G.: Recent advances in the understanding of fault zone internal structure: a review, In: Wibberley, C.A.J., Kurz W., Imber, J., Holdsworth, R.E. and Collettini, C. (eds.): The Internal Structure of Fault Zones: Implications for Mechanical and Fluid-Flow Properties. Geological Society, London, Special Publications, 299, 5 – 33, https://doi.org/10.1144/SP299.2, 2008.

Williams, J., Toy, V., Massiot, C., McNamara, D., and Wang, T.: Damaged beyond repair? Characterizing the damage zone of a fault late in its interseismic cycle, the Alpine Fault, New Zealand, Journal of Structural Geology, 90, 76 – 94, https://doi.org/10.1016/j.jsg.2016.07.006, 2016.

Williams, J., Toy, V., Smith, S., and Boulton, C.: Fracturing, fluid-rock interaction and mineralization during the seismic cycle along the Alpine Fault, Journal of Structural Geology, 103, 151 – 166, https://doi.org/10.1016/j.jsg.2017.09.011, 2017.

Williams, J., Toy, V., Massiot, C., McNamara, D., Smith, S., and Mills, S.: Controls on fault zone structure and brittle fracturing in the foliated hanging wall of the Alpine Fault, Solid Earth, 9, 469 – 489, https://doi.org/10.5194/se-9-469-2018, 2018.

Wirth, R.: A novel technology for advanced application of micro- and nanoanalysis in geosciences and applied mineralogy, European Journal of Mineralogy, 16, 863 – 876, https://doi.org/10.1127/0935-1221/2004/0016-0863, 2004.

Wirth, R.: Focused Ion Beam (FIB) combined with SEM and TEM: advanced analytical tools for studies of chemical composition, microstructure and crystal structure in geomaterials on a nanometre scale, Chemical Geology, 261, 217 – 229, https://doi.org/10.1016/j.chemgeo.2008.05.019, 2009.

Zoback, M., Hickman, S., and Ellsworth, W.: The role of fault zone drilling, in: Treatise on geophysics, edited by Schubert, G., p. 649 – 674, Elsevier, Amsterdam, 2007.

Table 1: Summary of observed hanging-wall cataclasite microstructures. PSZ: principal slip zone.

	poor	localization	high
	DFDP-1A	**Waikukupa Thrust**	**Martyr River**
fractures	X	X	X
- amount increases towards PSZ	X	X	/
microfaults	~ 5 - 130 µm wide	~ 5 - 130 µm wide	/
detrital clasts			
- main phases	quartz & feldspar	quartz & feldspar	polymineralic aggregates (mainly quartz, feldspar & chlorite)
- minor phases	/	micas (elongated, kinked & fractured), hornblende & chlorite aggregates (up to 0.6 × 1 mm large)	quartz & feldspar (< 5 %)
- roundness	angular - rounded	angular - rounded	angular - rounded
- sphericity	low - moderate	low - moderate	low - moderate
- amount			
- PSZ-proximal	~ 50 % (at ~ 3 m above PSZ)	~ 60 - 70 % (at ~ 70 cm above PSZ)	not sampled
- at contact to PSZ	~ 10 %	~ 20 - 25 %	~ 40 - 50 %
- size			
- PSZ-proximal	~ 100s of µm (at ~ 3 m above PSZ)	~ 100s of µm (at ~ 70 cm above PSZ)	not sampled
- at contact to PSZ	~ 100 µm	~ 100 µm	~ 100 - 200 µm
- maximum	~ 550 × 600 µm	~ 550 × 600 µm	~ 200 µm
fragments			
- schist	1.6 × 3.4 mm large	2.8 × 5.4 mm large	1.1 mm large
- fractured & gouge-filled	X	X	/
- mylonite	/	9 - 12 mm large	/
- fractured & gouge-filled	/	X	/
matrix clasts	X	X	/
- first observation	~ 1.35 m above PSZ	~ 10 cm above PSZ	/
- max. size	650 × 750 µm	1.3 × 3.4 mm	
patches of authigenic chlorite crystallites	X	X	/
- amount increases towards PSZ	X	X	/
bright matrix clasts	X	X	X
calcite			
- occurrence	all samples	mostly in direct vicinity to PSZ	all samples
- kind: cement	within some fractures; local	within some fractures; generally insignificant; slightly more pronounced within ~ 3 cm of PSZ	within some fractures; finely-dispersed & abundant
- kind: lenses	up to 1.2 × 4 mm	/	/
- kind: veins	frequent with increasing abundance towards the PSZ; mostly restricted to clasts; up to 5 - 300 µm thick; typically between 50 - 70 µm thick	~ < 15 µm thick; mutually cross-cutting with small (< 20 µm), dextral offsets	/

	poor	localization	high
	DFDP-1A	**Waikukupa Thrust**	**Martyr River**
foliation	locally & weak; formed by clasts and microfaults; locally with SC-geometry	clast-lenses parallel to PSZ	/
other	/	breccias (< 100µm large) within some centimeters above the PSZ; clay-clast-aggregates	/

Table 2: Summary of observed principal slip zone (fault gouge) microstructures. PSZ: principal slip zone; HW: hanging-wall; FW: footwall.

	poor		localization		high
	Havelock Creek	**Gaunt Creek**	**DFDP-1A**	**Waikukupa Thrust**	**Martyr River**
contact HW - PSZ	transitional over 8 cm	not sampled	not sampled	sharp at macro- & mesoscale; transitional over 4 mm at microscale & sharp at macro- & mesoscale; difficult to identify at microscale	
major differences compared to hanging-wall	not sampled	not sampled	~ 90 % of PSZ is cemented	FW-prox. gouge: dense anastomosing network of mutually cross-cutting calcite veins	I) clasts are small individual mineral phases and not chloritized aggregates; II) no calcite cement, but less porous due to authigenic phyllosilicates
kind of PSZ	single structure	single structure	single structure	layered HW-prox. gouge 2 cm thick FW-prox. gouge 2 cm thick	layered HW-prox. gouge 0.8 – 1 cm thick FW-prox. gouge 0.3 – 0.5 cm thick
- contact between PSZ layers	/	/	/	sharp & undulating & poorly developed at microscale	
- major differences between PSZ layers	/	/	/	FW-prox. gouge hosts dense, anastomosing network of mutually cross-cutting calcite veins	20 - 25 % clasts in HW-prox. gouge vs. 25 - 30 % clasts in FW-prox. gouge
similarities between investigated PSZs	HW-prox. gouge at Waikukupa Thrust	FW-prox. gouge at Waikukupa Thrust	/	Havelock Creek (HW-prox. gouge); Gaunt Creek (FW-prox. gouge)	/
detrital clasts					
- main phases	quartz & feldspar	quartz & feldspar	quartz & feldspar	quartz & feldspar	quartz & feldspar
- minor phases	hornblende & mica fragments (50 × 350 µm large)	/	/	/	hornblende; mica fragments (< 20 µm large) & needle-shaped serpentines (< 20 µm large)
- roundness	(sub)angular - rounded	(sub)angular - rounded	(sub)angular - rounded	(sub)angular - rounded	(sub)angular - rounded
- sphericity	elongate - moderate	elongate - moderate	elongate - moderate	elongate - moderate	elongate - moderate
- amount	10 %	< 1 %	/	HW-prox. gouge: 5 - 10 %; FW-prox. gouge: < 1 %	20 - 30 %
- size	~ 75 µm	~ 15 µm	/	~ 100 µm; decreases towards FW	HW-prox. gouge 10s - 200 µm; FW-prox. gouge < 100 µm
- maximum	160 × 250 µm	90 × 130 µm	/	110 × 180 µm	1 mm
- fragments					
- kind	schist	/	/	/	schist, mylonite, cataclasite

	poor		localization		high
	Havelock Creek	**Gaunt Creek**	**DFDP-1A**	**Waikukupa Thrust**	**Martyr River**
- roundness	subangular - -rounded	/	/	/	subangular - -rounded
- sphericity	low - moderate	/	/	/	low - moderate
- size	15 - 50 µm	/		/	/ 100s of micrometer (schist)
- maximum	400 × 450 µm	/	/	/	> 2.2 × 3.7 mm (schist); 3 × 7.5 mm (mylonite); 5 × 6 mm (cataclasite)
- other	/	/	/	clast size decreases towards FW	/
matrix clasts	prevailing type of clast	/	/	prevail at HW-prox. gouge	< 5 % of clasts
- maximum size	650 × 830 µm	/	/	3 µm – > 6 mm	~ 20 µm – 3 × 3.5 mm
patches of authigenic chlorite crystallites	/	/	associated with non-cemented fractures	/	/
bright matrix clasts					
- abundance	high	high	low (local)	/	low (local)
calcite veins	very rare	network	rarev	rare (HW-prox. gouge); network (FW-prox. gouge)	rare
- thickness					
- vein network	/	350 - 800 µm	/	~ 2 cm (FW-prox. gouge)	/
- individual veins	/	5 - 10 µm, up to 30 µm, increases slightly towards FW	up to 350 µm	HW-prox. gouge ~ 10 µm; FW-prox. gouge typically ~ 60 µm, between 1.5 - 200 µm decreases to FW	15 - 900 µm
- spacing	/	20 - 30 µm; between 10 - 80µm	/	200 µm (close to HW-prox. gouge), 10 µm (close o FW)	/
- orientations	/	/	/ FW-prox. gouge; I) subparallel to displacement; II) oblique to displacement; III) normal to displacement	/	
- CL color	/	mostly uniform yellow – orange; slightly brighter and more yellow to FW	/	uniform yellow – orange	/
- other	/	/	/	small (< 5 µm), blocky & euhedral crystals	/
foliation	/	/	/	/	in HW-prox. gouge; weak; parallel to PSZ; formed by clasts
other	/	/	slickolite	HW-prox. gouge: CCAs & breccias (0.6 × 1.2 mm)	/

Table 3: Summary of observed footwall (Quaternary gravel) microstructures. PSZ: principal slip zone; FW: footwall.

	poor	**localization**	**high**
	Gaunt Creek	**Waikukupa Thrust**	**Martyr River**
contact PSZ - FW	sharp	sharp	not sampled
detrital clasts			
- main phases	quartz & feldspar	quartz & feldspar	quartz & feldspar
- minor phases	mica	mica	mica, serpentine
- roundness	subangular - subrounded	subangular - subrounded / subangular - subrounded	
- sphericity	low - moderate	low - moderate	low - high
- amount	25 - 30 %	40 - 50 %	50 - 60 %
- size	~ 140 - 185 µm	~ 60 - 130 µm	~ 100 - 200 µm
- trend	/	increases with increasing distance to PSZ	increases with increasing distance to PSZ
- fragments	schist & cataclasite & schist, mylonite	cataclasite	schist & cataclasite
- maximum size			
- schist	~ 4.1 × 5.3 mm	~ 1 × 1.5 cm	0.7 × 1.4 cm
- mylonite	/	~ 0.7 cm	/
- cataclasite	~ 3.4 × 5.6 mm	0.5 - 0.7 cm	0.5 × 1.1 ,cm
matrix clasts	~ 300 µm (up to 4.3 × 7.4 mm)	/	/
patches of authigenic chlorite crystallites	X	/	/
bright matrix clasts			
- abundance	high	/	low
calcite		in general, mostly restricted to ~ 3 mm within contact to PSZ	
- kind: cement		finely dispersed	
- kind: veins	up to ~ 350 µm thick; cross-cut detrital clasts	veinlets & a few displacement-normal veins extending from FW-prox. gouge into footwall	/
- kind: other	lenses (up to 1 × 1.4 mm large) within detrital clasts	calcite rims (< 5 µm) at clasts parallel to displacement	/
foliation	/	/	weak; parallel to PSZ; formed by slightly imbricated clasts
other	0.75 - 1.6 cm thick lens of matrix clasts (size: ~ 100 - 300 µm; up to 1.4 × 2.1 mm); fractures between individual clasts are gouge-filled; < 5 % detrital clasts	/	/

Table 4. Mineralogical composition [wt%] of investigated samples as determined by XRD and subsequent Rietveld refinement. Mineral abbreviations are: Qtz: quartz; Plg: plagioclase; KFsp: potassium feldspar; Cc: calcite; Ank: ankerite; Chl: chlorite; Kln: kaolinite; Ms: muscovite; Ill: illite; Bt: biotite; Amp: amphibole; Ep: epidote; Srp: serpentine group minerals; Ap: apatite; Py: pyrite.

sample	location	lithology	dist. to PSZ[a]	Qtz	Plg[b]	KFsp	Cc	Ank	Chl	Kln	Ms	Ill	Bt	Amp[c]	Ep	Srp[d]	Ap	Py
129	Havelock Creek	gouge	0 cm	23	25	4	11		19	2	4	5	3	3				< 1
130_1	Gaunt Creek	gouge	0 cm	22	14	7	6		6		46							
130_2		gravel	- 2.5 cm	23	21	7	6		12		3	25	2					
130_3		gravel	- 4.75 cm	25	20	15	6		8	1	14	6	5					
120	DFDP-1A	cataclasite	292 cm	32	9	4	3		10	1	20	14	7				< 1	
119		cataclasite	270 cm	26	26	7	5		9	2	23		2				< 1	
118		cataclasite	135 cm	29	7	4	2		14	22	18	3	< 1				1	
117		cataclasite	87 cm	37	11	7	8		11	1	23	2	1					
116		cataclasite	25 cm	22	6	18	18		22	4	3	4	2				< 1	
115		gouge	0 cm	27	8	5	2		5	30	10	11	2				< 1	
132	Waikukupa Thrust	cataclasite	70 cm	23	41		3	1	16	< 1	2		4	9				< 1
124		cataclasite	25 cm	29	36	1	2		9	1	1	1	2	12	6			< 1
125_1		cataclasite	8 cm	32	36	1	2		11	1	1		3	8	6			< 1
131_2		gouge	2 cm	22	17	4	16		10	1	28	< 1	1	1			1	< 1
131_1		gouge	0 cm	11	8	2	29	1	5	1	< 1	41	1				1	< 1
133		gravel	- 10 cm	31	33	1	1		7		4	10	7	4	2			
127_3	Martyr River	cataclasite	2 cm	20	23	5	10		15	17	3	1	1		7			
127_4		gouge	0 cm	13	9	4	3		9	38	4	8	2			5	< 1	

[a)] Datum to calculate distance to PSZ refers to center of PSZ at Martyr River, Havelock Creek and the DFDP-1A borehole and to the contact between PSZ and footwall at Waikukupa Thrust and Gaunt Creek.

[b)] Albite is the main plagioclase phase.

[c)] Amphibole minerals encountered are typically hornblende.

[d)] Main serpentine group minerals are to equal amounts lizardite and amesite.

Table 5. Geochemical composition [wt%] of investigated samples as determined by XRF.

sample	location	lithology	dist. to PSZ[a]	MnO	P_2O_5	TiO_2	Na_2O	K_2O	CaO	MgO	Fe_2O_3[b]	Al_2O_3	SiO_2	LOI	total
129	Havelock Creek	gouge	0 cm	0.13	0.20	0.81	1.77	1.39	7.85	4.20	6.49	13.60	51.7	11.49	99.62
130_1	Gaunt Creek	gouge	0 cm	0.13	0.19	0.76	1.94	3.27	6.78	3.64	6.66	13.43	51.40	11.38	99.58
130_2		gravel	- 2.5 cm	0.10	0.21	0.84	2.08	3.01	4.84	3.81	6.38	14.11	54.56	9.67	99.61
130_3		gravel	- 4.75 cm	0.11	0.21	0.74	2.11	2.86	5.60	3.53	5.72	13.73	56.13	8.90	99.63
120	DFDP-1A	cataclasite	292 cm	0.06	0.17	0.70	1.15	4.20	1.94	3.01	5.66	16.12	60.54	6.08	99.63
119		cataclasite	270 cm	0.07	0.15	0.63	2.32	2.42	3.79	2.23	3.95	12.72	53.31	18.2	99.79
118		cataclasite	135 cm	0.04	0.17	0.58	1.19	4.17	1.76	2.52	4.20	14.31	65.95	4.88	99.76
117		cataclasite	87 cm	0.08	0.16	0.54	0.84	3.16	3.97	3.13	4.23	11.75	53.10	18.77	99.73
116		cataclasite	25 cm	0.17	0.18	0.71	0.38	3.56	10.99	4.48	5.70	11.64	44.66	17.15	99.62
115		cataclasite	0 cm	0.06	0.18	0.56	1.29	3.80	2.03	2.12	4.00	13.25	62.62	9.71	99.62
132	Waikukupa Thrust	cataclasite	70 cm	0.13	0.11	0.89	4.20	0.52	3.74	4.93	7.73	14.37	59.25	3.77	99.64
124		cataclasite	25 cm	0.12	0.09	0.52	3.25	0.30	4.41	3.16	5.58	12.81	55.58	13.81	99.64
125_1		cataclasite	8 cm	0.11	0.10	0.61	3.11	0.44	4.34	3.44	5.57	12.73	58.13	11.00	99.57
131_2		gouge	2 cm	0.15	0.16	0.72	1.38	2.11	10.09	2.98	6.15	12.75	50.31	14.73	101.53
131_1		gouge	0 cm	0.27	0.13	0.57	0.85	1.78	24.96	2.42	5.18	10.07	38.62	12.73	97.58
133		gravel	- 10 cm	0.11	0.15	0.81	3.03	1.82	2.47	2.74	6.12	14.75	64.98	2.74	99.73
127_3	Martyr River	cataclasite	2 cm	0.11	0.18	0.69	2.27	1.80	8.74	4.50	6.11	13.45	52.67	8.96	99.47
127_4		gouge	0 cm	0.10	0.14	0.56	2.09	1.55	3.50	10.59	5.99	11.07	56.61	7.34	99.54

[a)] Datum to calculate distance to PSZ refers to center of PSZ at Martyr River, Havelock Creek and the DFDP-1A borehole and to the contact between PSZ and footwall at Waikukupa Thrust and Gaunt Creek.

[b)] Fe_2O_3 is total Fe content.

Table 6. Slope *m* of the isocon and derived mass change [%], enrichment (positive values) and depletion (negative values) of elements for samples investigated relative to the host rocks. Geochemical composition of fault rocks is taken from table 5 and composition of host rocks from Table S1. All concentrations are in wt%.

sample	location	unit	dist. to PSZ[a]	m	mass	MnO	P_2O_5	TiO_2	Na_2O	K_2O	CaO	M
129	Havelock Creek	gouge	0 cm	~~0.74~~ 0.78	~~35.12~~ 27.40	~~251.30~~ 94.85	~~117.61~~ 65.08	~~126.88~~ 55.91	~~-21.93~~ -31.00	~~-7.63~~ -35.68	~~587.26~~ 395.11	~~324.5~~
130_1	Gaunt Creek	gouge	0 cm	~~0.74~~ 0.78	~~35.85~~ 28.07	~~258.65~~ 98.89	~~101.63~~ 52.93	~~115.38~~ 47.97	~~-13.97~~ -23.97	~~118.48~~ 52.11	~~496.81~~ 329.87	~~269.9~~
130_2		gravel	- 2.5 cm	~~0.78~~ 0.83	~~28.45~~ 21.15	~~167.18~~ 48.23	~~110.93~~ 60.06	~~125.06~~ 54.69	~~-12.78~~ -22.89	~~90.15~~ 32.45	~~302.83~~ 190.29	~~266.1~~
130_3		gravel	- 4.75 cm	~~0.80~~ 0.85	~~25.34~~ 18.29	~~180.77~~ 55.86	~~102.86~~ 54.02	~~93.24~~ 32.90	~~-13.66~~ -23.63	~~76.30~~ 22.87	~~354.81~~ 227.92	~~231.0~~
120	DFDP-1A	cataclasite	292 cm	~~0.86~~ 0.91	~~16.28~~ 9.66	~~46.51~~ -18.72	~~55.14~~ 17.71	~~69.33~~ 16.38	~~-56.35~~ -61.41	~~140.18~~ 67.28	~~46.17~~ 5.32	~~161.8~~
119		cataclasite	270 cm	~~0.76~~ 0.80	~~31.56~~ 24.44	~~94.71~~ 8.34	~~58.91~~ 20.93	~~71.30~~ 18.08	~~-0.36~~ -11.66	~~56.58~~ 9.38	~~223.08~~ 133.48	~~119.4~~
118		cataclasite	135 cm	~~0.93~~ 0.98	~~7.96~~ 2.07	~~-7.16~~ -48.36	~~41.48~~ 7.62	~~29.32~~ -10.89	~~-58.06~~ -62.83	~~121.40~~ 54.59	~~23.11~~ -11.07	~~103.5~~
117		cataclasite	87 cm	~~0.76~~ 0.80	~~32.43~~ 25.34	~~111.89~~ 17.97	~~62.06~~ 23.40	~~48.71~~ 2.57	~~-63.69~~ -67.78	~~105.81~~ 43.86	~~240.66~~ 146.35	~~210.1~~
116		cataclasite	25 cm	~~0.64~~ 0.68	~~55.21~~ 46.33	~~430.81~~ 194.38	~~121.78~~ 68.22	~~128.28~~ 56.85	~~-80.75~~ -82.99	~~171.74~~ 89.20	~~1005.22~~ 696.11	~~420.2~~
115		gouge	0 cm	~~0.88~~ 0.93	~~13.47~~ 7.37	~~31.62~~ -26.74	~~60.35~~ 22.07	~~33.33~~ -8.06	~~-52.22~~ -57.62	~~112.06~~ 48.18	~~49.25~~ 7.90	~~79.9~~
132	Waikukupa Thrust	cataclasite	70 cm	~~0.84~~ 0.89	~~19.03~~ 12.28	~~219.01~~ 77.01	~~3.37~~ -21.55	~~120.21~~ 51.38	~~63.20~~ 44.30	~~-69.56~~ -78.79	~~188.46~~ 107.89	~~339.0~~
124		cataclasite	25 cm	~~0.79~~ 0.84	~~26.61~~ 19.72	~~206.41~~ 70.42	~~-6.04~~ -28.52	~~37.69~~ -5.12	~~34.33~~ 19.06	~~-81.32~~ -86.96	~~261.79~~ 161.36	~~199.3~~
125_1		cataclasite	8 cm	~~0.82~~ 0.87	~~21.60~~ 15.00	~~165.08~~ 47.46	~~-8.80~~ -30.61	~~54.27~~ 6.33	~~23.45~~ 9.43	~~-73.69~~ -81.62	~~241.94~~ 147.07	~~212.9~~
131_2		gouge	2 cm	~~0.72~~ 0.76	~~38.66~~ 30.82	~~324.29~~ 135.48	~~71.86~~ 30.45	~~108.28~~ 43.20	~~-37.54~~ -44.76	~~43.89~~ 0.26	~~806.52~~ 553.46	~~209.1~~
131_1		gouge	0 cm	~~0.56~~ 0.60	~~78.51~~ 67.79	~~853.23~~ 427.04	~~83.21~~ 38.54	~~112.72~~ 45.71	~~-50.47~~ -56.36	~~56.27~~ 8.47	~~2786.97~~ 1973.23	~~223.1~~
133		gravel	- 10 cm	~~0.92~~ 0.97	~~9.28~~ 3.22	~~146.97~~ 37.22	~~32.00~~ 0.31	~~83.50~~ 26.31	~~8.09~~ -4.30	~~-2.19~~ -31.77	~~74.89~~ 26.22	~~124.0~~
127_3	Martyr River	cataclasite	2 cm	1.05	- 4.44	- 43.42	26.05	- 21.40	- 9.39	189.57	- 25.18	- 4
127_4		gouge	0 cm	1.09	- 8.54	- 49.46	- 1.42	- 39.56	- 20.16	138.65	- 71.32	2

[a] Datum to calculate distance to PSZ refers to center of PSZ at Martyr River, Havelock Creek and the DFDP-1A borehole and to the contact between PSZ and footwall at Waikukupa Thrust and Gaunt Creek.

[b] Fe_2O_3 is total Fe content.

Referee Comment (RC) 1

We are grateful to Christoph Schrank (CS) for his in-depth, well-structured and critical review. We think that in addressing his comments we will substantially improve the manuscript. He presented three major criticisms of the work (points RC1 – 1 to RC1 – 3). We respond to these first by repeating the referee's comments in bold font, then our responses are in plain text. Christoph Schrank also provided additional specific comments in an annotated pdf. We have also copied these comments into this document (except for typos, which we just corrected) so that it is easy to demonstrate what modifications are made in the revised manuscript in response to them.

RC1 – 1

The attempt to correlate microstructural and hand-specimen scale geochemical data to fault architecture on scales of up to > 100 km is problematic, mainly due to data sparsity and observational bias.

We agree with the reviewer that data sparsity likely imposes observational bias in our study. However, we do not claim to provide a complete model of the Alpine Fault's architecture. Instead, we highlight that our microstructural and geochemical data from four key sites suggest that the architecture of this particular fault could be more complex than previously thought. However, some upscaling/extrapolation of our results to other scales is feasibly accomplished by discussing our observations in the context of existing seismic investigations (see lines 546 – 549).

Our methodology is similar to that employed by previous studies of the Alpine Fault rocks, which, because of the nature of outcrop, have to rely on detailed investigations of one or only a few locations (e.g. Boulton et al., 2012; Sutherland et al., 2012; Toy et al., 2015). Barth et al. (2013) employed a very similar approach to ours (in terms of methods used and amount of locations studied) to investigate the architecture of the Alpine Fault's southern segment. Our study essentially extends the work of Barth et al. (2013) to the fault's central segment.

In my opinion, the authors are a bit too optimistic when it comes to drawing rather general conclusions in regards to correlating geometric properties of the studied fault to (micro- and mesostructural) host-rock properties. Since this correlation constitutes a core focus of the manuscript, it deserves particular care. Let me give some examples in the following

Lines 271 – 273: "Amount and size of clasts generally decrease towards the PSZ and vary systematically with PSZ thickness (Table 1): locations with thinner PSZ contain more clasts in the hanging-wall, which tend to be larger, compared to locations with thicker PSZ."

I admit I find this statement problematic. Table 1 provides hanging-wall observation for three locations. However, PSZ-proximal detrital clasts and matrix clasts are only sampled at two out of the three locations. Two data points with different values always display an apparent linear trend. I do not think that such a general statement is warranted based on

the very sparse data. Moreover, it has been shown in continuous fault outcrops that PSZ width can easily vary by a factor of 10 on along-strike scales of tens of meters without changes in host rocks (see for example the very nice recent paper by Kirkpatrick et al. 2018 – highly relevant to the work at hand).

Regarding the first part of this comment we agree that our statement "locations with thinner PSZ contain more clasts in the hanging-wall, which tend to be larger, compared to locations with thicker PSZ" is problematic because the outcrop situation provides only two locations, where the relationship between amount / size of grains and PSZ thickness can be investigated. The intention of this statement is to describe an observation. We highly encourage others to provide additional observations supporting or disproving our statement. Furthermore, we like to emphasize that this statement is not further exploited in the discussion of this manuscript, i.e. no general conclusions are based on this statement, which reflects that it describes an observation.

The decrease of amount and size of clasts towards the PSZ described in the manuscript is based on thin section analyses and is in accordance with outcrop observations (i.e. can be observed at all four outcrops) and previous work (e.g. Boulton et al., 2012; Toy et al., 2015). We will state this in the revised version of the manuscript. Please note, while PSZ-proximal detrital clasts have not been sampled, matrix clasts have not been observed at Martyr River.

The second comment, that "PSZ width can easily vary by a factor of 10 on along-strike scales of tens of meters without changes in host rocks" has motivated us to take a closer look at previous studies that examined PSZ width and consider comparisons to the work we present.

A few past studies report dramatic thickness variations in fault gouges. Shervais and Kirkpatrick (2016) and Kirkpatrick et al. (2018) report extreme thickness variations over short distances within the most recently-active of 13 slip zones that make up the so-called "inner fault core" of a fault that accumulated a total displacement in the order of 10 – 30 km (Shervais and Kirkpatrick, 2016). While the fault's total displacement is fairly-well constrained, it is unknown how much displacement each individual slip layer accumulated. It could easily be that the particular layer ("layer m") with thickness variations only accommodated a couple of meters of slip. Other studies of faults that accommodated displacements ranging between 1cm and 1km have reported large thickness variations over short distances parallel to displacement (e.g. Sagy et al., 2007; Sagy and Brodsky, 2009; Brodsky et al., 2011; note: it is debatable if these three studies are at all comparable in this context – see response to aspect RC1 – 3[c](2)).

With ~470km (Sutherland et al., 2007) the Alpine Fault has accommodated a much larger total offset than the slip zones investigated by e.g. Shervais and Kirkpatrick (2016) and Kirkpatrick et al. (2018). This difference suggests that variations in fault thickness are not as comparable as they appear on first hand. In addition, many studies dealing with thickness variations as function of displacement generally note that "faults smooth with increasing slip" (Brodsky et al., 2011; see also Sagy and Brodsky, 2009). In this context, thickness variations of e.g. *layer m* from Shervais and Kirckpatrick (2016) and Kirckpatrick

et al. (2018) appear to reflect rough contacts between the slip zones and the surrounding units. The Alpine Fault, with its substantially larger amount of slip accommodated, displays – where sufficiently exposed – smooth contacts between fault gouge and hanging- and footwall, respectively (see Figures 4b-d and 5b-d in the manuscript; see also Sagy and Lyakhovsky, 2019). These observations further suggest that thickness variations reflect different amounts of accommodated displacement.

Sagy and Brodsky (2009) document a fault where there is "a monotonic, nonlinear positive correlation between the displacement on the fault and the thickness of the cohesive granular layer". In other words, they observe that thickness increases with displacement (see also their Figure 10), so assuming comparable incremental displacements, an individual fault plane that accommodated more earthquakes will be thicker than a fault plane that accommodated fewer events. This is in accordance with previous studies (e.g. Evans, 1990; Faulkner et al., 2010; Ben-Zion and Sammis, 2003), and also one of our major conclusions (see paragraph lines 519 – 529).

Mineralogical differences could be another factor limiting the comparability of results described by e.g. Sagy and Brodsky (2009) or Shervais and Kirckpatrick (2016) and our study. Sagy and Brodsky (2009) describe a fault with layered damage architecture. In their setting, thickness variations are not related to the layer hosting the principal slip surfaces but to a layer containing a cohesive granular material mostly (> 90%) composed of plagioclase. This layer is interpreted to be "more cohesive than the surrounding damage zone". This contrasts with the Alpine Fault gouge, which is phyllosilicate-rich (between ~30 to ~60wt% in investigated samples; see also Figure 8 in the manuscript) and incohesive (Boulton et al., 2012). Slip zones described by Shervais and Kirckpatrick (2016) contain phyllosilicates but amounts are typically smaller compared to the Alpine Fault.

While we are still convinced that – despite the limitations of poor outcrops – it is appropriate to discuss variations in Alpine Fault gouge thickness in the context of fault zone architecture, we acknowledge that variations in fault zone thickness should be discussed in a broader context than it has been done in the manuscript. Consequently, we will include the above discussion in the revised version of the manuscript.

Lines 294 – 295:" The type of contact between hanging-wall cataclasites and fault gouge correlates with PSZ thickness: where the PSZ is thicker, contacts are transitional manifested by decreasing grain sizes (Table 2) and correlate with increasing amounts of phyllosilicates [...]".

The cited table also reveals that only two of the five studied locations expose, or allowed sampling of, the contact between hanging-wall cataclasites and PSZ. So again, two data points only are available and do not inspire tremendous statistical confidence in the validity of the above statement.

Similar to our statement "locations with thinner PSZ contain more clasts in the hanging-wall, which tend to be larger, compared to locations with thicker PSZ" the statement "the type of contact between hanging-wall cataclasites and fault gouge correlates with PSZ thickness […]" here describes an observation. However, this statement is repeated in the

discussion section (lines 492 – 493). While we consider this statement as a valuable observation to be (not) confirmed by succeeding studies, we agree that data are too scarce to derive any conclusions from it. We will remove this statement from the discussion.

RC1 – 2

The isocon analysis as conducted here is problematic.

Before replying to the individual aspects of this comment, we realized that equations 1 and 2 of the manuscript contained typos. Eq. 1: there should be super- instead of subscripts to index concentrations of altered and host rock, respectively; Eq. 2: it should have been m^{-1} instead of m (compare to equation 6 in Grant, 1986). We will change this in the new version. Fortunately our original calculations already employed the correct equation.

[a] Line 214: The authors emphasize that the choice of host rock is important for isocon analysis. In this context, it would be interesting if they added an explanation for their choices. For example, for the Alpine schist, they averaged compositional data from three samples obtained across a linear distance of < 20 m in a single drill hole. This drill hole is far away from most of the sites studied in this manuscript. Hence, one wonders: how heterogeneous is the Alpine schist chemically? Even in the three host rock samples used for averaging certain oxide proportions vary by a factor of 2, for rocks just a few meters apart. How large is this variability on the scales of tens of kilometres? In this context, it would be instructive, as a first test, to check if the chemical variability implied by the presented isocon plots is of the same order as that observed in the chosen (and ideally other) host-rock samples.

We agree that the protolith geochemistry is poorly constrained. In order to improve this, the revised version of the manuscript will include all other published geochemical analyses of the Alpine Schist, namely Tables 1 and 2 of Roser and Cooper (1990) and the data provided by Grapes et al. (1982). These additional data in combination with the ones already used in the manuscript cover the entire central segment of the Alpine Fault.

These additional data are in agreement with those already reported in the manuscript and do not substantially change the results of the isocon analyses (Figure 1). On average, slopes derived from analyses with better constrained protolith geochemistry are 0.045 larger than slopes solely based on protolith geochemistry provided by Toy et al. (2017). These modifications do not affect the overall behavior; i.e. all outcrops with the Alpine Schist as protolith are still affected by mass gains owing fluid-related alteration but absolute gains are on average 7.6% smaller (new: 26.7% vs. old: 34.3). However, slightly larger isocon slopes imply that some individual elements in some samples are less enriched or even depleted (e.g. Al is now depleted in 3 out of 6 samples in the DFDP-1A core).

[b] Moreover, it may be interesting to consider additional constraints on the slopes of the isocons. Given that the deformation pT-conditions are quite well known, it appears potentially useful to identify elements, which can be considered as relatively immobile a priori, for the choice of an isocon rather than a simple (least-squares?) linear fit (compare Schleicher et al. 2009).

In the preceding study of Schuck et al. (2018) we also performed an isocon analysis. In this, we assumed either Al or Ti to be immobile, respectively. However, results revealed that both phases are mobile (up to 28% enrichment of Ti based on immobile Al; up to 22% depletion of Al based on immobile Ti). We will refer to this previous study more explicitly in the revised manuscript. For a detailed evaluation of the process providing the isocon please refer to the reply to aspect c (below).

[c] Conversely, it would be instructive to discuss/consider if the best-fit isocon obtained in the present manuscript is consistent with geochemical expectation. For example, Na appears to be immobile while Al is relatively mobile according to the isocon example in Fig. 1 below. The same trend is implied for quartz relative to Al. Does this really make sense?

Grant (2005) discusses several possibilities to derive the isocon: (I) clustering of C_i^A/C_i^O (concentration of an elemental species i determined from an altered sample A divided by the one determined from the protolith O); (II) a best fit of data forming a linear array through the origin in an isocon diagram (the graphical equivalent of I); (III) the a priori assumption that certain components were immobile; (IV) the assumption of constant mass during alteration; (V) the assumption of constant volume during alteration.

By using option (III) one often assumes immobile Ti and / or Al. This assumption has been shown to be invalid for the fault in our past work (Schuck et al., 2018) – see reply to [b] (above). Assuming other elements than Ti and Al to be immobile (such as Zr as in Schleicher et al., 2009), implies that concentrations of these elements are commonly determined. However, Zr is not always measured (see for example Toy et al., 2017) limiting the amount of potentially available protolith data. Furthermore, it is debatable if the elements assumed to be immobile are actually immobile.

Options (IV) and (V) appear to be inconvenient, because increasing amounts of phyllosilicates towards the PSZ (e.g. Sutherland et al., 2012) suggest mass changes and substantial formation of calcite veins within the PSZ suggests significant volume increases (see Schuck et al., 2018).

Option (I) and its graphic equivalent option (II) are worthy of a closer examination: the four data points (Si, Ti, Al, Cu) chosen by Grant (2005) to determine the isocon cluster around 1 (maximum difference between individual points: 0.057; standard deviation: 0.026; Table 1, *Panel A*). However, Fe, Mg, Na and Zn cluster around 0.73 and appear to better constrain the isocon as their spread is 0.029 (standard deviation: 0.013). Furthermore, while the option chosen by Grant (2005) does not suggest substantial mass changes, the second option presented here suggests mass changes. In our opinion, this highlights that even data-based methods to derive the isocon may be biased.

In order to minimize the bias related to the determination of the isocon, we decided to derive the isocon with a best-fit of all data as this approach does not require any assumptions.

Results of isocon analyses with better constrained protolith geochemistry still show Al enrichment / depletion. However, absolute values are smaller: up to 15% enrichment / up to 5% depletion with better constrained data vs. up to 44% enrichment in the original manuscript. Comparison of Tables 6 and S2 of this manuscript with Table 4 of Schuck et al. (2018), where immobile Ti has been assumed, indicates that the results of both isocon analyses are in general agreement with each other.

Furthermore, results of isocon analyses with better constrained protolith geochemistry now indicate Na depletion except for the cataclasites at Waikukupa Thrust. Na depletion is in accordance with alteration of albite to phyllosilicates (see Figure 6a of the manuscript). However, Na enrichment in the cataclasite at Waikukupa Thrust (Table 6 of the manuscript) is not easily explained.

[d] On this note, linear fitting can entail a bias towards high-concentration elements (depending on the mathematical fitting method), which can constitute a problem. This issue is explained in the caption of Fig. 1 in more detail. This bias can be avoided by data scaling, as discussed in Grant's seminal paper of 1986. It is also interesting to recall that Grant (2005), the principal developer of the method, recommended to avoid the use of log-log-diagrams in isocon plots in this review paper. I echo his concerns here. It is easier to recognize elements not fitting the isocon on a linear scale (Fig. 1 below).

In the caption of his Figure 1 the reviewer states that "the given linear fit implies that SiO_2 is less mobile than Al_2O_3, which may be an artefact of the fitting method." However, isocon analyses indicating relatively immobile SiO_2 are not necessarily an artefact of the fitting method. Mineral dissolution simultaneous with phyllosilicate formation is a better explanation for the apparent immobility of SiO_2.

Data scaling would not resolve a potential bias resulting from linear fitting: by taking the data presented in Tables 6 or S1 (summarized in the reviewer's Figure 1) and scaling SiO_2 concentrations by a factor of 0.5 (see Grant, 1986) one would still get the same slope for the isocon.

We agree that isocon analysis should not be performed in log-log space. Fortunately, ours was not, as can be seen in our equations 1 and 2 of the manuscript. After having derived all important parameters (namely the slope of the isocon, mass changes and element enrichment / depletion) we plot element concentrations and the isocon in a diagram and use a logarithmic scale for its axes. This has the advantage that now there is no clustering of data points with concentrations smaller than 10wt% (compare Figure 1 from the reviewer and Figure 9 of our manuscript; see also Figure 6 in Schleicher et al. 2009). This means that we derived mass changes and element enrichment / depletion from mathematical operations and not graphically from the isocon. The plotted isocon diagrams (Figure 9) are a condensed, hence simplified, visualization of Tables 6 and S1.

Finally, in the light of the comments above, the following statement (line 226 – 227) appears problematic: "The method nevertheless allows relative geochemical changes within the fault zone at this location to be accounted for." This is probably not the case for elements where the variability within the host-rock samples is of the same order as those measured in the altered rock, or, even worse, for which the host-rock composition or isocon are chosen incorrectly. In summary, I recommend a careful revision, replotting, and subsequent reinterpretation of the isocon analysis. If one accepts this recommendation, section 5.1 of the discussion will most likely have to be rewritten substantially. It is important, but not discussed, that the isocon analysis conducted here differs significantly, both in methodology as well as outcomes, from a similar study on SAFOD samples conducted by Schleicher et al. 2009.

We agree that the choice of the protolith or the isocon might have substantial impacts on the results of the isocon analysis. However, as indicated in the reply to aspect [a], better constraining protolith composition by using all available data has an impact on some of the elemental species analyzed (absolute values of enrichment / depletion change), but has no impact on the overall behavior. This meets our expectations: Isocon slopes of analyzed fault rocks being substantially smaller than 1 indicate substantial amounts of fluid-related alteration, which lead to mass gains (e.g. formation of authigenic mineral phases). This is in accordance with microstructural observations of this and preceding studies (e.g. Sutherland et al., 2012) which demonstrate pervasive authigenic mineralisation. On these bases, we would have been very surprised if slightly modified protolith compositions resulted in isocon slopes of 1 (no fluid-related alteration) or greater than 1 (mass losses associated with fluid related alteration). Note that the situation at Martyr River differs, as already discussed at lines 401-402 of the manuscript.

We conducted our isocon analysis based on the equations provided by Grant (1986). Our equation 1 corresponds to equation 5 in Grant (1986) and our equation 2 corresponds to equation 6 in Grant (1986). In this, the approach is comparable to the one used by Schleicher et al. (2009). However, there are a few key differences: Schleicher et al. (2009) assume immobile Ti and Zr and derive the slope of their isocons by applying a best-fit to these two data points, whereas we chose a best-fit to all data points; as we justified in our reply to aspect [c]. Furthermore, they assumed constant densities, which we do not, because we expect that volume and mass change during authigenic alteration.

Schleicher et al. (2009) report two mass changes: (I) one for the entire fault rock (their Figure 6) and (II) one for individual elemental species (their Table 1). These mass changes of individual elemental species are calculated following equation 6 of Grant (1986), which corresponds to equation 2 of our manuscript. However, the results do actually not reflect mass changes but "change[s] in concentration of a component relative to its concentration prior to alteration" (Grant, 1986); i.e. element enrichment (positive values) or depletion (negative values).

In contrast to Schleicher et al. (2009), we decided to not perform a mass transport calculation, because this calculation is not necessary to assess the general pattern of fluid-related alteration, which was our motivation for the performance of the isocon analysis.

As will be discussed below in our reply to the comment in line 408 of the annotated manuscript, major differences between the study presented here and the one presented by Schleicher et al. (2009) – predominant element enrichment vs. predominant element depletion – probably reflect that the hydrological systems and host rock compositions of the Alpine Fault and the San Andreas Fault differ, so the nature of fluid-related alteration also differs. In this context we do not see any need to discuss our results with regard to the methodology / results presented by Schleicher et al., 2009.

RC1 – 3

The discussion linking geometrical characteristics of fault core and principal-slip zone to microstructures, geochemistry, and rheology is partially not well aligned with the cited literature. It would also benefit from consideration of additional articles on this field. Finally, some physical/mechanical processes of potentially high relevance are mentioned for the authors' kind consideration.

I have a number of concerns related to section 5.5.2 – Alpine fault core.

[a] I noticed a few occasions where certain statements and the associated references do not align very well. I point them out in the annotated PDF.

We address these concerns below, where we reply in detail to comments provided in the annotated pdf.

[b] Fig. 10 contains a mistake – please, see annotated PDF for explanation.

We appreciate the reviewer pointing out that what we had written in lines 471 – 485, which relate to Figure 10, was confusing (see also RC3). The figure we presented is correct and indeed implies that most strain is accommodated in the FW-proximal gouge.

Lines 471 – 476 describe briefly observations of Cowan et al. (2003) of low-angle detachment faults in the Death Valley. These faults juxtapose strong footwall rocks on weakly consolidated hanging-wall sediments, and have layered fault gouges.

Lines 477 – 485 aim to explain that the Alpine Fault is comparable to these low-angle detachment faults, in having a layered fault gouge and juxtaposing strong hanging-wall rocks on weakly consolidated footwall sediments (see also Biegel and Sammis, 2004). In both cases the fault gouge layers in contact with the weakly consolidated sediments (Death Valley low-angle detachment fault: hanging-wall; Alpine Fault: footwall) are microstructurally comparable (fine-grained, clast-poor).

Cowan et al. (2003) concluded that the gouge layer in contact with the weakly consolidated hanging-wall sediments accommodated more strain than the gouge layer in contact with the stronger footwall rocks (see their Figure 11b). Guided by this, we hypothesised that – when adjusted for the different kinematic situation (i.e. thrust vs. normal movement) – in the Alpine Fault Zone the footwall-proximal layer in contact with weakly consolidated sediments accommodated more strain than the hanging-wall-proximal layer. This situation is sketched in our Figure 10.

We will include this revised and – and hopefully clearer – explanation in the revised manuscript.

[c] As already explained in section 1, I have some reservations in regards to generalisations about factors controlling PSZ thickness presented here. In a nutshell:

1) Due to sampling difficulties, data are too sparse to conduct statistically meaningful tests – two or three data points are not enough.

As discussed above, we agree that data are sparse. However, we have described all known fault gouge outcrops NE of Martyr River. Data coverage can only be improved by more expensive approaches (such as drilling projects). We will clearly acknowledge this in the revised manuscript.

2) Relevant existing literature (Kirkpatrick et al. 2018 and references therein; the work of Emily Brodsky and Amir Sagy, etc.) on thickness variations of PSZ is not considered but highly relevant to the study at hand.

As outlined above, we agree that recent work on PSZ thickness variations (e.g. by Sagy et al., 2007; Sagy and Brodsky, 2009; Shervais and Kirkpatrick, 2016; Kirkpatrick et al., 2018) needs to be discussed in the revised manuscript.

However, we also note, that it is questionable, if results of e.g. Sagy et al. (2007), Brodsky et al. (2011), and Sagy and Lyakhovsky (2019) are comparable with ours. These studies investigate fault planes and analyze their roughness by examining the geometric properties of bumps and depressions. For us, it does not imply that these geometric features directly link to fault gouge thickness variations as there are no data along transect oriented normal to the fault plane (compare with Sagy and Brodsky, 2009, where fault plane bumps and depressions have been attributed to deformation in a layer located structurally below the fault gouge).

3) Given thickness variability of PSZ on the scale of metres (see literature in point 2), the question arises: is it at all useful to compare thickness variations at locations of up to tens of kilometres apart? This question warrants some careful discussion.

We agree that it would be optimal to study the fault zone architecture of the Alpine Fault in outcrops being located closer to each other. Nonetheless (and as outlined above), in absence of more outcrops than studied in the investigated fault segment, we consider it useful – though not ideal – to compare thickness variations at locations being as apart as they are in our study. While this approach does not allow to provide a detailed model of the fault zone architecture, we are confident that we are able to demonstrate that the Alpine Fault is more complex than previously thought (e.g. Norris and Cooper, 2007), and think that it is valuable to highlight this.

Our work is also valuable, because the Alpine Fault has accommodated so much more displacement than faults examined in previous studies of fault principal sip zone geometry

(see references introduced in our reply to point 2), which mostly focused on displacement-thickness- and displacement roughness-relationships.

[d] More generally, I feel that the pre-existing ideas from the mechanical literature on fault-zone width are not as well conidered as they could be. I choose one sentence to kick off my little discussion of this criticism (noting that there are other statements which inspire further critical thought):
Lines 512 – 513: "This suggests that strain localization within the fault core might be governed by processes insensitive of rheological variations caused by differing fault rock composition."

Problem 1: It is well known that materials of identical composition can have very different rheological properties because of, say, differences in microstructure (porosity, grain size, grain shape, grain alignment or lack thereof), fluid pressure, strain rate, etc. So this statement is not surprising or new and not well supported by references to existing literature.

We agree that there are other properties than mineralogy, which could affect rheology. However, the grain shapes and alignment we were able to examine appear to display only minor variations between individual outcrops. In the revised version, we will highlight that there could be other factors causing the observed thickness differences but that it is not possible to identify them owing to the scarce data.

We disagree with the reviewer that "this statement is not surprising or new and not well supported by references to existing literature". In the past it has been proposed that the Alpine Fault's architecture is consistent with the conceptual model of Caine et al. (1996) (e.g. Williams et al., 2016). However, we argue that this view is most likely an oversimplification and that the conceptual model presented by Faulkner et al. (2003) might be more suitable to describe the Alpine Fault (lines 566 – 568). We realize that this conclusion needs to be pointed out more explicitly in the revised manuscript.

The criticized sentence at lines 512 – 513 should be considered in context with its preceding sentence "[…] unlike other fault zones worldwide, the Alpine Fault displays a negative correlation between phyllosilicate content and fault core thickness", which is one of the key-messages of this study.

Problem 2: One important assumption in this statement is that the process of strain localisation within the PSZ postdates the formation of fault rock containing it quite significantly.
There is good experimental literature on monophase, homogeneous materials with strain softening that shows that the localization process of the first fault itself happens during the transient strain-softening response of the material. During this period, the fault width and basic architecture are basically fixed and remain constant for quite some time during steady-state flow (provided that there are no other huge external changes such as a change in plate velocity or the arrival of an exotic block of wall rock with vastly different properties). I am

going to do the terrible, terrible deed and sneak in some advertisement of our own work in this context (Schrank et al. 2008, Schrank and Cruden 2010), mainly because it is very easy to understand since the experiments are very simple but well controlled. So, once the fault core has formed, one obtains a weak material with irregular interfaces to the adjacent wall rocks, which in turn quite likely have different material properties. Such a state can easily lead to highly heterogeneous stress and strain distributions, which in turn control further localization within the fault rock. I illustrate this point with a (really quick and dirty) numerical simulation shown in Fig. 2.

In summary: local geometrical perturbations can play a very significant role in strain localisation and, accordingly, PSZ geometry. Moreover, the first localisation step likely occurs in the transient strain-softening domain – which is poorly understood mechanically because it is very difficult to run good experiments in this domain at geological conditions and it is also painful mathematically – and can easily introduce complex geometries even in simple materials with simple loading geometry.

There is little doubt that the fault gouge at some stage of its history was weaker than its parent rock, and thus strain softening must be considered in interpreting localisation geometries.

There is no doubt that the experiments reported in Schrank et al. (2008) are valuable to understand strain localization in general. However, their use to understand the geometry evolution of the Alpine Fault might be limited, because these experiments assume isochoric, isothermal, isochemical conditions and no changes in deformation mechanisms.

After having been uplifted along a single fault plane from a detachment at ~35 km depth (Little et al., 2005), the typical fault rock sequence encountered at the Alpine Fault (Figure 2c of the manuscript) records (a) progressively increasing strain from the hanging-wall towards the fault plane and (b) a change from ductile (mylonite formation; distal to the fault plane) to brittle (cataclasite formation; proximal to the fault plane) deformation mechanisms. We agree that the basic architecture of the fault might have been fixed at the onset of faulting. The Alpine Fault Zone rocks were deformed ductilely at depth then this was overprinted by brittle deformation. It is very likely the planar architecture and specific mineralogical arrangement imposed on the mylonites during creep have an impact on the fault gouges we focus on. This is dissimilar to the models the reviewer presents, but it is probably important in localization of deformation. However, our observations do not address this aspect. We are not looking at the results of early shear (i.e. fault zone evolution). Instead we focus on the description of the result of fault gouge evolution.

Fault rocks encountered in DFDP-1B (Figure 3a in the manuscript) demonstrate the complexity of the Alpine Fault Zone in the brittle regime. There, two PSZs were sampled, both surrounded by brittle fault rocks. We can interpret these two PSZs in two ways: (I) displacement was localized at more than one PSZ, which is dissimilar to the common view that Alpine Fault Zone uplift occurred along a single fault plane, and /or (II) that one PSZ

was abandoned and displacement transferred to another PSZ (fault gouge dating could help to resolve this issue, but is beyond the scope of this paper).

By writing this down, we realize that this line of reasoning is poorly explained in the manuscript (see lines 531 – 532) and needs revision.

These points highlight some issues I deem very relevant to the work at hand and well established in the literature but not considered here. I also noted a few smaller but relevant issues with the logical chain of arguments leading to some of the proposed conclusions in this discussion section in the annotated PDF.

In conclusion: due to the concerns outlined above, I believe that most of the discussion section would greatly benefit from a substantial overhaul, informed by revisiting and reassessing already cited and new literature, and considering the issues I mentioned in sections [1], [2], and [3]. It follows that the conclusion then should also be rewritten.

Below we respond to the specific comments on the manuscript except for cases where e.g. typos are highlighted. Numbers refer to the line in the pdf where the reviewer placed his comment

l. 45: It [the Punchbowl Fault] has a single PSZ.

CS: In Chester and Logan 1986, it can be seen that the longest continuous along-strike outcrop has a length of < 600 m. All other outcrops expose much shorter segments. I am mentioning this here to highlight that your study looks at a very different length scale. Moreover, one cannot be entirely certain that the Punchbowl fault consists of a continuous PSZ/core.

Our response: We briefly review published work on the Punchbowl Fault, because it is the classical example for the fault model proposed by Caine et al., (1996). However, we do not try to directly compare our observations with those obtained from the Punchbowl Fault, because the displacement on that structure and its overall geometry is dissimilar to the Alpine Fault.

l. 47: The core of the Punchbowl Fault is surrounded by an approx. 15 m thick damage zone […].

CS: In C&L 1986, they state 30 m as average DZ width.

Our response: Chester and Logan (1986), p. 83, last paragraph states: “These features increase in intensity towards the main gouge zone and define a zone of intense deformation that is laterally continuous but variable in width, averaging 15m.”

l. 60: Atypical for fault zones hosted in quartzofeldspathic protoliths […].

CS: I am not aware of a study that convincingly establishes this link in such general terms. Could you please add the related citation?

Our response: Here is an example: Faulkner et al. (2003) in their study comparing the quartzofeldspathic Punchbowl and San Gabriel Faults with the phyllosilicate-rich Carboneras

Fault state that “extreme localization, such as that seen more commonly in quartzo-feldspathic fault zones, suggests strain weakening and/or velocity weakening” (section 3.2, 1st paragraph).

l. 242: These [PSZ] thickness variations appear to be not systematically controlled by protolith lithology […].

CS: Can you really assess this? How much lateral displacement has occurred in each outcrop? What constitutes "lithology" in your case? Composition? Grain size? Grain shape? A relatively large number of microstructural properties determine the mechanical properties of a material - not just composition - and, of course, finite strain is quite important for the PSZ thickness.

Our response: Figure 2(b) shows that four out of five sample locations have the Alpine Schist (Torlesse Terrane) as protolith. In this case “lithology” refers to mineralogical composition. However, to acknowledge the referee’s valid concern, we will reformulate the sentence to: “Except for Martyr River, these locations have the same protolith (Fig. 2b.; see section 4.3). Furthermore, there is no systematic variation of PSZ thickness along-strike. This highlights that the fault core has a very variable character at different locations.”

l. 279: In addition, some microfaults have cores made of coarser-grained matrix and clasts or calcite veins surrounded by fine-grained gouge.

CS: Do you know the relative timing between microfaulting and calcite veins?

Our response: We re-examined the images displaying microfaults with calcite veins. We definitely cannot derive relative ages from cross-cutting relationships in them. Consider Figure 6i (below “B” of “BSE”) – here the microfault-matrix contains calcite clasts, which may originate from comminution of a calcite vein, which would imply that vein formation predated microfaulting. However, calcite veins are also seen in the cores of some other microfaults (no images shown in the manuscript), which indicates that vein formation postdates microfaulting. So… there are no systematic cross-cutting relationships and we cannot define one simple sequence of events.

l. 306: Where the PSZ is thinner, clasts tend to be more abundant and sizes tend to be larger.

CS: One could simply conduct a statistical test to quantify the correlation strength. Please, feel encouraged.

Our response: These observations are qualitative not quantitative.

l. 340: There are no discrete slip planes within the fault gouges.

CS: You did not sample any – preservation / recognition potential are an issue…

Our response: We will reformulate this sentence.

l. 364: They [Qtz and Fsp phases] do not exhibit any clear trend towards the PSZ.

CS: I find it difficult to discern trends from looking at tables. I am also uncertain of the meaning of "towards the PSZ" - as a function of orthogonal distance to PSZ?

Our response: Prior to the initial submission of the manuscript, we considered generating a figure demonstrating mineralogy. However, the number of samples investigated as well as sampling distance with respect to PSZ varies so much between locations that such a figure would be very hard to read. Also, there are only minor qualitative compositional changes between individual locations. The most important result of the mineralogical analysis is actually that thicker PSZs appear to contain fewer phyllosilicates than thinner ones. This is clearly shown in Figure 8. However, we have now realized that a description of the mineralogy of the footwall gravels was missing. It will be included (new section 4.3.3) for completeness in the revised manuscript.

l. 408: In summary, both microstructures and the predominant enrichment of elements show that fluids are not responsible for stress-driven dissolution processes or for substantial mass transfer out of the fault zone.

CS: Given my methodological criticism of the isocon analysis as well as potentially overlooked slickolites/stylolites in other samples, I believe that this point remains to be tested. Moreover, what about the large amount of authigenic micas? Your conclusions here at complete odds with the SAFOD paper by Schleicher et al. 2009, which you cite below but in a different context.

Our response: Please refer to the comment on Figure 6 below for our discussion of potentially overloocked slickolites / stylolites. Better constrained protolith composition did not substantially affect the general results of the isocon analysis (i.e. predominant enrichment of elements; see reply to RC1 – 2). While we admit that this is basically the opposite of what Schleicher et al. (2009) found for the San Andreas Fault ("most of the elements are depleted in the fault-related grains compared to the wall rock lithology"), we emphasize, as we did in our response to this referee's major comments, that this difference could originate from the fact that the San Andreas Fault has a different hydrological systems compared to the Alpine Fault (compare Xue et al., 2016, describing the San Andreas Fault hydrological system with Menzies et al., 2016, analyzing the Alpine Fault hydrology). Furthermore, the hydrological system of the hanging-wall is very active leading to intensive fluid-related alteration (Sutherland et al., 2012). One example of this process is shown in Figure 6a of the manuscript where plagioclase is altered to phyllosilicates. The same alteration mineralogy was shown by Schleicher et al. (2009) in the San Andreas Fault ("[…] albite/anorthite minerals […] altered into I-S clay minerals"). In this context, the "large amounts of authigenic micas" (which increase towards the PSZ; Sutherland et al., 2012) reflect rather element enrichment than dissolution.

l. 480: Fault gouge contains fewer and preferentially smaller clasts than the overlying hanging-wall-proximal layer […] and bounds mechanically weak gravels.

CS: What is your evidence?

Our response: See response to comment on line 306.

l. 483: Consequently, layered fault gouges and associated microstructural evidence demonstrate that strain localization and associated structural complexities within the Alpine Fault core are […] affected by shallow, hence late, processes.

CS: I am not convinced that you present clear evidence to support this statement. It appears rather difficult to figure out when the PSZ/gouge was active

Our response: This statement is supported not by observations of the gouge itself, but by the fact that the PSZ gouge cross-cuts all other structures in the fault core, so it must be the last active part of the fault system, and accommodate coseismic displacements. Furthermore, we know that Alpine Fault slip displaces the ground surface, because there are offsets of Quaternary features (e.g. Cooper and Norris, 1990; Berryman et al., 2012). So the gouge must accommodate slip in the very near-surface. We will include this argument in the revised manuscript.

l. 493/494: It has been suggested that such variations [in PSZ thickness] may results from different mechanisms of deformation (Hobbs et al., 1990; Schrank et al., 2008).

CS: In this context, it is important to look at the paper of Kirkpatrick et al. 2018. The references therein point to other relevant papers in this field. These papers, more correctly, speak about the effect of the constitutive model - which is an upscaled response of a microphysical deformation mechanism.

Our response: Will be elaborated in the revised version.

l. 500: These explanations do not appear to be responsible for observed variations as there is no correlation between PSZ thickness and sample location along-strike.

CS: Given your poor data situation – mainly due to exposure conditions and perhaps an inappropriate choice of length scale of observation – you cannot test this notion.

Our response: We agree that observations might be biased by outcrop situation and availability. However, the statement is based on the five locations investigated, where we do not observe a systematic increase / decrease of PSZ thickness from SW to NE.

l. 505: This is astonishing, because phyllosilicate-rich fault gouges generally tend to be wider (Faulkner et al., 2003; Schleicher et al., 2009) owing [to] the frictionally weak nature of these phases (Moore et al., 1997; Moore and Lockner, 2007; Lockner et al., 2011; Carpenter et al., 2015.

CS: These papers do not explicitly establish the statement made by the authors. I have other comments noted in the letter to the authors.

Our response: Faulkner et al. (2003), section 5.1: "The thickness of the zone of deformation […] is thought to be due to the mechanics of deformation of phyllosilicate-rich fault gouge." We agree, we erroneously cited Schleicher et al. (2009) here, and will remove that citation.

l. 508: The very narrow fault gouge at Martyr River contains frictionally extraordinary weak serpentine phases which elsewhere have typically dominated in fairly thick fault zones (Moore et al., 1997; Moore and Rymer, 2007, 2012).

CS: I feel that these statements and citations do not align very well. For example, Moore and Rymer 2007 show that serpentine is too strong to explain the weakness of the SAF - they find talc as the culprit for weakness. So speaking of "extraordinary weak serpentine phases" with these papers is not a great idea. Moreover, the fault dimensions noted in their 2012 paper do not vary much from the range of APF discussed here. Please, revisit.

Our response: We re-examined the cited literature with this specific comment in mind. It is debatable that talc causes the weakness of the San Andreas Fault (see e.g. Warr et al., 2014: "The hypothesis that talc causes creep at the depth of the borehole (Moore and Rymer, 2007; Wibberley, 2007) has not gained support due to the rare occurrence of this mineral in SAFOD fault gouge"), and thus removed the reference to Moore and Rymer (2007).

Also, we acknowledge that while serpentinite can have a quite low coefficient of friction (Moore and Reyhnolds, 1997; Moore and Lockner, 2004; Moore and Rymer, 2012), it is not "extraordinarily low", so we will remove that term. However, it is true that Moore and Rymer (2012) describe a 3 – 50 m wide "tectonic shear zone of serpentinite", which is more than two orders of magnitude thicker than the PSZ at Martyr River, so this part of the comment was correct. We also realize that we should change the emphasis to highlight the fact that the gouge from Martyr River is phyllosilicate- rather than serpentine-rich, as this probably has a greater influence on the way the gouge accommodates deformation, and we will make this change in the revised manuscript.

l. 510: Conversely, fault zones with similar quartzofeldspathic composition to the Alpine Fault are typically narrower (Chester et al., 1993; Faulkner et al., 2003). Consequently, unlike other fault zones worldwide, the Alpine Fault displays a negative correlation between phyllosilicate content and fault core thickness.

CS: Another example of somewhat tenuous alignment of the author's statement and the literature cited in support of it. Both papers examine a single particular field example of one fault. Thus, it seems quite bold to claim that they "are typically narrower". Similarly, I'd be curious to see the references for the statement in the next sentence regarding "fault zones worldwide".

Our response: We agree that we generalized the statement too much and will revise it.

l. 514: In addition, orientation of the fault (Figs. 2a & b), magnitude of stress and the stress field itself (Boese et al., 2012; Warren-Smith et al., 2017) are fairly constant along the central segment of the Alpine Fault.

CS: See my comments in the letter to the authors – I don't think this is true. Local geometrical perturbations can easily induce large local stress differences.

Our response: We stated this because the overall tectonic plate motions driving slip and generating stress fields within the Alpine Fault are fairly constant along its length, and the fault planes we investigated are all similar in orientation so the traction vectors resolved on them will also be similar. However, we recognise there are substantial topographic variations along strike of the Alpine Fault as it is cut by large glacial (and post glacial) valleys. Recently Upton et al. (2017) modelled the topographically-induced variations in stress and

demonstrated these indeed yield substantial local variations. We realise that we need to acknowledge this possibility, and will consequently add to the revised manuscript "However, it is still possible that the extreme variations in topography typical of the Alpine Fault hanging-wall generated quite different stress fields at our investigated sites (cf. Upton et al., 2017)."

l. 518: Biegel and Sammis (2004) suggested to explain along-strike variations of gouge thickness as record of rupture arrest. However, our observations (and the nature of Alpine Fault outcrops in general) do not easily lend themselves to a systematic analysis of this kind in the Alpine Fault zone.

CS: Absolutely correct – but that does not mean that you can rule out that these effects mattered. It would be instructive and convenient for the reader if you stated, which thickness variations this effect can cause.

Our response: We addressed a variety of potential mechanisms explaining PSZ thickness variations. We are quite confident that our proposed explanation (we actually investigated different faults planes having accommodated different amounts of displacement) is reasonable.

However, we are aware that the difficult outcrop situation prevents us from completely ruling out other explanations, which is not satisfying. Thickness variations as consequence of rupture arrest are mentioned for completeness. However, we do not see any mechanism explaining how rupture arrest could cause these variations. The original reference suggests that Biegel and Sammis (2004) had the same issue: "It is well known that the thickness of the gouge and breccia layers vary significantly along strike. Is it possible that these variations record the arrest of rupture?"

l. 521: However, quantitative models of fault core evolution have so far failed to reproduce datasets compiled on natural faults (e.g. Blenkinsop, 1989; Evans 1990; Sibson, 2003).

CS: Another example of poorly chosen references: these papers do not provide quantitative models of fault core evolution – they deal with empirical scaling relations and do not offer physics-based forward models. This problem is unsolved!

Our response: We disagree that these references are poorly chosen. Scholz (1987) summarizes empirical relations showing that thickness increases with displacement and "offer[s] a simple model that quantitatively accounts for this behavior". Hull (1988) states that he "[presents] empirical relationships between thickness and displacement" and quantifies this relationship by stating that "faults exhibit a linear correlation […] and an average displacement / thickness ratio of 63". The references we cited criticize the Scholz and Hull models; for example Evans (1990) states: "Conceptual and quantitative models which rely heavily on thickness-displacement relationships should be considered with caution until further data are collected on the topic. […] The linear and logarithmic plots of these data indicate a general increase in displacement with thickness, but the scatter of data show that this is a qualitative relationship […]." In the revised version we will emphasize the empirical character of these relationships.

l. 524: In other words: the more earthquakes a fault has seen, the thicker its PSZ may be (Ma et al., 2006; Li et al., 2013).

CS: There are alternatives. Slow creep along the fault can also modify the width to growth when the fault core is strain-hardening. See Schrank et al. 2008 as an experimental example.

Our response: We are only referring to relationships previously empirically-determined in earthquake-generating faults that slip episodically and have strain-weakening fault cores. The alternative indicated in Schrank et al. (2008) is not very relevant for the Alpine Fault, which is seismically locked down to 12 – 18 km (Beavan et al., 2007) and has displayed no measureable creep in historic times (see Schuck et al., 2018 for a discussion).

l. 526: […] the Alpine Fault's central segment, which is considered to rupture entirely during an earthquake (Sutherland et al., 2007; Howarth et al., 2018) […].

CS: This is a big assumption - how can you be sure that this was the case over the lifetime of the structure?

Our response: Berryman et al., (2012) showed the Alpine Fault accommodates earthquake ruptures, with ground displacements sufficient to dam rivers and create peat bogs, every ~300 years, and has done so for the last >5000 years. Coffey (2014) demonstrated evidence for three earthquakes of sufficient magnitude to create sieches in pro-glacial lakes with similar return periods c. 17ka. It is more difficult to understand why the fault would have behaved in a significantly different way prior to that than it is to assume it behaved the same. However, we will acknowledge this possibility by adding to the revised manuscript "and to have done so for at least the last ~5000 years (Berryman et al., 2012)".

l. 527/528: PSZ thickness variations suggest that studied fault gouges accommodated different amounts of displacement. This implies the studied PSZs are not part of the same shear plane, and that the Alpine Fault zone hosts multiple fault strands […].

CS: I disagree. Shear displacement is the integral of shear strain over sz width. See my simple numerical model. As soon as you have the slightest change in thickness, shear strain is no longer constant in the PSZ even if the applied displacement is the same at the far field. In other words: your statement is only true if the shear strain is identical everywhere in the PSZ - and one can rule out this assumption almost categorically at the scale of investigation. If you accept my criticism on the preceding sentence, this logical conclusion is no longer valid. However, I would agree that the statement is likely correct but for different reasons: it would be incredibly amazing and surprising to observe a fault on the scales of tens to hundreds of kilometers which features only on fault strand!

Our response: The comment inspires us to be more explicit here, and so we will modify the sentence to read "If we employ the simple relationship that shear strain in a fault zone is equal to zone width multiplied by boundary displacement, and assume constant strain distribution within the PSZ gouges, then the PSZ thickness variations we describe suggest the studied fault gouges accommodated different amounts of displacement. This implies the PSZs are not part of the same shear plane, and therefore that the Alpine Fault zone hosts multiple fault strands."

l. 534: This is unexpected given the small separation between boreholes and thus sample spacing of less than 100m.

CS: I have seen many rock, which are compositionally heterogeneous, and in terms of fabric, on the 10 to 100-m scale. Again, the opposite would be a surprise in schists and gravels as host rock. A flood basalt may be different...

Our response: We agree, compositional and microstructural heterogeneities on the 10 to 100 meter scale are not uncommon. However, the situation encountered at DFDP-1A and DFDP-1B differs, as indicated by Boulton et al., 2014: "Because each PSZ gouge has a distinct mineral assemblage representative of high or low temperature alteration, experimental results quantify how frictional properties vary within mineralogy, temperature and pressure". In our view, these dramatic differences appear conspicuous, if one assumes that both PSZs (less than 100m apart) are part of the same fault plane sharing the same record of P and T. We do realize now that it is necessary to explicitly paraphrase the observations of Boulton et al. (2014) in our revised discussion.

l. 543: […] which is atypical for quartzofeldspathic faults but typical for carbonate or phyllosilicate-hosted ones.

CS: I would appreciate more careful linking with existing literature to establish this point. At the moment, I feel doubt that the literature and your data support this notion firmly. But I'd be keen to be falsified in this feeling!

Our response: Please refer to the reply to our comment on line 510.

l. 553: Conclusions […]

CS: Given my criticism regarding the isocon data/method and mechanical interpretation, etc., I can expect the need to echo this in the conclusion. Forgive me if I do not do this for the sake of avoiding redundancy!

Our response: We will modify our conclusions to reflect the revisions we make to the discussion to accommodate the reviewer's major comments about this aspect.

Figure 6: The reviewer suggested we had overlooked the presence of stylolites in the images shown Figures 6c and 6e. We have systematically reexamined these images and still think we were correct in our interpretation sated at lines 404 – 405 ("furthermore, except for the slickolite observed in the DFDP-1A fault core (Fig. 7g), there is no microstructural evidence for pressure-solution such as dissolution seams or indented and embayed clasts").

Figure 6c of the manuscript contains a feature of undulatory shape that resembles a stylolite, but closer examination reveals no unambiguous evidence for pressure-solution, such as indented and embayed clasts. The feature undulates where it abuts clasts in the gouge it transects, but does not truncate them. We therefore prefer the interpretation that the featured formed by fracturing of a heterogeneous material.

The same is valid for Figure 6e of the manuscript, where there are definitely no indented and embayed clasts. The corresponding optical image (Figure 6g of the manuscript) shows the seam the reviewer indicated is a crack (white / transparent line in plain polarized light).

As recommend by the reviewer, where possible (locations WT, GC and MR), we will indicate the orientation and shear sense of the shear plane relative to the images in Figures 6 and 7.

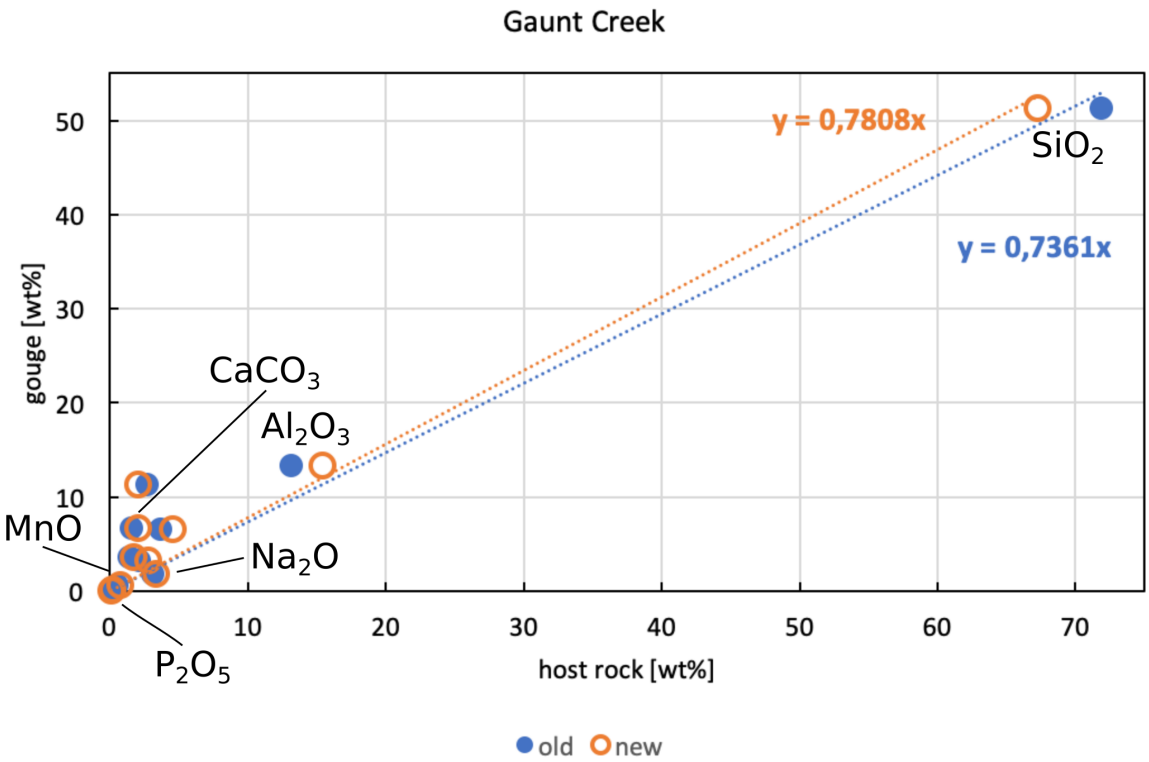

Figure 1: Isocon analyses of Alpine Fault PSZ at Gaunt Creek with host rock composition used in the initially submitted manuscript ("old") and the updated, better constraint one ("new"). The slightly larger slope of the new isocon implies a slightly lower mass gain (new: 28.1% vs. old: 35.9%).

References

Barth, N.C., Boulton, C., Carpenter, B.M., Batt, G.E. and Toy, V.G. (2013): Slip localization on the southern Alpine Fault, New Zealand. Tectonics 32, 620 – 640, doi:10.1002/tect.20041.

Beavan, J., Ellis, S., Wallace, L. and Denys, P. (2007): Kinematic constraints from GPS on oblique convergence of the Pacific and Australian plates, central South Island, New Zealand. In: Okaya, D., Stern, T.A. and Davey, F. (Eds.): A continental Plate Boundary: Tectonics at South Island, New Zealand. AGU Geophysical Monograph 175, 75 – 94.

Ben-Zion, Y. and Sammis, C.G. (2003): Characterization of Fault Zones. Pure and Applied Geophysics 160, 677 – 715.

Berryman, K.R., Cochran, U.A., Clark, K.J., Biasi, G.P., Langridge, R.M. and Villamor, P. (2012): Major Earthquakes Occur Regularly on an Isolated Plate Boundary Fault. Science 336, 1690 – 1693.

Biegel, R.L. and Sammis, C.G. (2004): Relating fault mechanics to fault zone structure. Advances in Geophysics 47, doi:10.1016/S0065-2687(04)47002-2.

Boulton, C., Carpenter, B.M., Toy, V. and Marone, C. (2012): Physical properties of surface outcrop cataclastic fault rocks, Alpine Fault, New Zealand. Geochemistry, Geophysics, Geosystems 13, doi:10.1029/2011GC003872.

Boulton, C., Moore, D.E., Lockner, D.A., Toy, V.G., Townend, J. and Sutherland R., (2014): Frictional properties of exhumed fault gouges in DFDP-1 cores, Alpine Fault, New Zealand, Geophyiscal Research Letters 41, 356 – 362.

Brodsky, E.E., Gilchrist, J.J., Sagy, A. and Collettini, C. (2011): Fault smooth gradually as a function of fault slip. Earth and Planetary Science Letters 302, 185 – 193.

Caine, J.S., Evans, J.P. and Forster, C.B. (1996): Fault zone architecture and permeability structure. Geology 24, 1,025 – 1,028.

Coffey, G. (2014): Sedimentology and neo-tectonics of the Cascade River, South-Westland, NZ. MSc Thesis, University of Otago.

Cooper, A.F. and Norris, R.J. 1990): Estimates for the timing of the last coseismic displacement on the Alpine Fault, northern Fiordland, New Zealand. New Zealand Journal of Geology and Geophysics 33, 303 – 307.

Evans, J.P. (1990): Thickness-displacement relationships for fault zones. Journal of Structural Geology 12, 1,061 – 1065.

Faulkner, D.R., Lewis, A.C. and Rutter, E.H. (2003): On the internal structure and mechanics of large strike-slip fault zones: field observations of the Carboneras Fault in southeastern Spain. Tectonophysics 367, 235 – 251, doi: 10.1016/S0040-1951(03)00134-3.

Faulkner, D.R., Jackson C.A.L., Lunn, R.J., Schlische, R.W., Shipton, Z.K., Wibberley, C.A.J., Withjack, M.O. (2010): A review of recent developments concerning the structure, mechanics and fluid flow properties of fault zones. Journal of Structural Geology 32, 1,557 – 1,575, doi: 10.1016/j.jsg.2010.06.009.

Grant, J.A. (1986): The isocon diagram – a simple solution to Gresens' equation for metasomatic alteration. Economic Geology 81, 1,976 – 1,982.

Grant, J.A. (2005): Isocon analysis: a brief review of the method and applications. Physics and chemistry of the Earth 30, 997 – 1004.

Grapes, R., Watanabe, T. and Palmer, K. (1982): X-ray fluorescence major and trace element analyses of metabasites, Southern Alps, New Zealand. Publication of the Geology Department no. 24 (Analytical Facility Contribution no. 8), Victoria University of Wellington.

Kirkpatrick, J.D., Shervais, K.A.H. and Ronayne, M.J. (2018): Spatial Variation in the Slip Zone Thickness of a Seismogenic Fault. Geophysical Research Letters 45, 7,542 – 7,550.

Little, T.A., Cox, S., Vry, J.K. and Batt, G. (2005): Variations in exhumation level and uplift rate along the oblique-slip Alpine Fault, central Southern Alps, New Zealand. GSA Bulletin 117, 707 – 723, doi: 10.1130/B25500.1.

Menzies, C.D., Teagle, D.A.H., Niedermann, S., Cox, S.C., Craw, D., Zimmer, M., Cooper, M.J. and Erzinger, J. (2016): The fluid budget of a continental plate boundary fault: Quantification from the Alpine Fault, New Zealand. Earth and Planetary Science Letters 445, 125 – 135.

Norris, R.J. and Cooper, A.F. (2007): The Alpine Fault, New Zealand: Surface geology and field relationships. In: Okaya, D., Stern, T.A. and Davey, F. (Eds.): A continental Plate Boundary: Tectonics at South Island, New Zealand. AGU Geophysical Monograph 175, 157 – 175.

Roser, B.P. and Cooper, A.F. (1990): Geochemistry and terrande affiliation of Haast Schist from the western Southern Alps, New Zealand. New Zealand Journal of Geology and Geopohysics 33, 1 – 10, doi:10.1080/00288306.1990.10527567.

Sagy, A., Brodsky, E.E. and Axen, G.J. (2007): Evolution of fault-surface roughness with slip. Geology 35, 283 – 286.

Sagy, A. and Brodsky, E.E. (2009): Geometric and rheological asperities in an exposed fault zone. Journal of Geophysical Research 114, doi:10.1029/2008JB005701.

Sagy, A. and Lyakhovsky, V. (2019): Stress Patterns and Failure Around Rough Interlocked Fault Surface. Journal of Geopyhsical Research Solid Earth 124, 7,138 – 7,154.

Schleicher, A.M., Tourschner, S.N., van der Pluijm, B.A. and Warr, L.N. (2009): Constraints on mineralization, fluid-rock interaction, and mass transfer during faulting at 2 – 3 km depth from the SAFOD drill hole. Journal of Geophysical Research 114, B04202, doi:10.1029/2008JB006092.

Schrank, C.E., Boutelier, D.A. and Cruden, A. (2008): The analogue shear zone: From rheology to associated geometry. Journal of Structural Geology 30, 177 – 193.

Schuck, B., Janssen, C., Schleicher, A.M., Toy, V.G. and Dresen, G. (2018): Microstructures imply cataclasis and authigenic mineral formation control geomechanical properties of New Zealand's Alpine Fault. Journal of Structural Geology 110, 172 – 186, doi: 10.1016/jsg.2018.03.001.

Shervais, K.A.H. and Kirkpatrick, J.D. (2016): Smoothing and re-roughening processes: The geometric evolution of a single fault zone. Journal of Structural Geology 98, 130 – 143.

Sutherland, R., Eberhart-Phillips, D., Harris, R.A., Stern, T., Beavan, J., Ellis, S., Henrys, S., Cox, S., Norris, R.J., Berryman, K.R., Townend, J., Bannister, S., Pettinga, J., Leitner, B., Wallace, L., Little, T.A., Cooper, A.F., Yetton, M. and Stirling, M. (2007): Do great earthquakes occur on the Alpine Fault in central South Island, New Zealand? In: Okaya, D., Stern, T.A. and Davey, F. (Eds.): A continental Plate Boundary: Tectonics at South Island, New Zealand. AGU Geophysical Monograph 175, 235 – 251.

Sutherland, R., Toy, V.G., Townend, J., Cox, S.C., Eccles, J.D., Faulkner, D.R., Prior, D.J., Norris, R.J., Mariani, E., Boulton, C., Carpenter, B.M., Menzies, C.D., Little, T.A., Hasting, M., De Pascale, G.P., Langridge, R.M., Scott, H.R., Lindroos, Z.R., Fleming, B. and Kopf, A.J. (2012): Drilling reveals fluid control on architecture and rupture of the Alpine Fault, New Zealand. Geology 40, 1,143 – 1,146, doi:10.1130/G33614.1

Toy, V.G., Boulton, C.J., Sutherland, R., Townend, J., Norris, R.J., Little, T.A., Prior, D.J., Mariani, E., Faulkner, D., Menzies, C.D., Scott, H. and Carpenter, B.M. (2015): Fault rock lithologies and architecture of the central Alpine Fault, New Zealand, revealed by DFDP-1 drilling. Lithosphere 7, 155 – 173, doi:10.1130/L395.1.

Toy, V.G., Sutherland, R., Townend, J., Allen, M.J., Becroft, L., Boles, A., Boulton, C., Carpenter, B., Cooper, A., Cox, S.C., Daube, C., Faulkner, D.R., Halfpenny, A., Kato, N., Keys, S., Kirilova, M., Kometani, Y., Little, T., Mariani, E., Melosh, B., Menzies, C.D., Morales, L., Morgan, C.,

Mori, H., Niemeijer, A., Norris, R., Prior, D., Sauer, K., Schleicher, A.M., Shigematsu, N., Teagle, D.A.H., Tobin, H., Valdez, R., Williams, J., Yea, S., Baratin, L.-M., Barth, N., Benson, A., Boese, C., Célérier, B., Chamberlain, C.J., Conze, R., Coussens, J., Craw, L., Doan, M.-L., Eccles, J., Grieve, J., Grochowski, J., Gulley, A., Howarth, J., Jacobs, K., Janku-Capova, L., Jeppson, T., Langridge, R., Mallyon, D., Marx, R., Massiot, C., Mathewson, L., Moore, J., Nishikawa, O., Pooley, B., Pyne, A., Savage, M.K., Schmitt, D., Taylor-Offord, S., Upton, P., Weaver, K.C., Wiersberg, T., Zimmer, M. and DFDP-2 Science Team (2017): Bedrock geology of DFDP-2B, central Alpine Fault, New Zealand. New Zealand Journal of Geology and Geophysics, doi:10.1080/00288306.2017.1375533.

Upton, P., Song, B.R. and Koons, P.O. (2017): Topographic control on shallow fault structure and strain partitioning near Whataroa, New Zealand demonstrates weak Alpine Fault. New Zealand Journal of Geology and Geophysics, doi:10.1080/00288306.2017.1397706.

Warr, L.N., Wojatschke, J., Carpenter, B.M., Marone, C., Schleicher, A.M. and van der Pluijm, B.A. (2014): A „slice-and-view“ (FIB-SEM) study of clay gouge from the SAFOD creeping section of the San Andreas Fault at ~2.7 km depth.

Williams, J.N., Toy, V.G., Massiot, C., McNamara, D.D. and Wang, T. (2016): Damaged beyond repair? Characterising the damage zone of a fault late in its interseismic cycle, the Alpine Fault, New Zealand. Journal of Structural Geology 90, 76 – 94.

Xue, L., Brodsky, E.E., Erskine, J., Fulton, P.M. and Carter, R. (2016): A permeability and compliance contrast measured hydrologically on the San Andreas Fault. Geochemistry, Geophysics, Geosystems, doi:10.1002/2015GC006167.

Referee Comment (RC) 2

This comment is a post scriptum to RC 1 by Christoph Schrank. It provides a reference (Sagy and Lyakhovsky, 2019) we happily deployed to reply to RC 1.

References

Sagy, A. and Lyakhovsky, V. (2019): Stress Patterns and Failure Around Rough Interlocked Fault Surface. Journal of Geopyhsical Research Solid Earth 124, 7,138 – 7,154.

Referee Comment (RC) 3

We are grateful for the feedback provided by an anonymous referee (AR). The referee raises four (RC3 – 1 to RC3 – 4) main concerns, which are addressed in detail below. Furthermore, specific comments to individual points of the manuscript are provided in an annotated pdf. In the following, we will repeat the referee's statements (in bold font) and our reply to it. Below the responses to these main concerns, we respond to the specific comments on the manuscript except for cases where e.g. typos are highlighted.

RC3 – 1

The results section is sometimes hard to follow. My suggestion is to avoid wording, long sentences, the different classification of clast within the cataclasite (i.e. matrix clast, bright matrix clasts), the different sub-classification of cataclasite (i.e. hangingwall-proximal gouge, footwall-proximal gouge) and so on. I suggest to the author to shorten and simplify this part, maybe focusing on the striking differences between the different outcrops. In addition, within the description of the results there are several jumps from an outcrop to another. This confuses the reader. One solution can be to divide the results chapter with sub-sections based on the description of the different outcrops (i.e. sub-section 4.1 Havelock Creek, 4.2 Gaunt Creek, 4.3 Waikukupa Thrust, 4.4 Martyr River, 4.5 Borehole microstructures and so on). This will help the reader to have a better idea of the peculiar structures within the different locations.

In this paragraph, the reviewer expresses concerns regarding the style of the results section. Two aspects detail these concerns: (I) wording, long sentences and classifications introduced and (II) outcrop description being confuse as there are jumps from an outcrop to another.

With respect to aspect (I), we will aim to simplify our wording and shorten sentences in the revised version of the manuscript (examples where this has been suggested by the reviewer are very helpful). One aim of this paper is to provide a detailed characterization of Alpine Fault gouge with respect to microstructures, mineralogy and geochemistry. This requires a description of observations, which facilitates to compare observations made in different studies. For example, matrix clasts, though sometimes termed *reworked gouge clasts,* have been reported previously (see Boulton et al., 2012; Toy et al., 2015; Schuck et al., 2018). In this context and as described in the manuscript, bright matrix clasts are a distinct feature and *bright matrix clast* appeared to be a reasonable term to describe this feature. Similar reasoning applies regarding the terms *hanging-wall- and footwall-proximal gouge* (see also Schuck et al., 2018). These terms describe distinct features observed at two locations. Furthermore, as the formation of these features in discussed in the discussion section a proper labeling appeared necessary.

With respect to aspect (II) we disagree with the reviewer. To the end of characterizing the PSZ of the Alpine Fault, we report at the beginning of the subsections the main observations valid for all investigated locations (see e.g. lines 245 – 259 or lines 357 – 362) before presenting observations specific for one or some of the locations (e.g. lines 319 –

323); hence the structure of the sections is guided by individual observations. The suggested re-arrangement to base subsections on the description of the different outcrops has been tried in an earlier version of the manuscript. However, the description of microstructures, mineralogy and geochemistry was repetitive, which unnecessarily extend the results section. The chosen structure of the manuscript provides (a) a holistic description of Alpine Fault gouge and (b) shows differences between individual locations.

RC3 – 2

In addition, I suggest also to split the two figure of microstructures in three, in order to do figure with larger panels. In this way can be easier to see the detail of microstructures. Please, enlarge also Fig. 4 and 5 (two column wide).

Figures 2 – 7 and 9 are designed to be two columns wide. Their smaller width in the submitted manuscript originates from the template used. We hope that it will be possible to display these figures two-column-wide, if this manuscript will be published.

RC3 – 3

I suggest to draw a conclusive general sketch where the main microstructures are highlighted regarding to the different locations. For instance, a similar (but a lit of bit more detailed) sketch as that of Fig. 10, also with the other outcrops, and a map with arrows indicating the different positions of microstructures. In this case the reader will have a complete picture of the different microstructures according to position along the fault.

Figure 9 of Schuck et al. (2018) provides a conclusive general sketch highlighting the main microstructures. Microstructural differences between individual locations appear to be minor, hence it appears elusive to sketch these subtle differences. Nonetheless, we will consider including such a sketch in the revised manuscript once all referee comments will have been included in the manuscript.

RC3 – 4

Line 525-530. Seismological investigations showed that during a fault rupture the slip distribution along a fault plane is always heterogeneous, with zones characterized by high displacements and zones characterized by low to zero displacements, both at surface and at depth (e.g. Ma et al., 1999; Lin et al. 2001; Tinti et al., 2016). This can affect the production and the thickness of fault gouges and the distribution of fault rocks. The observed differences in gouge thickness could be explained also by different displacements occurred along the same fault plane, rather than the product of multiple displacements along several fault strands? Are there evidence of multiple fault strands at the surface or the area is too vegetated to map such complexity?

In this comment, the referee addresses two aspects: (I) potentially differing amounts of displacement accommodated and (II) the presence / absence of multiple faults strands and the dense vegetation obscuring their identification, respectively.

Regarding aspect (I), locations *DFDP-1 / Gaunt Creek*, *Havelock Creek* and *Waikukupa Thrust* are situated in the central segment of the Alpine Fault, location *Martyr River* is

located in the fault's southern segment (see Figure 2 of the manuscript). While it is known that the fault might rupture along its entire length, differing recurrence intervals for the central and southern segments suggest that individual fault sections might fail independently of each other (see also section 2.1 of the manuscript). However, the entire central segment is considered to rupture in case of an earthquake (see lines 524 – 526; Sutherland et al., 2007; Howarth et al., 2018). If one assumes that there is only one fault plane, earthquakes rupturing the entire central segment suggest that PSZs investigated in the central segment have accommodated the same displacement. However, in this case PSZ thicknesses should be more similar than they actually are.

Regarding aspect (II), the area is indeed densely vegetated, which is the reason for the sparsity of locations providing access to the PSZ. However, in two different settings there have been indicators of / direct evidence for more than one fault strand. (a) DFDP-1B is the only location of the central segment of the Alpine Fault, where there are two PSZs (see Figure 3a in the manuscript). Both PSZs are bound by fault rocks. However, the presence of these two PSZs has so far not been discussed in the context of fault zone architecture. At locations where both hanging- and footwall are covered by tens to hundreds of meter thick Quaternary sediments, shallow imaging techniques detected multiple fault strands (Kaiser et al., 2009; Carpentier et al., 2012) and there are indications that at least some of them might extend into the basement (see also lines 546 – 548; Lay et al., 2016; Lukács et al., 2018).

These aspects (two PSZs encountered in DFDP-1B and multiple fault strands detected by shallow imaging techniques) is also discussed in the reply to referee comment 1 and will be elaborated in more detail in the revised version of the manuscript.

Below we respond to the specific comments that were made as annotations on the manuscript. Numbers refer to the line in the original pdf where the reviewer placed his comment

l. 54:

AR*:* Please, synthesize from line 30 to 54.):

Our response: Lines 31 – 54 review fault zone architecture and the two end-member models of fault-zone architecture presented by Caine et al. (1996) and Faulkner et al. (2003), respectively. These provide a fundamental framework for the discussion of our observations and we would like to retain them.

l. 65: The fault is dominantly transpressive and runs through the South Island of New Zealand.

AR: dextral or sinistral?

Our response: We will modify this to "dominantly dextral transpressive"

l. 238:

AR: please insert coordinates in the caption of Fig. 2.
Our response: We will do this as requested.

l. 254/255:
AR: I suggest to avoid the term “matrix clast”, maybe is better only to use the term “clast”
Our response: The term *clast* is not unambiguous. A clast could also be a larger quartz grain embedded in the matrix. We prefer to retain the qualifying “matrix” to make it clear what there features are.

l. 313: Many of these fractures contain up to 305 µm wide calcite cores, locally surrounded by gouge, microstructurally similar to microfaults observed within the DFDP-1A cataclasites
AR: Cores” – you mean crystals? […] Figure of this microstructure.
Our response: We really do mean core. The corresponding figure is Figure 6i (reference in line 314).

l. 404: Slickolite
AR: stylolite?
Our response: As detailed in line 317 a slickolite is a special form of a stylolite, and this term describes the observed feature more appropriately than the more generic term *stylolite*.

l. 440: section 5.2.1
AR: all this is not a discussion of the results presented in this paper. This should be deleted or moved in the geological setting above
Our response: We reviewed the different views about the extent of the Alpine Fault’s brittle part (namely its damage zone and its fault core) presented in previous publications in section 5.2.1 and the first part of section 5.2.2, and then discussed how our results inform a better understanding of the Alpine Fault’s architecture in the rest of section 5.2.2. If we move section 5.2.1 to the *geological setting* section (as suggested by the reviewer), we would also have to move the first part of section 5.2.2 there, and then our new findings would be entirely without context so we prefer to keep it here.

l. 476:
AR: I imagine that this part is from your work. So I don't understand the relationship with the previous sentence regarding the faults in the death Valley
Our response: As discussed in our response to referee comment 1, we acknowledge that this paragraph (lines 471 – 476) and the succeeding one (lines 477 – 485) are misleading and will revise them.

l. 513: This suggests that strain localization within the fault core might be governed by processes insensitive of rheological variations caused by differing fault rock composition.
AR: Maybe related to greater fluid circulation a authigenic clay precipitation into narrow PSZ?
Our response: Please refer to our reply to referee comment 1 on this line.

Figure 2: Inserting a simplified section trace in Figure 2b is not possible, because (I) Figure 2c is a conceptual (composite) sketch depicting a shallow-depth transect across the Alpine Fault and (II) the scales of Figures 2b and c differ so much that the section trace would be too small to be recognized in Figure 2b. We will indicate the DFDP-2 borehole with a different symbol.

References

Boulton, C., Carpenter, B.M., Toy, V. and Marone, C. (2012): Physical properties of surface outcrop cataclastic fault rocks, Alpine Fault, New Zealand. Geochemistry, Geophysics, Geosystems 13, doi:10.1029/2011GC003872.

Caine, J.S., Evans, J.P. and Forster, C.B. (1996): Fault zone architecture and permeability structure. Geology 24, 1,025 – 1,028.

Carpentier, S.F.A., Green, A.G., Langridge, R., Boschetti, S., Doetsch, J., Abächerli, A.N., Horstmeyer, H., and Finnemore (2012): Flower structures and Riedel shears at a step over zone along the Alpine Fault (New Zealand) inferred from 2D and 3D GPR images. Journal of Geophysical Research 117, doi:10.1029/2011JB008749.

Faulkner, D.R., Lewis, A.C. and Rutter, E.H. (2003): On the internal structure and mechanics of large strike-slip fault zones: field observations of the Carboneras Fault in southeastern Spain. Tectonophysics 367, 235 – 251, doi: 10.1016/S0040-1951(03)00134-3.

Kaiser, A.E., Green, A.G., Campbell, F.M., Horstmeyer, H., Manukyan, E., Langridge, R.M., McClymont, A.F., Mancktelow, N., Finnemore, M. and Nobes, D.C. (2009): Ultrahigh-resolution seismic reflection imaging of the Alpine Fault, New Zealand. Journal of Geophysical Research 114, doi:10.1029/2009JB006338.

Howarth, J.D., Cochran, U.A., Langridge, R.M., Clark, K., Fitzsimons, S.J., Berryman, K., Villamore, P. and Strong, D.T. (2018): Past large earthquakes on the Alpine Fault, paleoseismological progress and future directions. New Zealand Journal of Geology and Geophysics 61, 309 – 328.

Lay, V., Buske, S., Lukáxc, A., Gorman, A.R., Bannister, S. and Schmitt, D.R. (2016): Advanced seismic imaging techniques characterize the Alpine Fault at Whataroa (New Zealand). Journal of Geophysical Research: Solid Earth 121, doi:10.1002/2016JB013534.

Lukács, A., Gorman, A.R. and Norris, R.J. (2018): Quaternary structural and paleo-environmental evolution of the Alpine Fault near Haast, New Zealand, from 2D seismic reflection and gravity data. New Zealand Journal of Geology and Geophyics, doi:10.1080/00288306.2018.1544153.

Schuck, B., Janssen, C., Schleicher, A.M., Toy, V.G. and Dresen, G. (2018): Microstructures imply cataclasis and authigenic mineral formation control geomechanical properties of New Zealand's Alpine Fault. Journal of Structural Geology 110, 172 – 186, doi: 10.1016/jsg.2018.03.001.

Sutherland, R., Eberhart-Phillips, D., Harris, R.A., Stern, T., Beavan, J., Ellis, S., Henrys, S., Cox, S., Norris, R.J., Berryman, K.R., Townend, J., Bannister, S., Pettinga, J., Leitner, B., Wallace,

L., Little, T.A., Cooper, A.F., Yetton, M. and Stirling, M. (2007): Do great earthquakes occur on the Alpine Fault in central South Island, New Zealand? In: Okaya, D., Stern, T.A. and Davey, F. (Eds.): A continental Plate Boundary: Tectonics at South Island, New Zealand. AGU Geophysical Monograph 175, 235 – 251.

Toy, V.G., Boulton, C.J., Sutherland, R., Townend, J., Norris, R.J., Little, T.A., Prior, D.J., Mariani, E., Faulkner, D., Menzies, C.D., Scott, H. and Carpenter, B.M. (2015): Fault rock lithologies and architecture of the central Alpine Fault, New Zealand, revealed by DFDP-1 drilling. Lithosphere 7, 155 – 173, doi:10.1130/L395.1.